3-24-2016

Effectiveness Based Design of a Tactical Tanker Aircraft

Andrew K. Petry

Effectiveness Based Design of a Tactical Tanker Aircraft

THESIS

Andrew K. Petry, First Lieutenant, USAF

AFIT-ENY-MS-16-M-233

DEPARTMENT OF THE AIR FORCE
AIR UNIVERSITY

AIR FORCE INSTITUTE OF TECHNOLOGY

Wright-Patterson Air Force Base, Ohio

AFIT-ENY-MS-16-M-233

EFFECTIVENESS BASED DESIGN OF A TACTICAL TANKER AIRCRAFT

THESIS

Presented to the Faculty

Department of Aeronautical Engineering

Graduate School of Engineering and Management

Air Force Institute of Technology

Air University

Air Education and Training Command

in Partial Fulfillment of the Requirements for the

Degree of Master of Science in Aeronautical Engineering

Andrew K. Petry, B.S.

First Lieutenant, USAF

March 24, 2016

AFIT-ENY-MS-16-M-233

EFFECTIVENESS BASED DESIGN OF A TACTICAL TANKER AIRCRAFT

THESIS

Andrew K. Petry, B.S.
First Lieutenant, USAF

Committee Membership:

Lt Col Anthony M. DeLuca, PhD
Chair

Edward J. Alyanak, PhD
Member

Maj Ryan P. O'Hara, PhD
Member

Abstract

An approach to drive conceptual aircraft design using mission effectiveness parameters is described and applied to an operational scenario. The scenario includes traditional aircraft refueling tankers and a proposed tactical tanker concept supporting fighter aircraft conducting offensive (OCA) and defensive (DCA) counter air patrols. Traditional conceptual design methodologies were used to generate a baseline design for a tactical tanker aircraft, which was evaluated using a MATLAB-based model to investigate Measures of Effectiveness (MOE). The model holds the traditional tanker and fighter capabilities constant, while varying the tactical tanker's specific fuel consumption, lift-to-drag ratio, fuel payload, mass fraction, and proximity to contested airspace. A sensitivity analysis was conducted to show the effect of technology variations on MOEs. Results show with a minimum of 45000 lb fuel payload, the tactical tanker can increase the fighter OCA penetration radius by 57%, and the DCA loiter time by 48%. However; optimal size is heavily dependent on gameboard layout, fighter size, and number of aircraft tasked to the tanker. Sensitivity analysis and full factorial trade space exploration show the MOEs are most sensitive to changes in proximity and mass fraction. These results provide recommendations for the prioritization of research efforts if the US Air Force decides to develop a tactical tanker aircraft in the future.

Acknowledgements

I am grateful for the support I received from my advisor, sponsor, professors, coworkers, fellow students, friends, and family. I would like to specifically thank Dr. Alyanak for suggesting this topic and providing me with the tools and guidance necessary to succeed. Thanks also goes out to Jeff Dubois, Frank Campanile, and Tom Jacobs, for their expertise.

I am also indebted to my fellow students, especially Mark Vahle, Josh Kim, Jason Torf, and James Sellers. I would have been hopelessly lost without your support!

Andrew K. Petry

Table of Contents

Page

List of Figures

Figure Page

List of Tables

EFFECTIVENESS BASED DESIGN OF A TACTICAL TANKER AIRCRAFT

I. Introduction

1.1 Motivation

The complexity and requirements of military aircraft have greatly expanded since the early days of aviation. US Army Signal Corps Specification 486, the 1907 document which set the requirements for the military's first-ever airplane acquisition, totaled only four pages [4]. Since then, technological advances and warfighter needs have conspired to drastically increase the number of systems onboard new military aircraft. These systems have complex interactions. With the increase in complexity comes an increase in cost. According to the RAND Corporation, the per unit cost of tactical aircraft has increased 10% annually since 1950 [5]. Cost overruns lead to a decrease in the number of procured aircraft, which increases the per unit cost, and can potentially further reduce the total number of aircraft procured. This cycle is known as the defense death spiral [9]. The F-22 Raptor is a recent example of the defense death spiral's consequences. Between 1991 and 2004, cost overruns led to a drop in the projected number of procured F-22s from 750 to 680 to 442 to 339 before reaching a final value of just 183 aircraft [27].

Modern military aircraft are designed in stages with increasing fidelity. Raymer illustrated the design process begins in the conceptual phase, then enters the preliminary phase, and reaches culmination in the detailed design phase [24]. Certain decisions and design actions occur within each phase, as shown in Figure 1.

In the conceptual design phase, the aircraft's size, configuration, and weight are

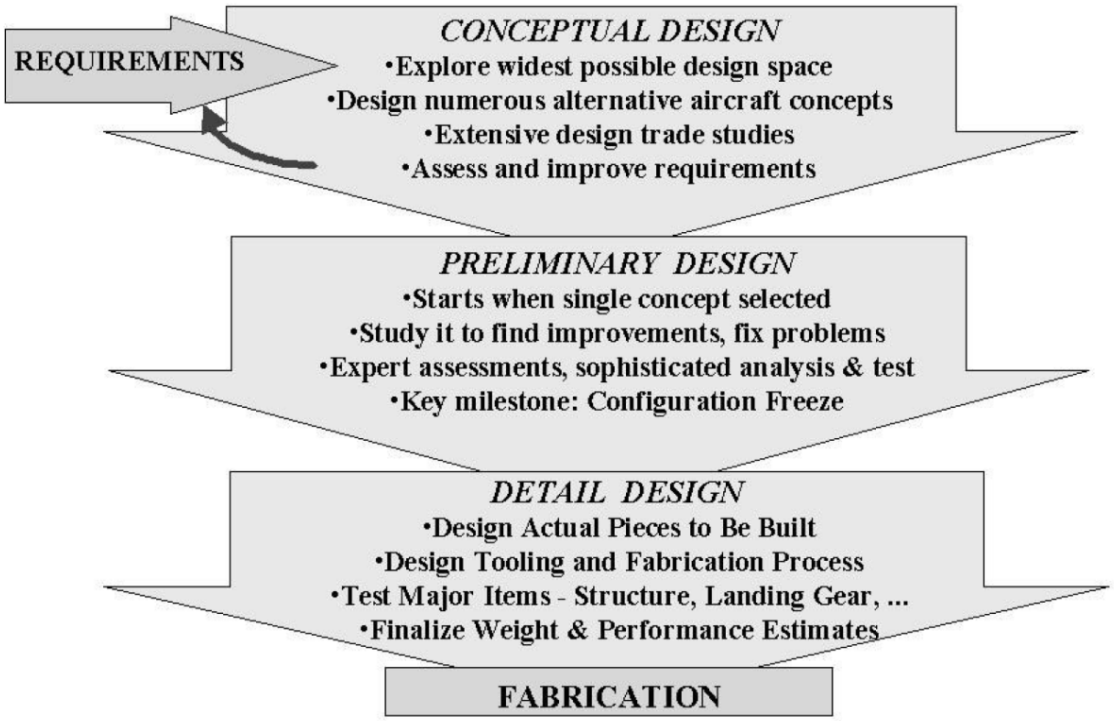

Figure 1. Aircraft design phases and accompanying tasks [24].

investigated. Simple modeling tools are used to predict preliminary aircraft performance in a chosen mission. Some of the analysis tools commonly used during this phase include trade studies, analysis of alternative designs, and comparisons with historical trends.

The preliminary design phase begins once the customer's requirements are known and major questions of configuration (*e.g.* canard vs. standard horizontal tail) and weight have been answered [25]. At this point, the design's general layout has been chosen, and engineering teams of various disciplines conduct in-depth analysis and subsystem design. In the case of the wing spar shown in Figure 2, the preliminary design phase shows the shape and size of the spar, but does not make considerations for fuel storage, attachment bolts, and wiring.

The increased fidelity of the preliminary design allows the use of more advanced computational tools, and perhaps an assessment of the design in a simulated opera-

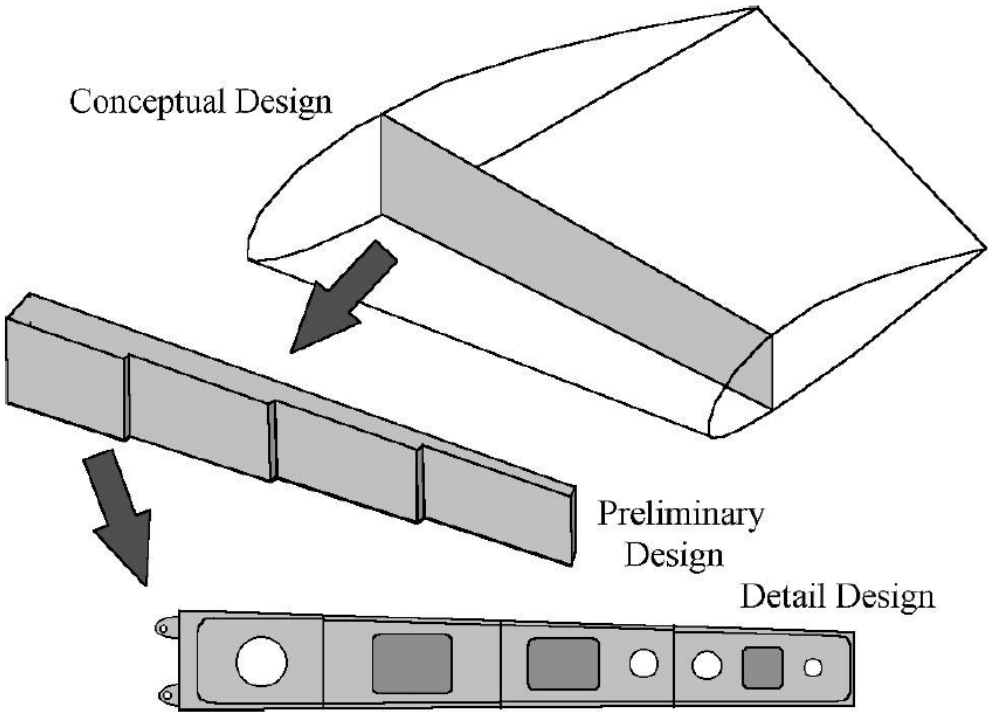

Figure 2. Evolution of wing spar design through each design phase [24].

tional environment, known as an Operational Assessment (OA). If the design satisfactorily meets mission requirements in OA, then the program enters into the detailed design phase. The culmination of the detailed design phase is a prototype aircraft.

1.2 Research Problem Description

If the OA unveils performance shortcomings, then the design program will either be terminated or follow one of two alternatives:

(1) Conduct a redesign

(2) Determine if the user will accept decreased performance

Conducting a redesign can be very expensive, and it increases a program's susceptibility to the defense death spiral. To avoid the death spiral, military aircraft designers must find a way to reliably and inexpensively determine the effectiveness of

a given design during the conceptual design phase. Effectiveness is determined by an analysis of parameters called Measures of Effectiveness (MOE). MOEs measure how well a system performs in its operational environment [15]. MOEs are expressed by mathematical equations and ratios using outputs from the OA. Changes in MOEs are driven by configuration and technology changes known as Technology Performance Measures (TPM). Examples of TPMs used in aircraft design include lift-to-drag ratio, specific fuel consumption, and mass fraction.

1.3 Scope and Assumptions

This research seeks to accomplish three objectives. The first objective is to use OA to quantify how changes in TPMs propagate through a scenario, and impact the aircraft's effectiveness. In other words, if designers improve a TPM by a certain percentage, how much better will the overall airplane perform? The second objective is to determine the sensitivity of each MOE to changes in TPMs. Understanding the importance of each TPM enables recommendations to be made for prioritization of research funding.

The research can be broken down into a series of steps. First, a capability gap must be defined, which can be filled by developing a new aircraft design. The capability under consideration is the use of a tactical tanker aircraft to support fighters performing offensive and defensive counterair (OCA or DCA) missions. The objective of an OCA mission is to destroy, disrupt, or degrade enemy air capabilities by engaging them as close to their source as possible. The objective of a DCA mission is to protect friendly forces from enemy airborne attacks [1]. Tactical tankers are distinguished from current Air Force tankers, such as the KC-10 and KC-135, by their smaller size and ability to operate closer to the battlefield. The US Navy and Marine Corps fill the tactical tanker role with the KC-130, or buddy refueling

from an F-18, but incompatible equipment prevents Air Force fighters from taking advantage of sister service capabilities [7]. In both OCA and DCA scenarios, fighters and tankers launch from friendly bases and fly towards the contested airspace. At a certain distance from the contested airspace, the fighters separate from the tankers and proceed alone. The tanker enters into a loiter orbit and waits for fighters to refuel. The introduction of a tactical tanker in this scenario improves the mission effectiveness of the fighter aircraft by providing fuel at a location much to the fight, which decreases the proportion of the total mission time the fighters spend transiting to and from the refueling point.

Once the scenario is fully defined, a set of traditional design requirements can be extracted. These requirements, such as speed, range, and payload, are familiar to all aircraft designers. From these requirements, a tactical tanker can be conceptually designed using techniques described in Raymer's aircraft design text [25]. Outputs of this design stage include baseline TPM values such as lift-to-drag ratio, fuel quantity, and mass fraction. Next, the design is evaluated in a MATLAB-based OA tool adapted for this research called the quick look model. The quick look model simulates the aircraft's performance in an operational scenario. Using design of experiments techniques and sensitivity analysis methods, the performance impacts of each TPM are investigated, and MOE values are quantified. Finally, the results are examined to provide recommendations in two distinct areas. First, tactical tanker design parameters initially identified using Raymer's techniques can be refined to provide a starting point for future design studies. Second, results from the TPM sensitivity analysis can inform decision makers about the relative importance of current research investments, and provide insight into future funding decisions.

1.4 Thesis Outline

Chapter I provides an overview of the motivation for this work, the research objectives, and the project's scope. Chapter II presents an in-depth review of previous research into conceptual design, MOEs, sensitivity analysis, and full factorial trade space development using design of experiments techniques. Chapter II also provides a brief history of military tanker aircraft. Chapter III outlines the methodology used to investigate this research problem, including an orderly overview of the scenario to be evaluated, the requirements derived from the scenario, and the steps to be taken to conduct the operational analysis. Chapter IV introduces and analyzes the results. Finally, Chapter V summarizes the results, provides conclusions, and makes recommendations for future work.

II. Literature Review

This chapter provides a review of background information necessary to understand, plan, and perform the research detailed in later chapters. Topics to be covered include an overview of traditional conceptual design techniques, a review of efforts to evaluate conceptual designs using measures of effectiveness, a review of sensitivity analysis and full factorial trade spaces, a description of current USAF tanker operations, and an introduction of the tactical tanker concept.

2.1 Conceptual Design

Raymer's aircraft design textbook provided an excellent overview of conceptual design methods [25]. The conceptual design phase begins with setting the aircraft's size and weight at levels capable of accomplishing the required mission profile. This determination is based on requirements for the number of crew, payload weight, fuel weight, and empty airframe weight. Ratios of fuel weight to takeoff weight, and empty weight to takeoff weight, are substituted into the weight summation to enable comparisons between a proposed design and historical weight trends. These ratios are incorporated into the takeoff weight equation shown in Equation 1 below, where W_0 represents the takeoff weight, and other values represent weights of the crew, payload, fuel, and empty aircraft.

$$W_0 = \frac{W_{crew} + W_{payload}}{1 - (W_{fuel}/W_0) - (W_{empty}/W_0))} \tag{1}$$

Raymer provided a semi-logarithmic plot and curve-fit equation (see Equation 2), which shows the trends of empty weight fraction versus loaded takeoff weight for fighters, transports, bombers, and other aircraft classes [1]. In general, Raymer's data show an inverse relationship between empty weight fraction and takeoff weight. In

the curve-fit equation, the constants A and C differentiate between aircraft classes. K_{vs} is an adjustment factor for aircraft with variable sweep-wing technology, which requires extra actuators and stronger, heavier components.

$$W_{empty}/W_0 = AW_0^C K_{vs} \tag{2}$$

Once the empty weight fraction is determined, the next design parameter to be found before takeoff weight is the fuel fraction, denoted by W_{fuel}/W_0, which is the ratio of fuel weight to total weight at takeoff. In general, aircraft with higher fuel fractions have longer range when compared with aircraft of similar total weight. Determination of fuel fraction requires a detailed understanding of the proposed aircraft's mission profile. Mission profiles describe the altitude, distance, and speed to be covered by each mission leg. Legs of a typical mission include takeoff; climb to altitude; cruise for a given distance; loiter over an area for a certain time; release payload in the form of weapons, cargo drops, or offloaded fuel; cruise home; and land. For added fidelity, designers can account for fuel used in warm-up, taxi, and other short mission legs. Mission profiles vary greatly depending on aircraft type. For example, mission profiles for a commercial airliner and an air superiority fighter are very different, as shown in Figure 3.

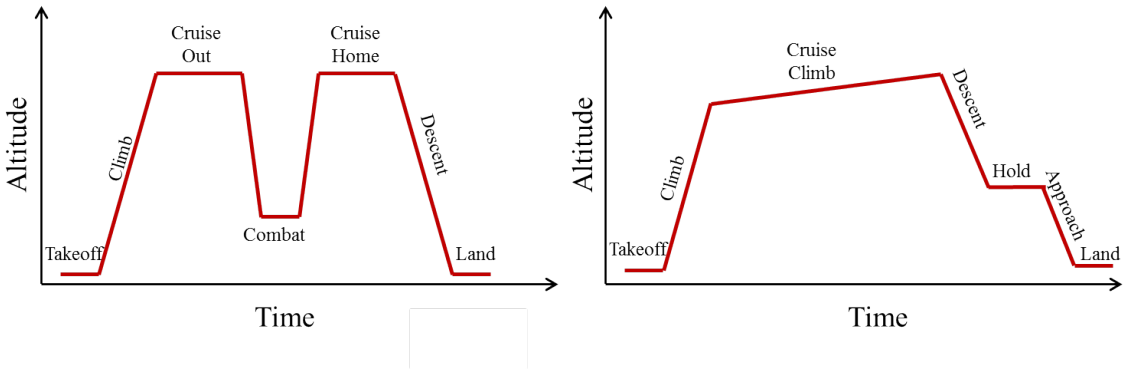

Figure 3. Typical mission profile for a fighter on a high-low-high mission (left) and commercial transport airliner (right).

Fuel fractions for each mission leg are assigned a ratio. For example, the takeoff mission leg is W_1/W_0, and the climb leg is denoted by W_2/W_1. The total mission fuel fraction is found by multiplying individual fuel fractions from each mission leg. Fuel fraction for an aircraft with four mission legs is shown in Equation 3.

$$\frac{W_4}{W_0} = \frac{W_1}{W_0} * \frac{W_2}{W_1} * \frac{W_3}{W_2} * \frac{W_4}{W_3} \tag{3}$$

Fuel fractions for takeoff, climb, and landing are approximated using historical data from similarly sized aircraft. Cruise, loiter, and combat legs are more complex, and require knowledge or estimation of the aircraft's required range and endurance, engine specific fuel consumption, velocity, and lift-to-drag ratio rather than historical data.

Once total fuel fraction and empty weight fraction are known, the aircraft's takeoff weight can be calculated. Knowledge of the aircraft weight allows the designer to conduct trade studies, which involve consulting with the user to determine the importance of each requirement. The purpose of these studies is to show the user the relationship between each requirement and the total weight. Raymer provided example calculations for a proposed anti-submarine warfare aircraft with an initial weight of 56,700 pounds, a range of 1,500 nautical miles, and a payload of 10,000 pounds. He showed a 500 nautical mile decrease in required range reduced takeoff weight by almost 15,000 pounds. Adding 5,000 pounds of additional payload increases the overall weight by more than 22,000 pounds [25]. Initial size determinations set the stage for calculations of thrust-to-weight ratio and wing loading.

Thrust-to-weight ratio (T/W) and wing loading (W/S) are the two most important parameters affecting a proposed aircraft's mission performance [25]. Thrust-to-weight ratio is described as the ratio between an aircraft's maximum thrust and takeoff weight at sea level static conditions. This ratio can be improved (increased) by installing a

more powerful engine which generates more thrust without increasing weight, or by finding a way to reduce weight from a certain aircraft components. Wing loading is the ratio between takeoff weight and wing area, and is measured in pounds per square foot. Wing loading can be improved (decreased) for cruise flight by substituting for a wing with larger area. However, some aircraft may desire a high wing loading in order to reduce surface area and associated drag. An aircraft with high thrust-to-weight ratio, or low wing loading, is more maneuverable than an aircraft with the opposite characteristics.

Raymer presented a method of converting individual requirements into curves-marking the boundary between feasible and infeasible values for T/W and W/S [25]. Figure 4 shows examples of these curves for a hypothetical fighter jet. This fighter has defined requirements for takeoff and landing distance, cruise speed, supersonic sprint, and sustained turn performance. Each of these requirements can be turned into an equation, using W/S as the independent variable, and T/W as the dependent variable.

The colored lines on Figure 4 represent the T/W vs. W/S curve for each requirement. Examining the takeoff distance requirement in isolation shows an aircraft with a low T/W and a low W/S, indicating a small engine with large wings, is equally as effective as an aircraft with a large T/W and a large W/S, indicating a powerful engine with small wings. Because the final design must simultaneously satisfy all of the customer's needs, requirements cannot be viewed in isolation. An overall feasibility region, denoted by the black dashed lines, can be constructed by selecting a T/W and a W/S point that lies on the feasible side of each curve. The optimal T/W and W/S combination lies at the black star. At this point, the airplane weighs as little as possible for a given engine and wing selection. Additionally, at this point in the design process, the airplanes unit cost is as small as possible, due to the correlation

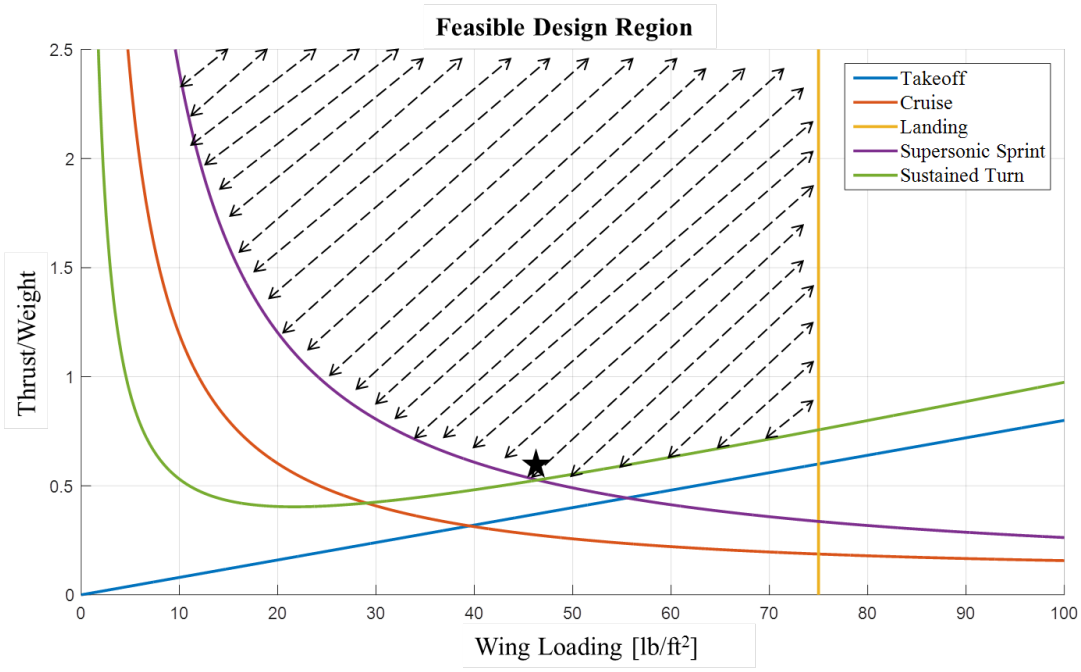

Figure 4. Plot of thrust-to-weight ratio vs. wing loading for a hypothetical fighter aircraft.

between increased weight and increased cost.

A designer should not design an airplane around the T/W and W/S pair denoted by the black star. This is because an aircraft's weight increases during the development process or later during operational life when extra systems, performance requirements, or mission requirements are added or modified [25]. If the optimal point had been chosen, then an increase in weight, without a corresponding increase in thrust, would cause the T/W ratio to cross from the solution space into the infeasible region. It is good practice to choose a design point with built-in T/W and W/S margins based on historical expectations of weight creep in past designs.

Once the T/W and W/S values have been chosen, the aircraft layout drawings are started for the fuselage, wings, engine(s), and tail. Considerations are made for locating subsystems such as landing gear, payload, and avionics. The layout can be facilitated with computer-aided design software. Once the conceptual design is

completed, the aircraft's predicted performance can be evaluated, analyzed, and altered during an iterative process. Eventually, the design will be mature, and the program will enter the preliminary design phase. It should be noted that the conceptual, preliminary, and detailed design processes do not necessarily have firm links to Department of Defense acquisition terminology.

2.2 Measures of Effectiveness

A Measure of Effectiveness (MOE) measures how well a system performs a specific function in its operational environment [15]. The goal of the aircraft design process is to create an aircraft which meets the most important customer requirements. Several methods have been created to evaluate a design's effectiveness.

2.2.1 Evaluating Overall Utility

Dimitri Mavris and Daniel DeLaurentis of the Georgia Institute of Technology Aerospace Systems Design Laboratory created a method of evaluating an aircraft design based on five attributes: affordability, availability, peacetime safety, mission capability, and wartime survivability [18]. Previous attempts at design evaluation and optimization focused on one or two of these attributes in isolation. Mavris and DeLaurentis created an overall evaluation criteria (OEC) metric to compare the utility of different designs. The OEC, shown in Equation 4, has terms for each of the five attributes, as well as importance coefficients which sum to one. The importance coefficients are shown by the Greek letters alpha through epsilon, and provide weighting to attributes that may be more or less important. Alternate design vectors are evaluated by comparing each attribute's value to the baseline value in the original design vector.

$$OEC = \alpha\frac{LCC_{BL}}{LCC} + \beta\frac{MCI}{MCI_{BL}} + \gamma\frac{EAI}{EAI_{BL}} + \delta\frac{P_{surv}}{P_{surv_{BL}}} + \epsilon\frac{A_i}{A_{i_{BL}}} \tag{4}$$

The five parameters in this equation are Life Cycle Cost (LCC), Mission Capability Index (MCI), Engine Related Attrition Index (EAI), Survivability (P_{surv}), and Inherent Availability (A_i). Each parameter is paired with an attribute listed above. The authors also presented a decision matrix technique for deciding which aircraft design, among a group of potential alternatives, offered the most utility. This design matrix enabled examination of each attribute's weighting coefficient. Visualizing the effects of small changes in importance coefficients provided the designer with potential trade studies, with the goal of providing the best fit for the customers needs. Ultimately, Mavris and DeLaurentis separated the design process into three steps:

1. Assess customer requirements and translate into design objectives and coefficient values
2. Generate feasible alternatives and calculate attribute values
3. Evaluate alternatives using the OEC decision matrix

Hugh McManus, Matthew Richards, Adam Ross, and Daniel Hastings of the Massachusetts Institute of Technology generated a method of incorporating certain MOEs into trade space studies for satellites flying in low earth orbit [19]. The authors describe MOEs as "ilities," which they define as "system properties that specify the degree to which systems are able to maintain or even improve function in the presence of change" [19]. They created an equation showing a satellites lifetime utility as a function of utility during periods of time known as epochs. In each epoch, the systems performance and configuration was held static, meaning no changes were occurring. This utility equation, shown in Equation 5, determines the sum of the utility in each epoch, multiplied by the length of the epoch, multiplied by the probability of

surviving a period of change. In their space application, the change typically comes from collision with space debris.

$$U_{lifetime} = U_1T_1 + P_2 * U_3T_3 \tag{5}$$

The satellite designs modeled in this scenario come from a range of values for four different satellite attributes: payload mass, propulsion type, fuel load, and debris shield mass. Each attribute has between four and eight options. Using full-factorial analysis, a total of 768 design vectors were created [19]. The authors evaluated each design, and presented three methods for interpreting the results. These methods are all variations of plotting techniques, with the main distinction being how the designer wants to display differences between each design vector.

The method shown in Figure 5 provides the best view of the Pareto-efficient region, where utility is maximized with respect to cost. The end result of plotting these design vectors is the discrimination between feasible and infeasible options, and identification of designs worthy of more detailed analysis. The red line shows the location of the example design vector.

2.2.2 Incorporating Future Technology Improvements

Michelle Kirby of the Georgia Institute of Technology investigated methods to create conceptual aircraft designs that incorporate future technological advancements, with the objective of designing for affordability and quality instead of traditional performance metrics [17]. Kirby gathers customer requirements and establishes a baseline conceptual design. Potential variations are gathered in a Morphological Matrix. An example Morphological Matrix for a new pen is shown in Table 1. In this simplified example, the pen has four characteristics, and each characteristic has several independent and mutually exclusive alternatives. Conceptual design vectors

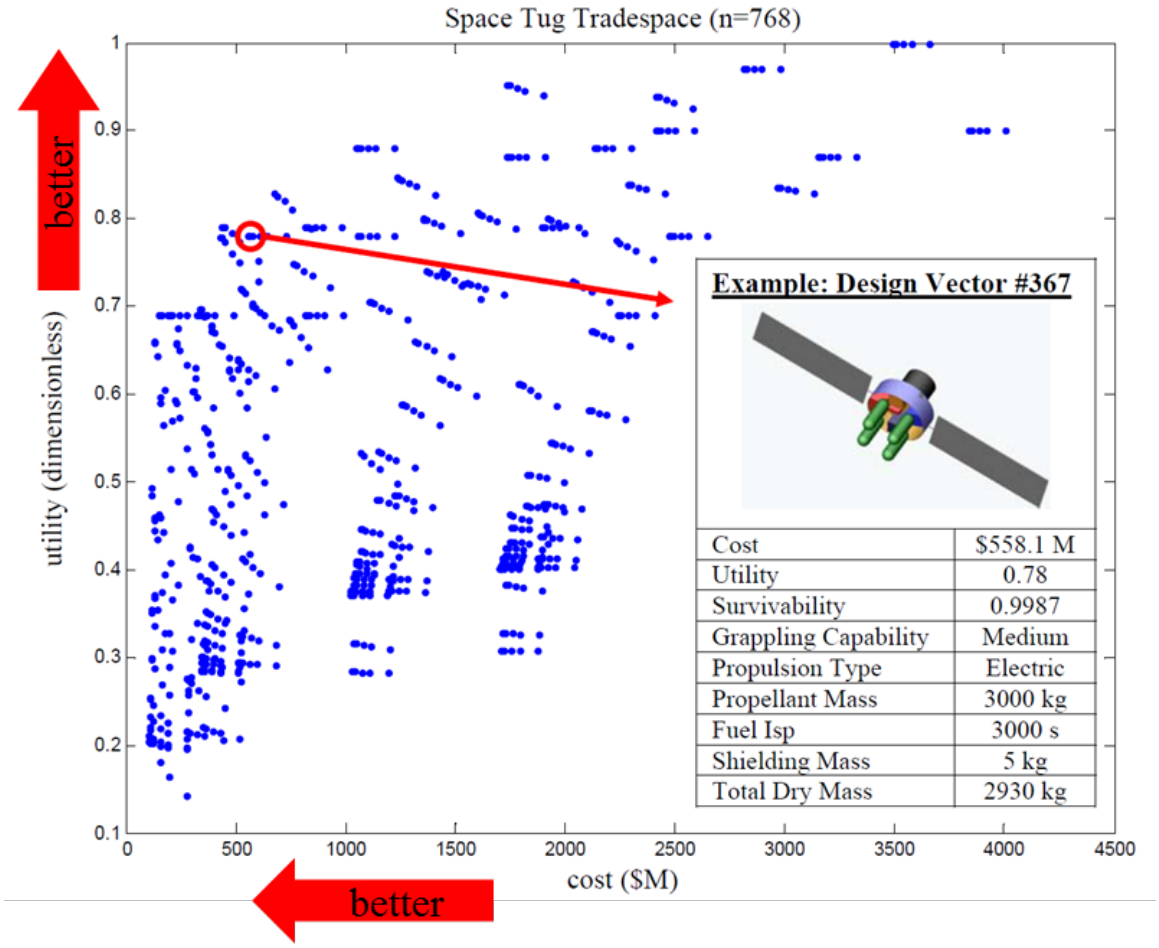

Figure 5. Trade Space Exploration for a Space Tug Spacecraft [19].

can be made by selecting one alternative for each of the four characteristics. The combined set of all possible design vectors is known as the alternative concept space.

Continuing the pen example, it is possible that a new type of writing tip is in development. Before investigating a design vector incorporating this new technology, Kirby says the designer must first consider three questions [17]:

1. Is the new technology compatible with the other characteristics?
2. What is the impact to the overall system from the new technology?
3. What is the technology's maturity?

Kirby assigns a Technology Readiness Level (TRL) to the new technology and uses a Weibull distribution to quantify the uncertainty associated with the technology's

Table 1. Sample Morphological Matrix for a New Pen [17].

	Design Alternatives		
	1	**2**	**3**
Casing	Plastic	Metal	Hybrid
Writing Tip	Felt	Ball	-
Color	Black	Red	Blue
Line Thickness	Fine	Medium	Heavy

TRL rating. The designer's confidence in eventual system performance increases as the TRL increases from 1 towards 9 [26].

Researchers David Panson, Edward Alyanak, Jeffrey Dubois, and Todd Van Woerkam of the Air Force Research Laboratory (AFRL) applied similar ideas about new technologies to the development of a next generation fighter aircraft [23]. With the increasing pace of technological advancement, the AFRL team saw the trade space for future systems growing exponentially more complex. The team sought to reduce the technology trade space of a conceptual fighter design in order to more accurately direct future design efforts. Their three objectives included [23]:

1. Develop a quick look model to identify the impact of various aerodynamic technologies on baseline and alternate aircraft performance in a representative mission context.

2. Reduce the technology trade space using a low-fidelity tool before transitioning to more computationally expensive simulation environments.

3. Evaluate and screen conceptual aircraft designs.

Panson *et al.* developed scenarios to test new fighter designs on OCA and DCA missions, then created alternate fighter design vectors with technological improvements over the baseline aircraft.

The results showed interesting tradeoffs in technology improvements depending on the desired optimization method, as shown in Figure 6. Units have been removed from

the plot. For the DCA scenario, the performance indices sought to maximize fighter loiter time or minimize fuel required by varying Mach number. Metrics accounted for included loiter time, number of fighter aircraft aloft, fuel required, and number of tanker sorties. Faster cruise leg speeds led to a small increase in loiter time, but came at the cost of increased fuel required and more tanker support. Minimizing single sortie fuel required achieved significant fuel savings but resulted in shorter loiter time.

In the OCA scenario, the optimization method searched the trade space to maximize efficiency or maximize speed, again by varying Mach number during each flight leg. The two performance indices led to significant impacts on penetration radius and time at risk.

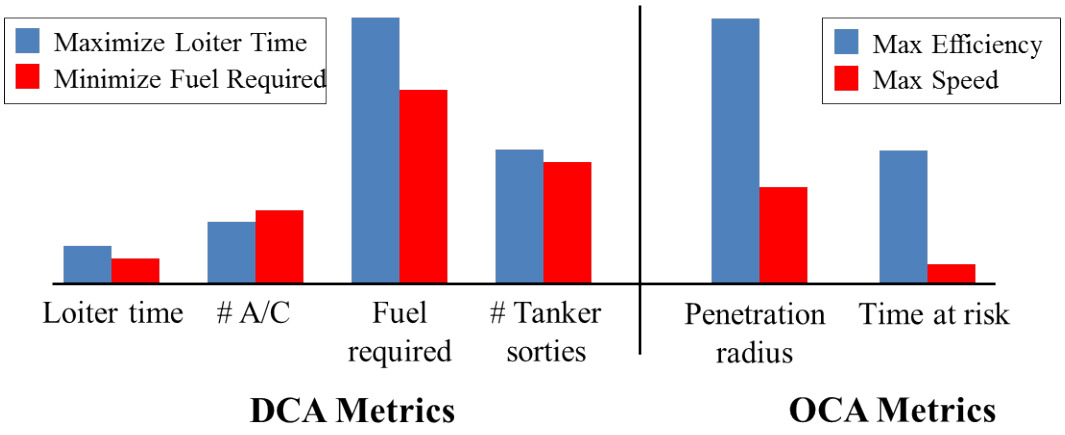

Figure 6. Baseline aircraft performance results [23].

These tradeoffs highlight the importance of coupling design analysis with operations research.

2.3 Sensitivity Analysis

Sensitivity analyses are conducted to determine the sensitivity of a given response function to changes in model parameters[29]. They have three common purposes[20]:

1. Determine the sensitivity of a configuration to its proximity to an optimal point.

2. Determine the sensitivity to a relaxation in mission constraints.

3. Determine the influence of changing a technology level.

The third purpose is most relevant to the development of a tactical tanker. Budget constraints necessitate that technology levels cannot be simultaneously increased at the same rate. Sensitivity analysis enables prioritization of technology improvement efforts predicted to provide the largest benefit to system performance. These prioritization decisions may require prior knowledge of the expected expenditure necessary to realize a certain technology improvement [20].

Sensitivity analyses use Taylor Series Expansions, as shown in Equation 6 to approximate derivatives. The procedure is valid for small changes in model parameters and when only one parameter is changed at a time.

$$y(x + \Delta x) = y(x) + \nabla y(x) * \Delta x + O(\Delta x^2) \tag{6}$$

Solving for $\nabla y(x)$ in the first-order Taylor Series Expansion results in a forward-difference approximation of the derivative, shown in Equation 28. In this equation, the $O(\Delta x)$ term represents truncation error. Smaller Δx perturbations will decrease truncation error. However, small enough perturbations lead to increased round-off error [29].

$$\nabla y(x) = \frac{y(x + \Delta x) - y(x)}{\Delta x} + O(\Delta x) \tag{7}$$

The forward-difference approximation finds sensitivities in y at the $(x + \Delta x)/2$ point because the numerator in Equation 28 can be interpreted as the average point between x and $(x + \Delta x)$ [10]. A similar technique, called backward-difference, finds

sensitivities using the value at $y(x - \Delta x)$ instead of $y(x + \Delta x)$. A third technique, shown in Equation 8, is known as the central-difference method. The central-difference method uses two points on either side of $y(x)$ to find sensitivities at exactly that point. It is second-order accurate.

$$\nabla y(x) = \frac{y(x + \Delta x) - y(x - \Delta x)}{2\Delta x} + O(\Delta x^2) \tag{8}$$

Adam Diedrich of the Massachusetts Institute of Technology applied sensitivity analysis to the development of an extremely quiet transport aircraft [11]. Diedrich varied the engine's weight and specific fuel consumption (SFC) and found the change in aircraft max takeoff weight. His results are shown in Figure 7. The slope of each line on this plot represents the sensitivity to a change in engine parameters. Steeper slopes correspond to higher sensitivity, and shallow or flat slopes correspond to low or zero sensitivity. Diedrich found that max takeoff weight was much more sensitive to engine SFC than to engine weight. Other researchers have applied similar techniques to the design of fighter aircraft [23] and the analysis of fuel consumption in commercial aircraft [12].

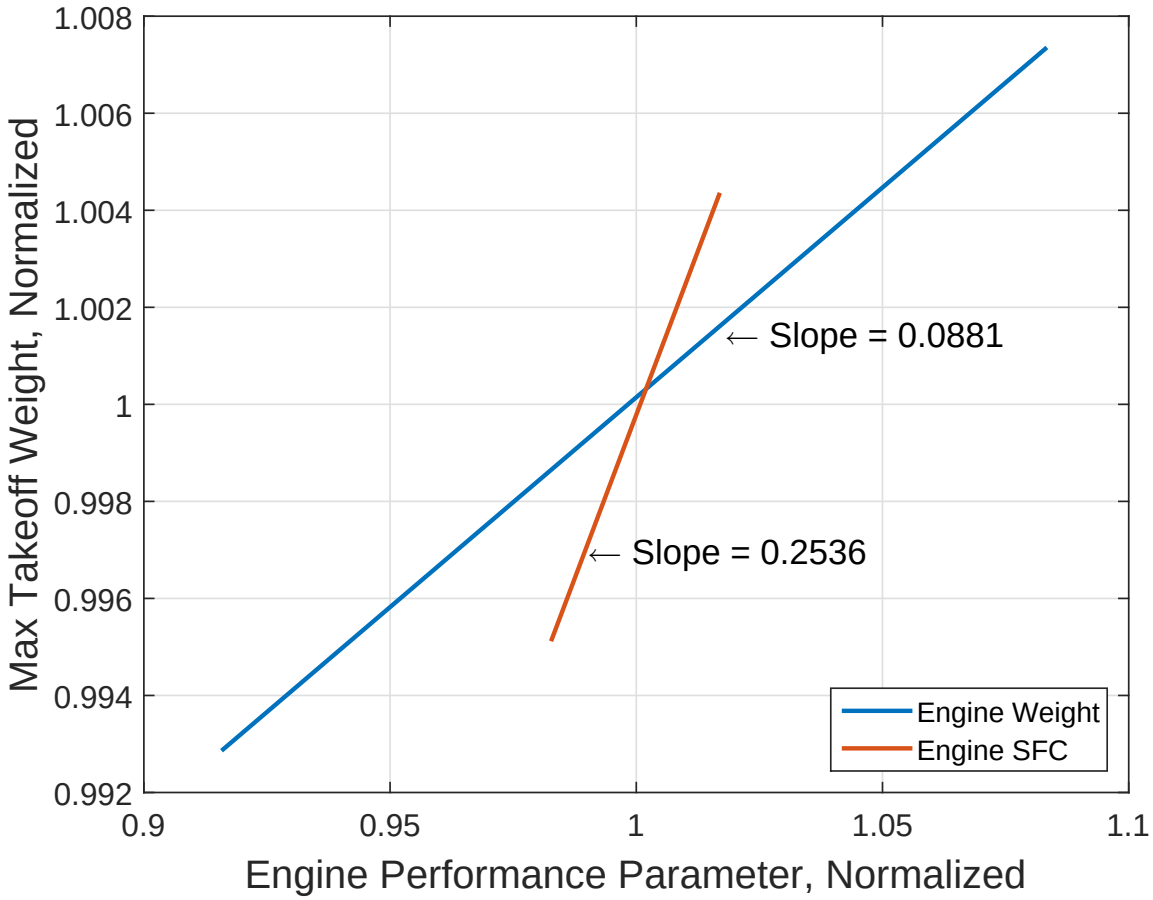

Figure 7. Sensitivity of Max Takeoff Weight with respect to Engine Performance [11].

2.4 Design of Experiments

Modern Design of Experiments (DOE) techniques were introduced in the 1920s by Ronald Fisher [13]. Their purpose is to quantify how a change in an input variable impacts an experimental outcome. Fisher introduced this concept by setting up a simple factorial scheme designed to experimentally study the effects of composition variations in a mixture containing several active ingredients. Two conditions must be met for the experiment to be worthwhile and valid [13]:

1. The ideal ingredient mixture must be unknown.

2. The efficacy of each mixture must be measurable by its effect in particular trials.

Suppose Fisher's mixture has three active ingredients, given as factors A, B, and C. Each factor may be included in the final mixture in a low or high concentration, known as levels. The total number of trials necessary to fill the 'full-factorial' design space is shown in Equation 9. Table 2 breaks down each trial.

$$Trials = Levels^{Factors} = 2^3 = 8 \tag{9}$$

Table 2. Experimental Trials in a 2^3 Factorial Design

Trial Number	Factor 1	Factor 2	Factor 3
1	Low	Low	Low
2	Low	Low	High
3	Low	High	Low
4	Low	High	High
5	High	Low	Low
6	High	Low	High
7	High	High	Low
8	High	High	High

Each trial consists of a unique combination of the factors and levels. The mixture's efficacy can be tabulated for each trial and the experimenter can determine the appropriate concentration level for each of the active ingredients. Every trial provides valuable information necessary to answer the relevant questions. Although the experiment did not fully explore the range of concentrations between low and high, it may have determined a promising direction for further experimentation [6].

2.5 Tanker Aircraft

The US military regards aerial refueling as an integral part of US airpower. According to Joint Publication 3-17, aerial refueling "significantly expands deployment, employment, and redeployment options available by increasing the range, payload, and flexibility of air forces...especially when overseas basing is limited or not available"

[28]. Current USAF conventional tankers include the KC-10 and KC-135, with the KC-46 expected service within the next two years. The USAF also operates variants of the C-130, known as the MC-130 and HC-130. These aircraft conduct refueling of helicopters and tilt-rotor aircraft, using a probe and drogue system to refuel without interference from the rotor blades.

The KC-135 aircraft entered the USAF inventory with the mission of refueling B-47 and B-52 bombers on intercontinental missions under the command of Strategic Air Command (SAC). The KC-135 used a flying boom system which transfers fuel at high rates using pump pressure. In this scenario, the tanker aircraft inserts its refueling boom into a receptacle on the receiver aircraft [28]. At maximum pressure, the KC-135 supplies fuel at a rate of approximately 1,000 gallons per minute [16]. Tactical Air Command (TAC), unlike SAC, preferred the probe and drogue refueling system. In probe and drogue refueling, a hose and basket system is reeled into the air behind the tanker. Receiver aircraft plug into the basket using an extended probe [28]. Probe and drogue tankers, such as the KB-50, had three separate refueling stations, and could support several fighters simultaneously, albeit at a slower fuel flow rate than with the flying boom systems. Another advantage of the probe and drogue system is its smaller size, which enabled its employment on smaller tanker aircraft. Figure 8 shows a comparison of the two refueling systems. Over time, the KB-50 became too expensive to sustain, and was retired from service in the early 1960s. This retirement meant TAC was completely reliant on flying boom tanker support from SAC, and USAF fighter aircraft since have been designed for compatibility with the flying boom rather than the probe and drogue. From this era emerged a gap which continues to the present, where USAF fighter aircraft rely on large, single-point refueling tankers.

The development of aerial refueling for the Navy was not subject to the doctrine which led the Air Force towards large tankers. Rather, naval aviation refueling tech-

Figure 8. Comparison between Flying Boom (left) and Probe and Drogue (right) aerial refueling systems.

nology was driven by the need to operate from aircraft carriers. Aircraft carriers limit the weight and dimensions of aircraft operating from their decks. These limitations led to reliance on tactical refueling from smaller aircraft such as the now-retired KA-6. Naval tankers incorporated the probe and drogue system due to its smaller size and lack of a boom operator crew position. Current Navy fighters, such as the F-18, can even refuel each other in a technique known as buddy refueling. Allied nations also have the capability to quickly modify fighters for buddy refueling. During the 2011 Libya campaign, the Italian Air Force modified Tornado fighter aircraft as buddy refuelers to extend the loiter time of other fighters [14]. The use of the probe and drogue system enables Navy fighters to refuel from Marine-operated KC-130 aircraft. To support naval aircraft in todays joint environment, newer Air Force KC-10s and K-135s have been modified to include retractable probe and drogue systems. The centerline station on KC-10 aircraft has both an extendable drogue and boom system, and two more drogue systems can be installed near the wingtips. KC-135s are not as flexible. They lack the capability to mount wingtip stations, and the configuration of the centerline station can only be changed on the ground, which prevents the aircraft from refueling different types of receiver aircraft on the same sortie [28].

KC-135 and KC-10 aircraft are limited in how close they can approach a combat area due to their high value and relative lack of defensive capabilities. Fighter aircraft are assigned to fly defensive counterair combat air patrols on High Value Airborne Asset (HVAA) sorties to protect tankers, airborne radar, and surveillance aircraft [1]. The objective of a HVAA sortie is to intercept or destroy enemy attempts to attack the high-value asset. Fighters assigned this task are constantly positioned near the tanker or other high-value asset, which decreases the number of fighters conducting offensive operations. Furthermore, the tankers are kept at a distance outside contested airspace, so the risk of enemy engagement is further decreased. This standoff distance increases the amount of time a fighter package spends transiting to and from combat, which decreases their mission effectiveness.

Conversely, finding a way to decrease the standoff operating distance between the tanker orbit and combat area would increase mission effectiveness. This type of aerial refueling aircraft is known as a tactical tanker, and is distinguished from a conventional tanker by its smaller size, enhanced survivability, and ability to operate from austere airfields with runways between 4,000 and 5,000 feet long [22]. Such an idea has been previously proposed, and AFRL is currently evaluating the tactical tanker concept and studying the value of providing fuel to fighters closer to their objective. Work is also underway to determine the best way to position a flying boom or probe and drogue refueling system on a smaller aircraft while maintaining an acceptable flow field to refuel a variety of aircraft [3].

In a report for the Air War College, Lt Col Douglas Cole outlined the need to develop a Tactical Aerial Refueling Platform (TARP) [8]. Writing near the end of the Cold War in 1989, Cole examined a hypothetical conventional war in Europe. In a conventional war against the Warsaw Pact, Cole foresaw critical vulnerabilities in the NATO war plans. NATO war planners assumed that in the event of hostilities

in Europe, the airspace over Belgium and Germany would be safe for aerial refueling. Cole argued this assumption was false, and stated his opinion that traditional tanker aircraft would be forced to remain west of the English Channel. He envisioned a scenario where fighters in the skies over Germany would be forced to fly across the English Channel to refuel, which could severely limit their effective time in the contested airspace.

Cole proposed a tactical tanker known as the TARP which would incorporate stealthy and vertical/short takeoff and landing technologies. However, Cole realized the low likelihood of funding such a program and suggested five modifications to improve the ability of traditional tankers to operate in a contested environment [8]:

1. Equip tankers with multi-point air refueling systems to increase the number of fighters than can simultaneously refuel.

2. Equip tankers with both flying boom and hose and drogue systems to enable support to joint and coalition receiver aircraft.

3. Enable tankers to receive fuel from other tankers during flight.

4. Enable tankers to perform their missions at altitudes as low as 1000 feet above ground level.

5. Equip tankers with defensive avionics systems.

The tactical tanker's smaller size and ability to operate from shorter runways has led to an emerging market in countries with smaller Air Forces than the United States. In 2006, Israel Aerospace Industries and Gulfstream partnered to develop a conceptual tactical tanker based on the G550 business jet [21]. The proposed jet would carry a total of 55000 pounds of fuel, about 15000 pounds more than the baseline G550. In 2013, BAE Systems announced plans to modify BAe 146 aircraft as tactical tankers [21]. These two proposed aircraft were marketed as small, relatively inexpensive aircraft for use in tactical missions or as a low-cost surrogate for larger

tankers such as the KC-135 and A330 Multi-role Tanker Transport.

III. Research Methodology

3.1 Gameboard Layout

The gameboard represents a realistic scenario in which the fighters, tactical tanker, and traditional tanker work together to complete a mission. In this case, mission success is furthered by maximizing the time fighters can spend over the objective area in an anti-access/area denial (A2/AD) environment. An A2/AD environment is characterized by zones of increasing susceptibility to enemy attack. Approaching the objective, the enemy's integrated air defense system (IADS), made up of radars, surface-to-air missiles, fighters, etc., increases in strength. Due to the hazardous nature of these zones, certain aircraft are limited by how close they can approach the objective.

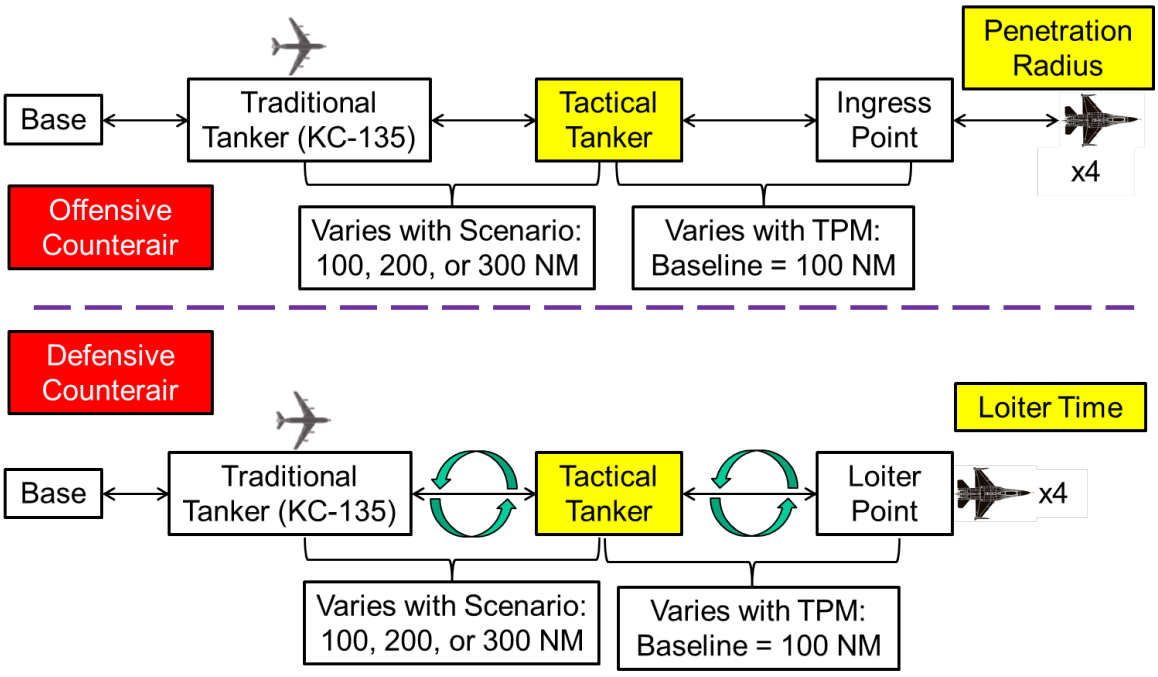

Figure 9. Gameboard layout showing aircraft operating regions (not to scale).

Figure 9 shows the gameboard layout for the OCA (top) and DCA (bottom) missions. The mission begins when the three aircraft types takeoff from one or more

friendly bases. The formation proceeds towards the contested airspace, refueling each other as necessary. At the border between permissive and contested airspace, the traditional tankers separate from the formation and enter into a loiter orbit. The tactical tankers and fighters proceed toward the contested airspace, refueling as necessary. At a certain point, the fighters top off their fuel tanks and continue flying on their own.

In the DCA mission, the fighters fly to the loiter point, loiter for certain period of time, then return for refueling before heading back for another loiter cycle. The tactical tanker cycles back and forth between its orbit location and the traditional tanker position. All aircraft return to the home base at the 8 hour mark. It is assumed that the traditional tanker never runs out of fuel; it is replaced by a fully fueled tanker if it burns or offloads all of its fuel payload.

In the OCA mission, the fighters fly towards the ingress point at their best range Mach number, then accelerate upon penetration. They fly as far as their fuel permits before returning to the tactical tanker. The fighters only enter contested airspace one time before all aircraft return to base. For comparison purposes, the ingress and loiter points are coincident. The OCA and DCA missions are divided into three different scenarios to investigate changes in aircraft positions.

Table 3. Scenario Distances in Nautical Miles.

Mission Leg	Scenario 1	Scenario 2	Scenario 3
Base to Traditional Tanker	300	300	300
Trad Tanker to Tact Tanker	100	200	300
Tact Tanker to Ingress/Loiter Point	100	100	100

Table 3 shows distances between the critical players on the gameboard. These parameters can be changed in the model to determine and investigate the tactical tankers

design sensitivity to changing parameters. These changes are necessary, because the exact situations in which the tactical tanker may be called upon are unknown. Factors influencing these parameters include geographic locations of friendly bases with respect to combat areas, contested airspace dimensions/strength, and each aircraft types susceptibility and vulnerability.

The distance from base to the traditional tanker orbit is constant in each scenario. The distance from the traditional tanker orbit to the tactical tanker orbit varies from 100 to 300 nautical miles in order to investigate how well the tactical tanker can perform as an intermediary between the fighters and traditional tanker, not at a technological performance change. The distance the fighters cover on their way to the loiter/ingress point is set at 100 nautical miles baseline value for each scenario. this distance changes by up to 20% in each scenario based on the tactical tanker's proximity technological performance measure.

3.2 Aircraft Designs

The Tactical Tanker Tradespace (TTT) quick look model includes three distinct aircraft types: fighters, tactical tankers, and traditional tankers. Users input the quantity and performance parameters of each aircraft. Model runs for this research included one tactical tanker, one KC-135, and four fighters with performance approximately equal to an F-16.

The tactical tanker's general characteristics were identified using Raymer's methods outlined in Chapter II [25]. These characteristics are driven by a comparison of TPM values with historical aircraft design trends.

3.2.1 Tactical Tanker Requirements

The baseline tactical tanker design was completed according to these trends. Equation 10 gives an aspect ratio (AR) of 6.63 for a maximum Mach number of 0.85. This equation is valid for military cargo and bomber aircraft.

$$AR = 5.57 * Mach_{max}^{-1.975} \tag{10}$$

Equation 11 uses the calculated aspect ratio to find the wing's span efficiency factor (e). This equation is valid for wings with a quarter chord sweep less than 30 degrees The tactical tanker's span efficiency factor is 0.85.

$$e = 1.78 * (1 - 0.045 * AR^{0.68}) - 0.64 \tag{11}$$

Equation 12 finds the lift coefficient at takeoff based on the maximum lift coefficient. Maximum lift coefficient equals 2.5, which is achievable using Fowler flaps or more advanced flap systems. The 1.2 value in the denominator is the ratio of takeoff speed to stall speed.

$$C_{L_{takeoff}} = \frac{C_{L_{max}}}{1.2^2} \tag{12}$$

Takeoff lift coefficient is used to generate a constraint curve for the takeoff requirement. The tactical tanker must be able to takeoff in less than 5000 ft. Equation13 generates this constraint curve. The minimum thrust to weight ratio is found as a function of wing loading. This equation is also a function of takeoff lift coefficient, σ, which is the ratio of field density to sea level density, and the takeoff parameter (TOP). TOP is a correction factor used to find takeoff distance for a jet aircraft over a 50 foot obstacle.

$$(T/W)_{takeoff} = \frac{1}{TOP * \sigma * C_{L_{takeoff}}} * (W/S) \tag{13}$$

The landing constraint is not a function of thrust to weight ratio. The maximum wing loading for safe landing is shown in Equation 14. The σ density ratio appears again in this equation. The tactical tanker must land in under 5000 ft, represented by $s_{landing}$. $s_{obstacle}$ is the added distance necessary to clear an obstacle on a 3 degree final approach glideslope. The tactical tanker's wing loading for a safe landing must be less than 125 lb/ft^2.

$$(W/S)_{landing_{max}} = \frac{s_{landing} - s_{obstacle}}{80} * \sigma * C_{L_{max}} \tag{14}$$

The thrust to weight ratio constraint during cruise flight is shown in Equation 15.

$$(T/W)_{cruise} = \frac{\beta^2 * K1}{\alpha * q} * (W/S) + \frac{C_{D_0} * q}{W/S} \tag{15}$$

In this equation, β is the percent fuel remaining at the start of the maneuver, α is the ratio of thrust at altitude to thrust at sea level static conditions, and q is the dynamic pressure. K1 and C_{D_0}, the parasite drag, are defined below:

$$K1 = \frac{1}{\pi * e * AR} \tag{16}$$

$$C_{D_0} = \frac{3 * \pi * e * AR}{16 * (L/D)^{-2}_{max}} \tag{17}$$

A T/W ratio vs. W/S plot was generated (see Chapter IV), and the design point was chosen as

$$(T/W)_{takeoff} = 0.3$$

$$(W/S)_{takeoff} = 115 lb/ft^2$$

3.2.2 Tactical Tanker Weights

Next, aircraft weight can be estimated. Raymer Table 6.1 provides empirical relationships between empty weight fraction and takeoff weight, aspect ratio, thrust-to-weight ratio, wing loading, and maximum Mach number. This relationship is derived from military cargo and bomber aircraft data [25].

$$\frac{W_{empty}}{W_{takeoff}} = 0.07 + 1.71 W_{takeoff}^{-0.1} AR^{0.1} (T/W)_{takeoff}^{0.06} (W/S)_{takeoff}^{-0.1} Mach_{max}^{0.05} \tag{18}$$

Empty weight and takeoff weight are then solved iteratively by guessing an initial takeoff weight value. This value is advanced through the weight fraction ratios corresponding to each mission leg to calculate empty weight and takeoff weight in Equations 19 and 20. The takeoff weight guess is adjusted until the guess equals the calculated value.

$$W_{empty} = \frac{W_{empty}}{W_{takeoff}} * W_{takeoff} \tag{19}$$

$$W_{takeoff} = \frac{W_{takeoff}}{W_{empty}} * W_{empty} \tag{20}$$

The baseline tactical tanker was designed to takeoff and land in under 5000 ft, cruise for 350 nautical miles at Mach 0.8 at 36000 ft, loiter for 5 hours, then cruise for another 350 nautical miles. Cruise performance is set at Mach 0.8 to match the KC-135.

3.2.3 Tactical Tanker Technology Performance Parameter Changes

Equations 21 through 26 show how each TPM can be adjusted from a given baseline value. The Δ quantity represents the parameter's change percentage. New parameter values are equal to the sum of the old value plus the percent change.

$$Parameter = Parameter_{baseline} * (1 + \Delta Parameter) \tag{21}$$

$$SFC = SFC_{baseline} * (1 + \Delta SFC) \tag{22}$$

$$L/D = L/D_{baseline} * (1 + \Delta L/D) \tag{23}$$

$$MassFraction = MassFraction_{baseline} * (1 + \Delta MassFraction) \tag{24}$$

$$FuelPayload = FuelPayloadbaseline * (1 + \Delta FuelPayload) \tag{25}$$

$$Proximity = Proximity_{baseline} * (1 + \Delta Proximity) \tag{26}$$

3.3 Model Development

The operational assessment model is a modified version of a MATLAB tool developed by AFRLs Aerospace Design and Analysis Branch. The original model was developed to conduct trade space exploration for proposed air superiority fighter concepts [23]. Its objective was to develop a quick look tool to answer a series of basic questions regarding the performance of a future fighter while conducting offensive or defensive counterair patrols. The modified model, hereafter known as the Tactical

Tanker Trade Space (TTT) quick look model, was heavily altered to suit the tactical tanker mission.

The TTT quick look model contains properties and methods. Public properties used in the TTT quick look model are user-provided inputs such as aircraft gross takeoff weight, lift-to-drag curves, Mach numbers, fuel capacity, and gameboard/scenario dimensions. Private properties include calculated quantities such as the amount of fuel offloaded from the tactical tanker, fuel burn rates, and mission performance. Calculation of the private properties enables calculation of the seven MOEs. The model's methods include the functions necessary to calculate, save, or display the values of public and private properties. In the TTT quick look model, key methods include calculation of private properties and MOEs, use of a secant method fuel burn optimizer, sensitivity analysis, and the setup of a design of experiments trade space. The secant method is a root finding algorithm used to find the amount of fuel the tactical tanker burns while the fighters are away conducting their mission. This method is necessary because the tactical tanker needs to keep enough fuel onboard to fly itself back to the traditional tanker. The method calculates a cost function value at two slightly different guessed quantities, then finds the gradient between the two results. The method is propagated until the root is found. In the OCA scenario, the secant method is used to find the amount of fuel the tactical tanker burns while the fighters are away conducting their mission. In the DCA scenario, the secant method finds the amount of fuel transferred between the traditional and tactical tankers during each refueling cycle. A selection of new equations developed to model interactions between the fighters, tactical tanker, and traditional tanker is shown in Appendix B.

3.4 Measures of Effectiveness and Technology Impacts

Technical Performance Metrics (TPMs) are aircraft technological characteristics that impact mission success. In the TTT model, TPMs are introduced by the user as public properties that can vary by some percentage. A percentage change in a TPM value reflects the incorporation of improved technology, techniques, or procedures into the aircraft or mission. TPMs used in the TTT model include lift-to-drag (L/D) ratio, specific fuel consumption (SFC), and mass fraction. L/D ratio is a measure of a wings aerodynamic efficiency. SFC is a measure of the mass flow rate of fuel per unit of thrust. Mass fraction compares an aircrafts mass with and without fuel. These TPMs are public properties that relate to an aircrafts range, according to the Breguet Range Equation shown in Equation 27.

$$Range = \frac{V(L/D)}{g} * \frac{1}{SFC} * ln\frac{W_{takeoff}}{W_{empty}} \tag{27}$$

According to Equation 27, range is maximized at high velocity, high lift-to-drag ratio, low specific fuel consumption, and high mass fraction. Each of these TPMs can be adjusted by up to 20% in the TTT quick look model to investigate the performance of future aircraft designs which incorporate improved technology. Each TPM can be adjusted independently, which enables investigation of the aircraft designs sensitivity to a change in that TPM.

When examined in combination with each other, the TPMs can be linked to mission success, which is recorded using Measures of Effectiveness (MOEs). The purpose of an MOE is to measure how well the tactical tanker performs its mission. The seven MOEs listed below investigate the tactical tanker's own performance as well as its impact on the performance of the fighters it is tasked to support in either offensive or defensive missions.

OCA CAP Effectiveness - see Equation 83

- Ratio of the fighter's distance away from the tactical tanker and traditional tanker

OCA CAP Penetration Effectiveness - see Equation 84

- Ratio of the fighter's penetration radius with and without the tactical tanker

OCA Tactical Tanker Fuel Effectiveness - see Equation 85

- Ratio of the tactical tanker's offloaded and burned fuel

DCA CAP Loiter Effectiveness - see Equation 118

- Ratio of the fighter's loiter time with and without the tactical tanker.

DCA CAP Loiter Percent Effectiveness - see Equation 119

- Ratio of the fighter's percentage time spent at the loiter point with and without the tactical tanker

DCA Tactical Tanker Effectiveness - see Equation 120

- Ratio of the tactical tanker's fuel offloaded to fuel loaded from the traditional tanker

DCA Tactical Tanker Fuel Effectiveness - see Equation 121

- Ratio of the tactical tanker's fuel offloaded to fuel burned

See Chapter IV for in-depth discussion of MOE values and their importance.

3.5 Sensitivity Analysis

Sensitivity analysis was conducted using a forward-step finite difference method with step size of 0.1%, described in Chapter II and shown in Equations 28 and 29.

$$\nabla y(x) = \frac{y(x + \Delta x) - y(x)}{\Delta x} + O(\Delta x) \tag{28}$$

Sensitivities of each MOE were found with respect to the five TPM changes. This process finds the sensitivity of MOE_i to a change in TPM_j by comparing the MOE

response at an initial and perturbed TPM value.

$$\frac{\partial MOE_i}{\partial TPM_j} \approx \frac{MOE_i(TPM_j + \Delta TPM_j) - MOE_i(TPM_j)}{\Delta TPM_j} \tag{29}$$

Raw sensitivities were normalized to one according to Equation 30 so the relative importance of each TPM could be compared and analyzed.

$$Sensitivity_{norm} = \frac{\dfrac{\partial MOE_i}{\partial TPM_1}}{\dfrac{\partial MOE_i}{\partial TPM_1} + \dfrac{\partial MOE_i}{\partial TPM_2} + \dfrac{\partial MOE_i}{\partial TPM_3} + \dfrac{\partial MOE_i}{\partial TPM_4} + \dfrac{\partial MOE_i}{\partial TPM_5}} \tag{30}$$

This equation normalizes the sensitivity of MOE_i to the first of five TPM variables.

3.6 Design of Experiments

The full factorial trade space includes five levels and five factors for a total of 3125 cases. The five factors are technology changes in SFC, L/D, mass fraction, fuel payload, and proximity. The five levels represent the technology change magnitudes: -20%, -10%, unchanged, +10%, and +20%. These levels include technology improvements as well as detriments. SFC can be improved by incorporating more efficient engines. Lift to drag ratio can be improved by using higher aspect ratio wings or reducing drag. Mass fraction could be improved by maximizing the use of lightweight composite materials. Proximity could be improved by incorporating technologies which enable the tactical tanker to operate closer to contested airspace. Note that for some factors, a technology improvement is a reduction in a particular metric. For example, engine efficiency improves as SFC decreases. Technology detriments were included in the full factorial trade space because of potential interactions between

factors. For example, an engine with improved SFC may weigh more than a baseline engine, which has a negative effect on mass fraction.

IV. Results

4.1 Baseline Aircraft Design

A plot of thrust to weight ratio vs. wing loading, was used to select the baseline tactical tanker's design point, which is marked by the red dot shown in Figure 10. The chosen design point lies just above the takeoff constraint line, and left of the landing constraint. The design point's location was not placed directly on either constraint according to recommendations by Raymer [25]. If the aircraft is designed with no growth margin, then any weight increase in the preliminary or detailed design phase may push the aircraft across a constraint, and into the infeasible design region.

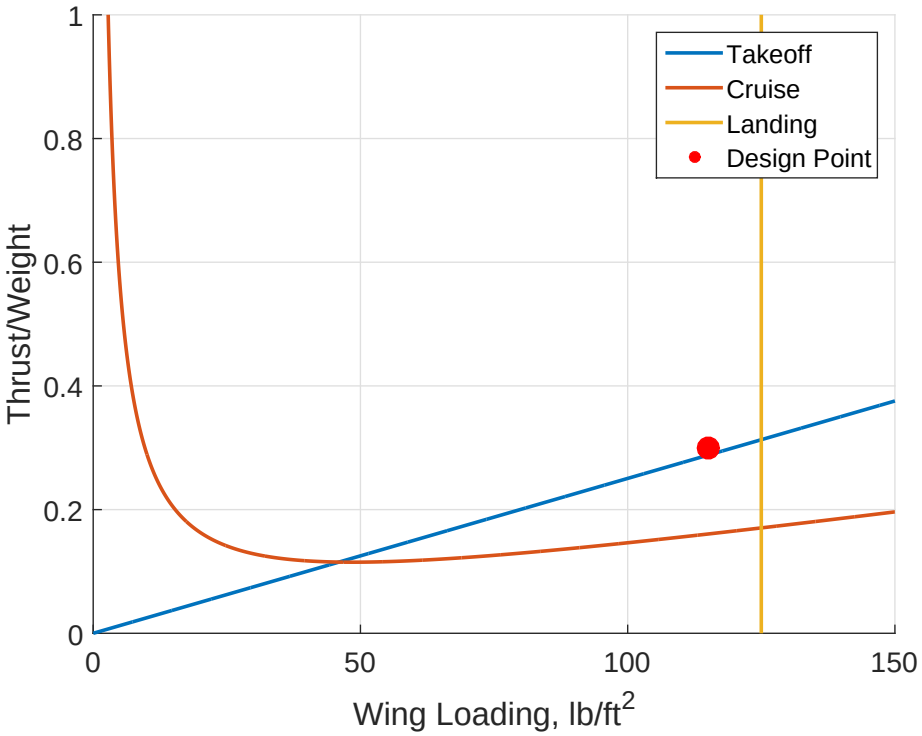

Figure 10. Design point on T/W vs. W/S plot.

The baseline tactical tanker aircraft has parameters shown in Table 4, which were found using the methodology, constraints, and historical trends shown in Figure 10 [25]. These values are independent of fuel payload.

Table 4. Tactical Tanker Design Point

Parameter	Baseline
SFC, 1/hr	0.572
L/D	16.0
T/W ratio	0.3
Wing Loading, lb/ft^2	115

Mass fraction, Gross Takeoff Weight (GTOW), and Fuel Burn Rate are all impacted by fuel payload. GTOW consists of two constituent parts: fuel weight and non-fuel weight. Non-fuel weight includes crew, structures, systems, and other permanent items. Mass fraction is the proportion of GTOW devoted to non-fuel weight. Equation 31 shows the relationship between GTOW, fuel, and mass fraction.

$$GTOW = \frac{TotalFuel}{1 - MassFraction} \tag{31}$$

Figure 11 shows a semi-logarithmic plot of mass fraction vs. fuel weight for fuel payloads between 25000 lb and 100000 lb. Mass fraction decreases as fuel payload increases. This downward trend, with values between 0.41 and 0.47, matches what's expected for aircraft of the tactical tanker's size class.

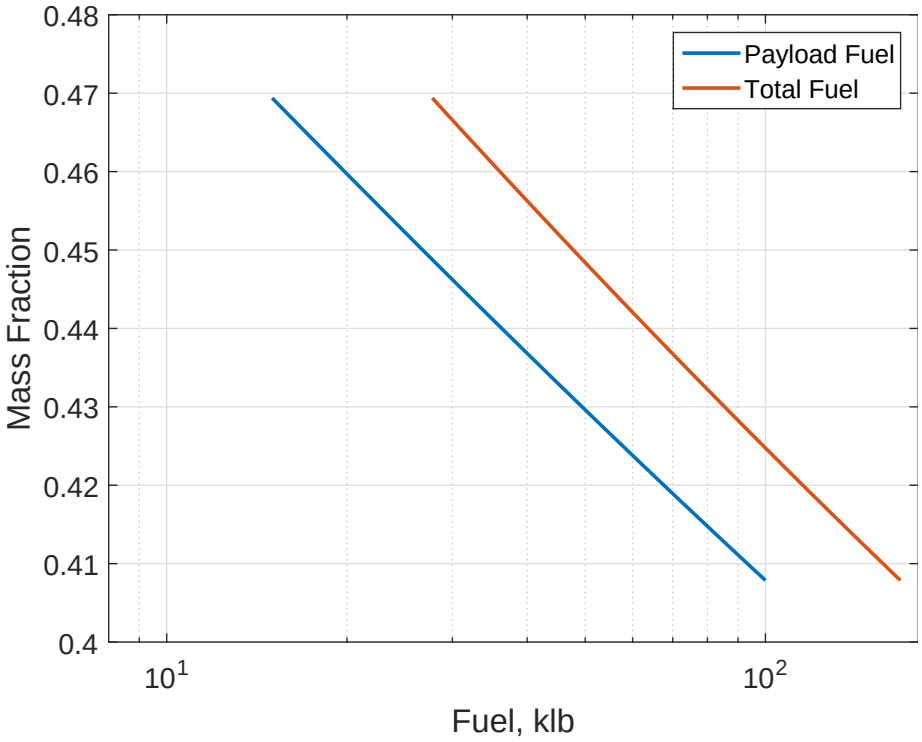

Figure 11. Semi-logarithmic plot of Mass Fraction vs. Fuel.

Figure 12 shows the relationship between GTOW and fuel weight for payloads between 25000 lb and 100000 lb. This figure also depicts the relationship between payload fuel and total fuel. Payload fuel is fuel designated to be offloaded to receiver aircraft, and total fuel is the sum of payload fuel and fuel required to fly. To determine total fuel from a given payload fuel, slide horizontally to the total fuel line, then read the corresponding fuel value off the x-axis. For example, a 50000 lb fuel payload corresponds to 86400 lb of total fuel, a 151600 lb GTOW, and 0.430 mass fraction.

Although the two fuel categories are displayed separately, modern tankers have sophisticated fuel management systems which enable them to move fuel between different locations. If the tactical tanker required less fuel for its own consumption, then the excess fuel could be transferred to receiver aircraft.

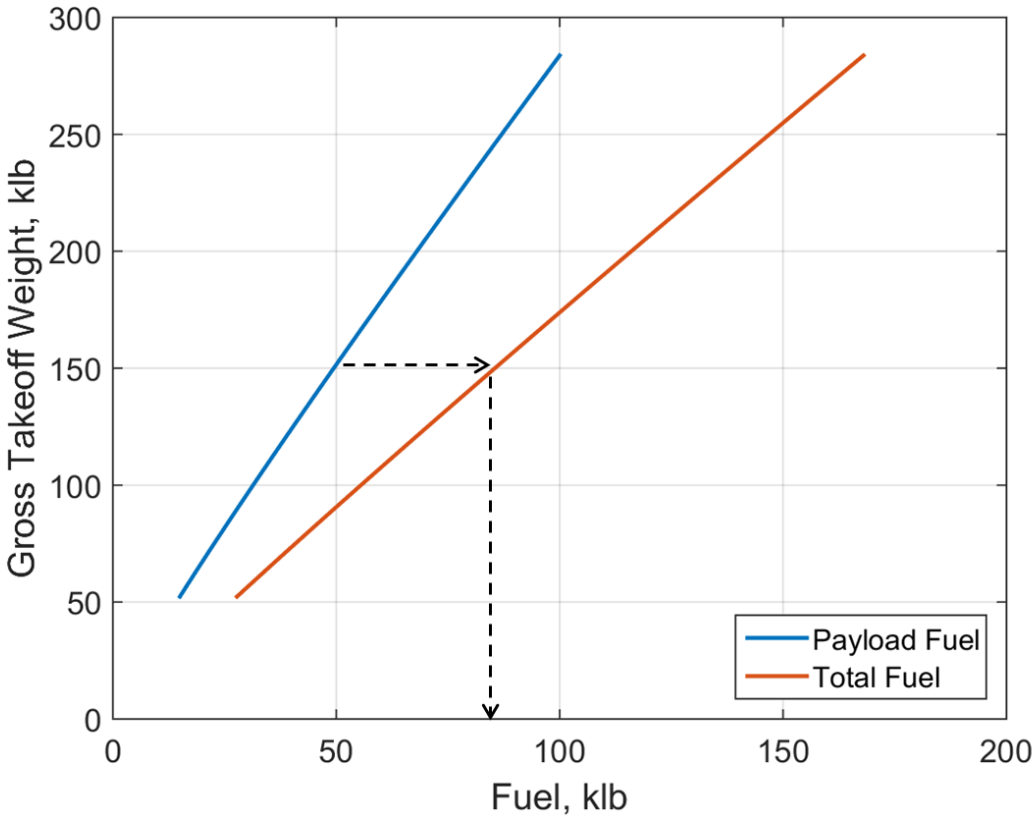

Figure 12. Gross Takeoff Weight vs. Fuel.

Figure 13 displays the same GTOW vs. total fuel line shown previously. This plot adds data points from existing traditional tankers to validate the design technique. The KC-135, KC-46, and KC-10 lie near the extrapolated line.

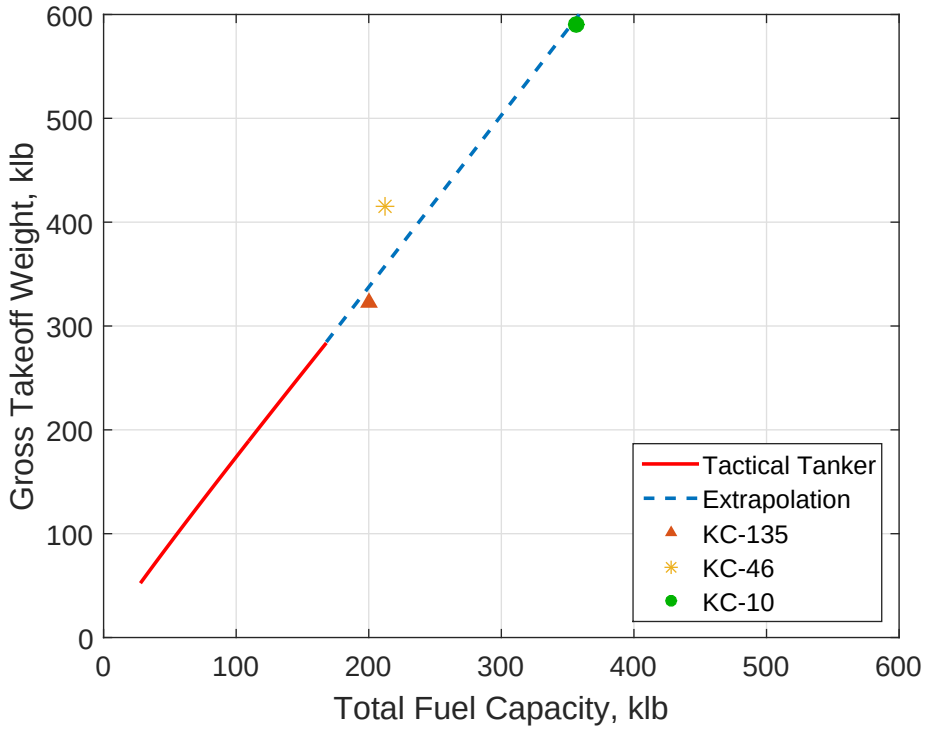

Figure 13. Comparison of Tactical Tanker, KC-135, KC-46, and KC-10 weights and fuel quantities.

Equation 32 shows that fuel burn rate increases with fuel capacity. This relationship is shown graphically in Figure 14, and provides a useful baseline for understanding the MOEs and TPM changes discussed below.

$$TactTankerFBR = \frac{FuelCapacity * SFC}{60 * L/D * \ln(1/massfraction)} \tag{32}$$

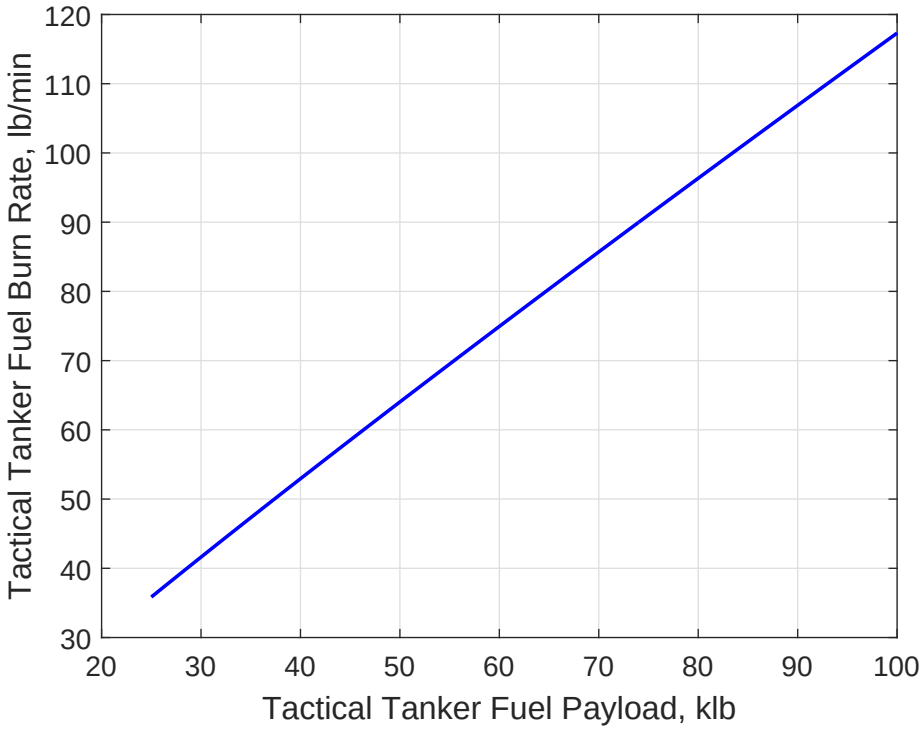

Figure 14. Tactical Tanker Fuel Burn Rate vs. Fuel Payload.

4.2 Measures of Effectiveness

The tactical tanker design parameters described above were input into the TTT quick look model, and the MOEs were calculated for three distinct scenarios. The distance from the base to the traditional tanker orbit is constant for all three scenarios, as shown in Table 5. The baseline distance between the tactical tanker and contested airspace is fixed at 100 nautical miles for finding the MOEs, because technology changes were not part of the MOE investigation. The distance between the traditional tanker and tactical tanker was varied from 100 to 300 nautical miles as another means of examining the model.

Table 5. Scenario Distances.

Mission Leg	Scenario 1	Scenario 2	Scenario 3
Base to Traditional Tanker, NM	300	300	300
Traditional Tanker to Tactical Tanker, NM	100	200	300
Tactical Tanker to Contested Airspace, NM	100	100	100

Figures 15 to 20 below show MOE values for each scenario plotted as a function of tactical tanker fuel payload. MOEs for fighters performing DCA missions are shown first, followed by fighters performing OCA.

4.2.1 Defensive Counterair

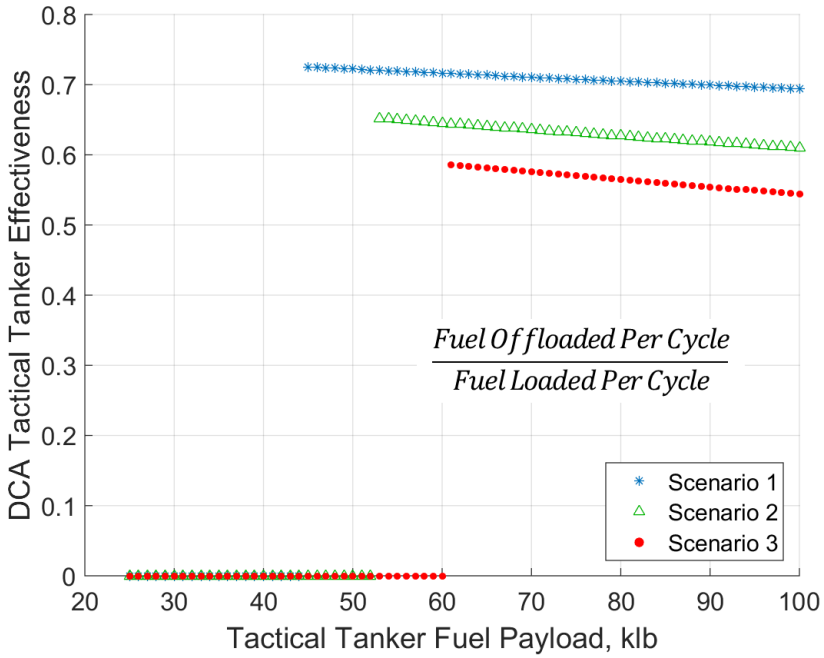

Figure 15. DCA Scenarios: DCA Tactical Tanker Effectiveness vs. Tactical Tanker Fuel Payload.

Figure 15 plots DCA Tactical Tanker Effectiveness against tactical tanker fuel payload for each scenario. This MOE, calculated in Equation 120, is the amount of

fuel offloaded to fighters each cycle divided by the amount the tactical tanker receives from the traditional tanker each cycle. This MOE is equal to zero when the tactical tanker cannot give the fighters enough fuel to conduct a complete loiter cycle. The amount of fuel each fighter needs for a full loiter cycle is constant; they are limited by their own fuel tank size. Therefore, the numerator is a constant when the tactical tanker can support a full loiter cycle.

In Scenario 1, the tactical tanker MOE peaks at 0.725 at 45000 lb fuel payload. This MOE value means the tactical tanker oggloads about 72.5% of the fuel it loads from the traditional tanker. The tactical tanker continues to provide the same amount of fuel to the fighters at higher fuel payloads, but becomes less effective due to increased fuel burn which accompanies the larger aircraft size. The other two scenarios show similar trends. In Scenario 2, the MOE peaks at 0.652 with a 53000 lb fuel payload. Scenario 3 peaks at 0.586 at 61000 lb. Tanker effectiveness decreases across the scenarios due to the increased distance between the two tanker types.

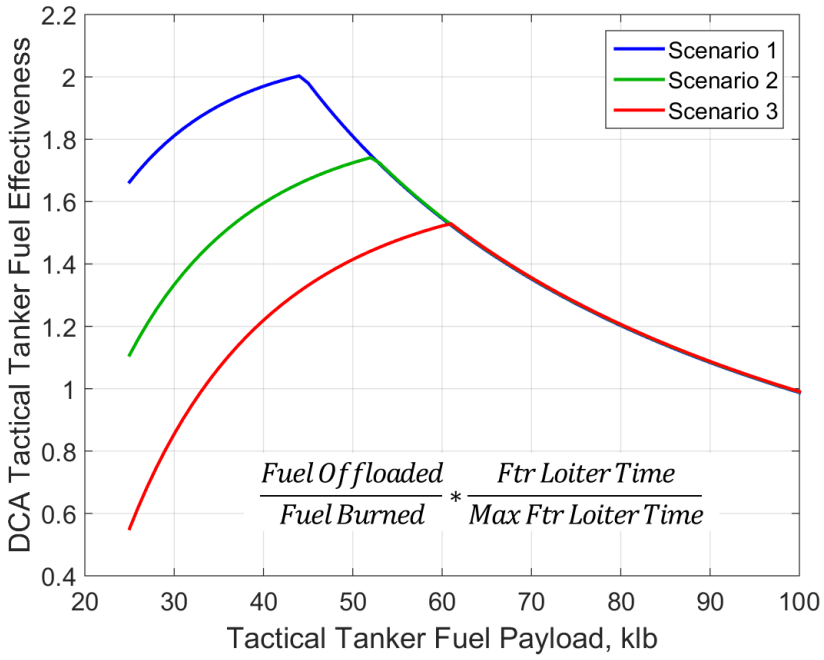

Figure 16. DCA Scenarios: Tactical Tanker Fuel Effectiveness vs. Tactical Tanker Fuel Payload.

In Figure 16, the DCA Tactical Tanker fuel Effectiveness MOE is plotted against fuel payload. This MOE, previously shown in Equation 121, is found by the ratio of fuel offloaded to fuel burned, and is then multiplied by a loiter time factor. The loiter time factor is necessary to create conditions for an optimum design point. Without this correction factor, the MOE would call for the smallest possible tactical tanker size because it could offload all of its available fuel and have a low fuel burn rate. This correction factor is less than one when the fighter cannot achieve a full loiter cycle, and is equal to one when it can perform the maximum length loiter cycle. Peaks occur at the same fuel payloads described above for the Tactical Tanker Effectiveness MOE. The same sizing trend appears for this MOE; tactical tankers larger than necessary to support exactly one fighter loiter cycle are carrying excess fuel.

The MOE values for each scenario overlap once the tactical tanker is large enough to support a full fighter loiter cycle. This occurs because the fuel offloaded and fuel burned are equal across each scenario. The amount of fuel burned depends only on fuel burn rate and mission duration. Since the mission duration is capped at exactly 8 hours regardless of scenario, the fuel burned is constant.

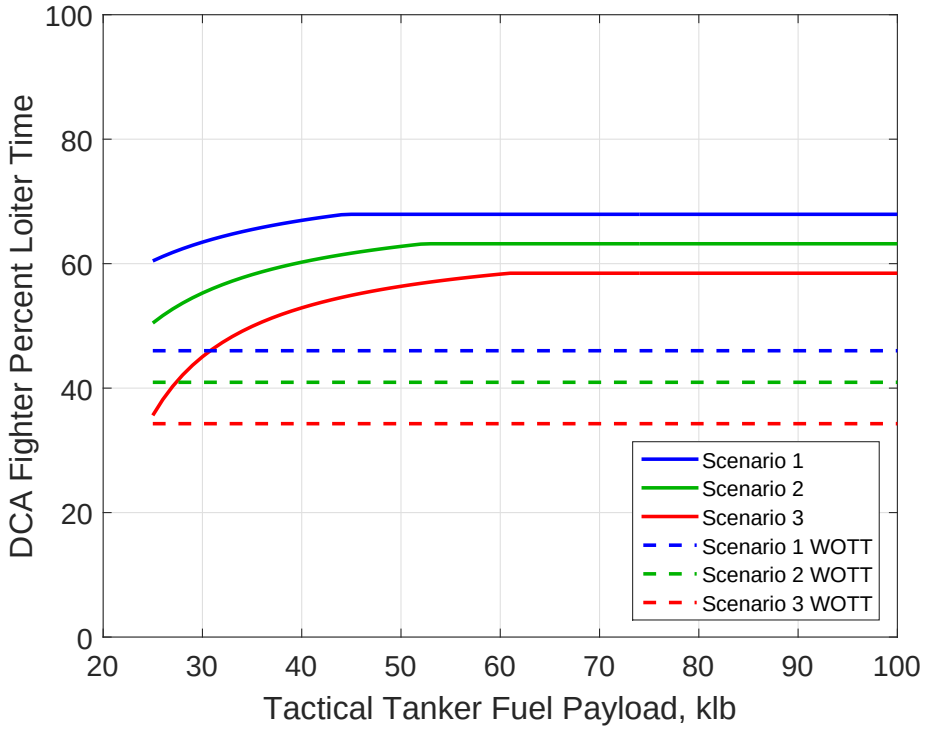

Figure 17. DCA Scenarios: Fighter Percent Loiter Time with and without Tactical Tanker vs. Tactical Tanker Fuel Payload.

Figure 17 graphs the percentage time the fighter spends at the loiter location as a function of tactical tanker fuel payload, and introduces a comparison between the presence and absence of the tactical tanker. The solid lines show the fighter's performance in each scenario when supported by the tactical tanker. Dashed lines show the fighter's performance without the tactical tanker (WOTT). As in the previous two plots, the tactical tanker fully fills the fighter's fuel tanks at 45000 lb, 53000 lb, and 61000 lb, in the respective scenarios. Loiter time percentage is the time spent at the loiter point divided by the total time the fighter can fly before needing to refuel. At the Mach numbers and altitudes specified in the model, the fighters can fly for 173 minutes before consuming their reserve fuel.

If the tactical tanker could orbit directly over the loiter point, then the fighters could spend this entire time at the loiter point, and the percentage would approach 100%. In Scenario 1, the fighters spend up to 68% of their cycle time loitering,

compared with 46% without the tactical tanker. This 48% increase corresponds to an extra 37.9 minutes on station for every refueling cycle. The fighters loiter at 36000 ft altitude to decrease their fuel burn. Table 6 includes these values as well as corresponding values for the other scenarios.

Table 6. Tactical Tanker Impact on Fighter Loiter Performance.

	% Loiter WOTT	% Loiter	% Increase	Time Increase, min
Scenario 1	46	68	48	37.9
Scenario 2	41	63	54	38.5
Scenario 3	34	58	71	41.8

Table 6 presents three potential benefits to the tactical tanker's presence. First, a given number of fighters spend a greater proportion of their flight time where they are needed. Second, an equivalent temporal presence at the loiter point can be achieved with fewer fighter aircraft, which permits the other fighters to conduct different missions. Third, the tactical tanker's beneficial impact increases as the distance between the traditional and tactical tankers increases.

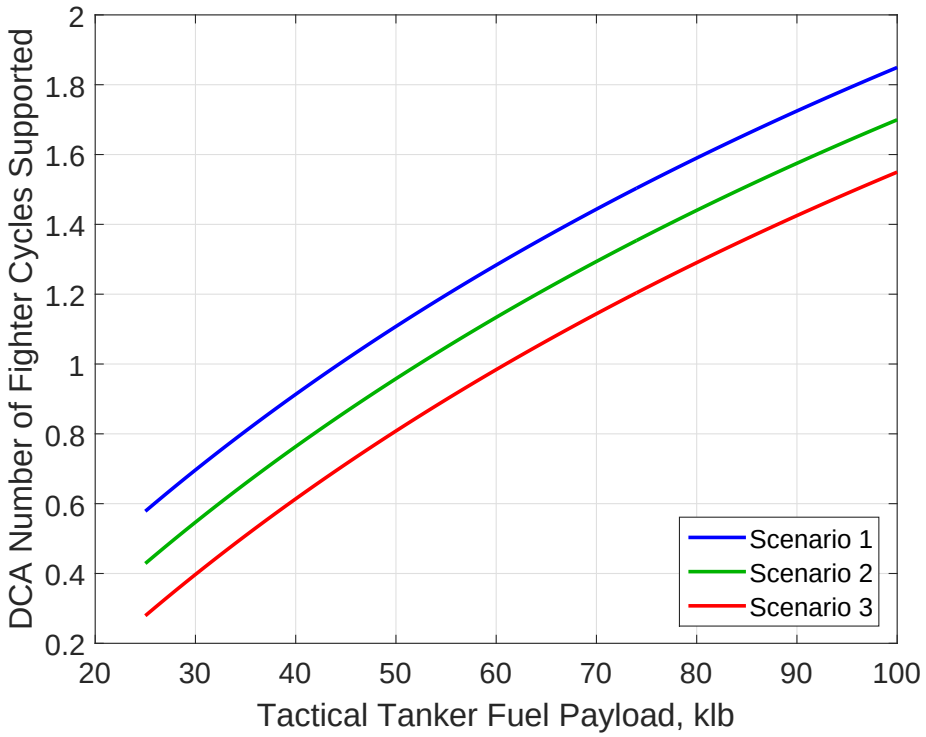

Figure 18. DCA Scenarios: Number of Fighter Cycles Supported vs. Tactical Tanker Fuel Payload.

Figure 18 shows the number of fighter cycles the tactical tanker can support at each fuel payload before needing to refuel from the traditional tanker. The tactical tanker must always have enough fuel to return to the traditional tanker, as well as not consume any of its 10% reserve. This requirement to keep enough fuel for the return trip is the driver behind the differences between each scenario. As previously discussed, the tactical tanker can support a complete fighter loiter cycle at 45000 lb, 53000 lb, and 61000 lb in the respective scenarios. The slope of each curve is steeper on the left side of the plot than on the right. This slope difference indicate the incremental improvement in cycle support for a given fuel payload increase is greater at smaller fuel payloads. When the number of fighter cycles supported is less than one, the fighters receive as much fuel as the tanker can safely give, then execute their loiter segment. Meanwhile, the tactical tanker returns to the traditional tanker

to refuel. For extremely small (less than 25000 lb fuel payload) tactical tankers, the fuel offloaded to the fighters may not be enough to cover the time the tactical tanker requires to cruise to and from the traditional tanker's position, and the mission may collapse. Also, it is important to note that this plot assumes a 4:1 ratio of fighters for each tactical tanker. The DCA MOE values will change if the tactical tanker must support more fighters, meaning the ideal fuel payloads discussed in this section may change.

4.2.2 Offensive Counterair

Figure 19 shows the fighter's penetration radius as a function of tactical tanker fuel payload. Solid lines on the plot represent the three scenarios with the tactical tanker present. Dashed lines show fighter performance without the tactical tanker.

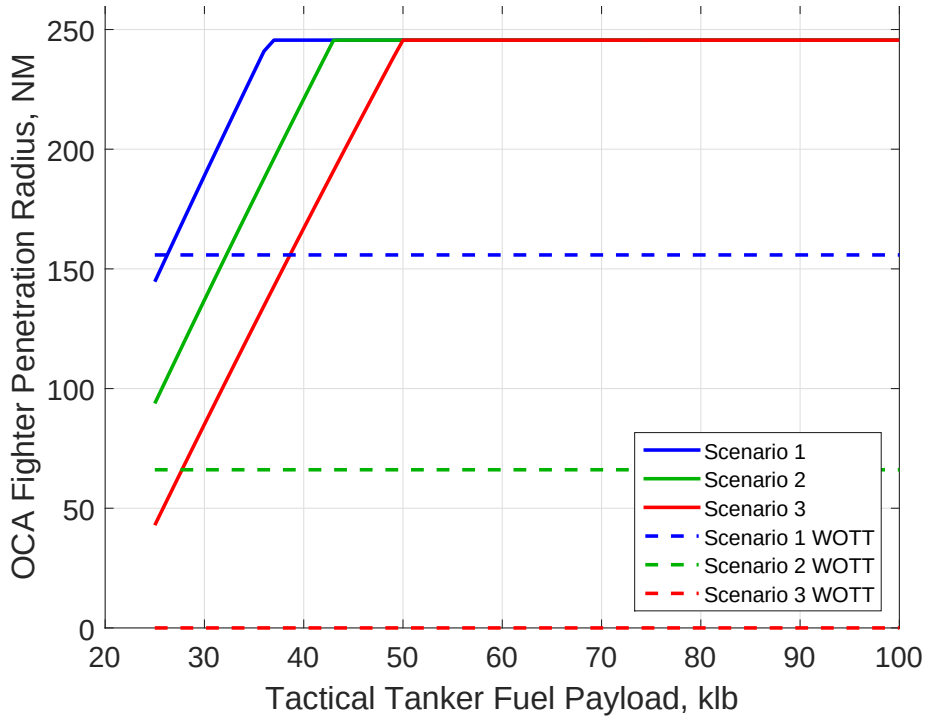

Figure 19. OCA Scenarios: Fighter Penetration Radius with and without Tactical Tanker vs. Tactical Tanker Fuel Payload.

Maximum penetration radius for each scenario occurs when the fighter departs

the tactical tanker with full fuel tanks. Penetration radius is therefore the distance the fighter can fly away from the tanker, minus the distance between the tanker and ingress point; the distance between the tactical tanker and ingress point is not counted towards penetration radius. In Scenario 3, for example, the fighter has zero penetration radius because of the 300 NM distance between the two types of tankers. The ingress point marks the point where the fighter increases speed and begins its offensive mission. This fuel level is achieved in each scenario at 37000 lb, 44000 lb, and 50000 lb, respectively. Table 7 summarizes the differences between the scenarios. All distances are measured in nautical miles.

Table 7. Tactical Tanker Impact on Fighter Penetration Performance.

	Pen Radius WOTT	**Pen Radius**	**% Increase**	**Distance Increase**
Scenario 1	155.8	245.6	57.6	89.8
Scenario 2	66.1	245.6	271.6	179.5
Scenario 3	0	245.6	-	245.6

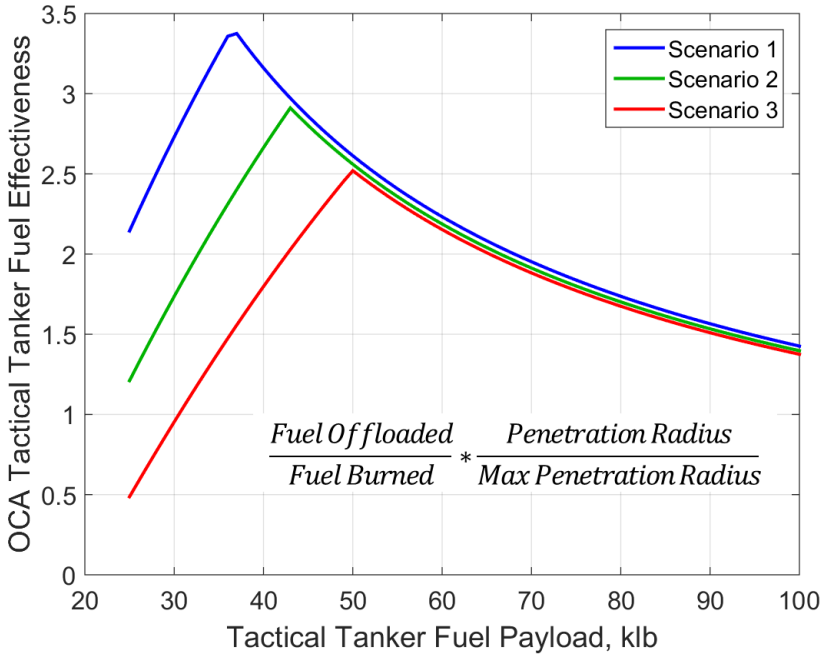

Figure 20. OCA Scenarios: Tactical Tanker Fuel Effectiveness vs. Tactical Tanker Fuel Payload.

Finally, Tactical Tanker Fuel Effectiveness is shown in Figure 20 plotted against tactical tanker fuel payload. Like the DCA Tactical Tanker Fuel Effectiveness MOE, this MOE is the ratio of fuel offloaded to fuel burned, multiplied by a correction factor. In this case, the correction factor equals the ratio of achieved penetration radius to the maximum possible penetration radius. It equals one when the fighter leaves the tactical tanker with full fuel tanks, and less than one when the tanks are not full. The MOE peaks at the fuel payloads listed above, where the tactical tanker can fill the fighter's fuel tanks, but is not encumbered by the higher fuel burn rate that accompanies larger fuel payloads.

Unlike the analogous plot for the DCA case, the MOE curves do not overlap at higher fuel payloads. The difference in mission duration between the OCA and DCA cases drives this disparity. On DCA sorties, the mission duration always equals the peak value of 8 hours because the fighters need to be on station as long as possible.

On OCA sorties, the mission ends once the fighter crosses back over the ingress point on the return leg. The total distance covered differs between the three scenarios, so the amount of fuel burned also differs, despite the fuel burn rate being the same. Scenario 1 has a slightly higher MOE because it lasts 26 minutes less than Scenario 2, and 52 minutes less than Scenario 3.

4.3 Sensitivity Analysis

MOE plots were shown at varying fuel payloads to find the ideal fuel payload for each mission type and scenario. All MOE values were computed using the baseline tactical tanker configuration. Sensitivity analysis can recalculate these MOEs based on small differences in the five TPMs: L/D, SFC, mass fraction, proximity, and fuel payload. The sensitivity of each MOE can be plotted at various fuel payloads to determine which technologies have the biggest impact on effectiveness.

Sensitivity plots are shown here only for Scenario 1. Similar plots for Scenarios 2 and 3 are shown in Appendix A.

4.3.1 Defensive Counterair

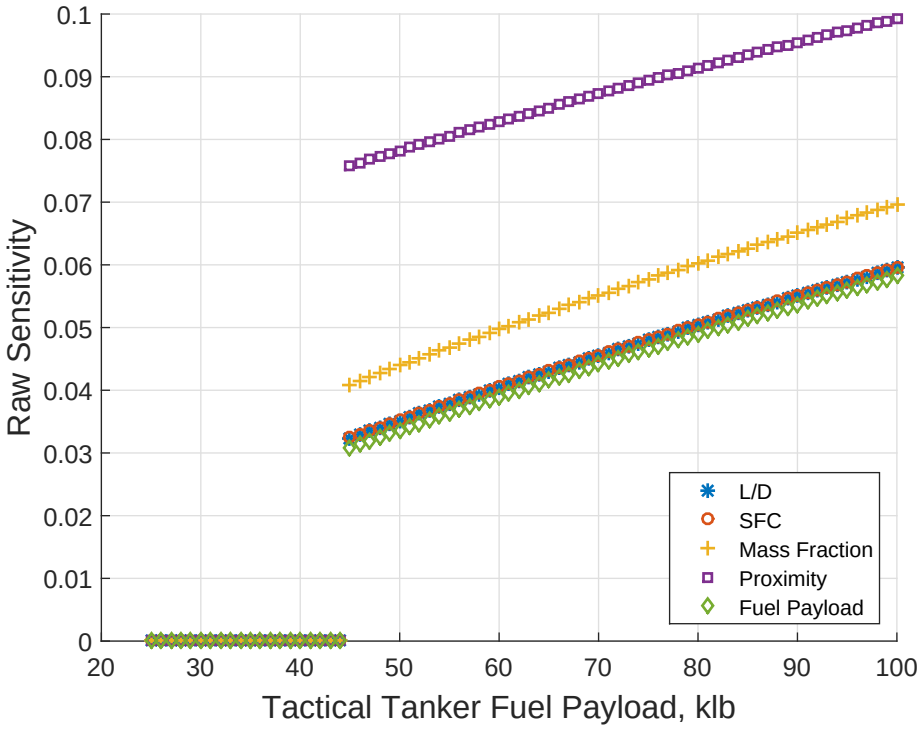

Figure 21. DCA Scenario 1: Sensitivity of Tactical Tanker Effectiveness at varying tactical tanker fuel payloads.

Figure 21 shows the sensitivity of DCA Tactical Tanker Effectiveness to changes in the five TPMs. This MOE is calculated by the amount of fuel offloaded per cycle divided by the amount of fuel the tactical tanker loads from the traditional tanker, as shown in Equation 33.

$$DCATactTankerEffectiveness = \frac{DCATactTankerFuelOffloadedPerTankerCycle}{DCATactTankerFuelLoadedfromTradTanker} \quad (33)$$

This MOE is most sensitive to changes in proximity, followed by mass fraction, then L/D and SFC, then fuel payload. The sensitivity to L/D and SFC are identical

because they are both equally important factors in determining the tanker's fuel burn rate. Mass fraction has slightly higher sensitivity because of the natural log term in the fuel burn rate equation. When examining why the MOE is so sensitive to proximity, it is important to recall that the finite difference method uses a forward step, which increases the TPM. An increase in the proximity TPM is a detriment; it forces the tactical tanker to orbit farther away than the original position. This MOE is highly sensitive to proximity because increasing the proximity TPM forces the tactical tanker to onload more fuel from the traditional tanker.

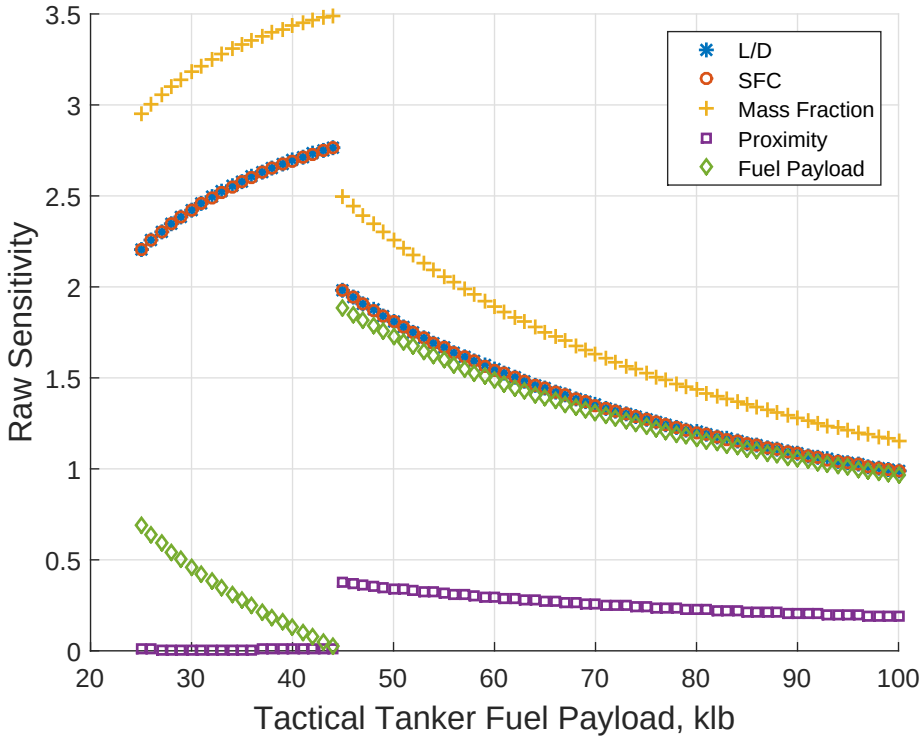

Figure 22. DCA Scenario 1: Sensitivity of Tactical Tanker Fuel Effectiveness at varying tactical tanker fuel payloads.

The sensitivity of DCA Tactical Tanker Fuel Effectiveness is shown in Figure 22 and the MOE is described by Equation 34.

$$DCATactTankerFuelEffectiveness = \frac{DCATactTankerFuelOffloadedPerMission}{DCATactTankerFuelBurnedPerMission} * \frac{DCAFtrLoiterTime}{DCAFtrLoiterTime_{max}} \quad (34)$$

For all fuel payloads, this MOE is least sensitive to proximity changes. A discontinuity appears at 45000 lb because the tactical tanker can thereafter support a full fighter loiter cycle. On the left side of the discontinuity, the sensitivity to mass fraction, L/D, and SFC increases as the sensitivity to fuel payload drops. On the right side of the discontinuity, sensitivities to all five TPMs display a downward trend.

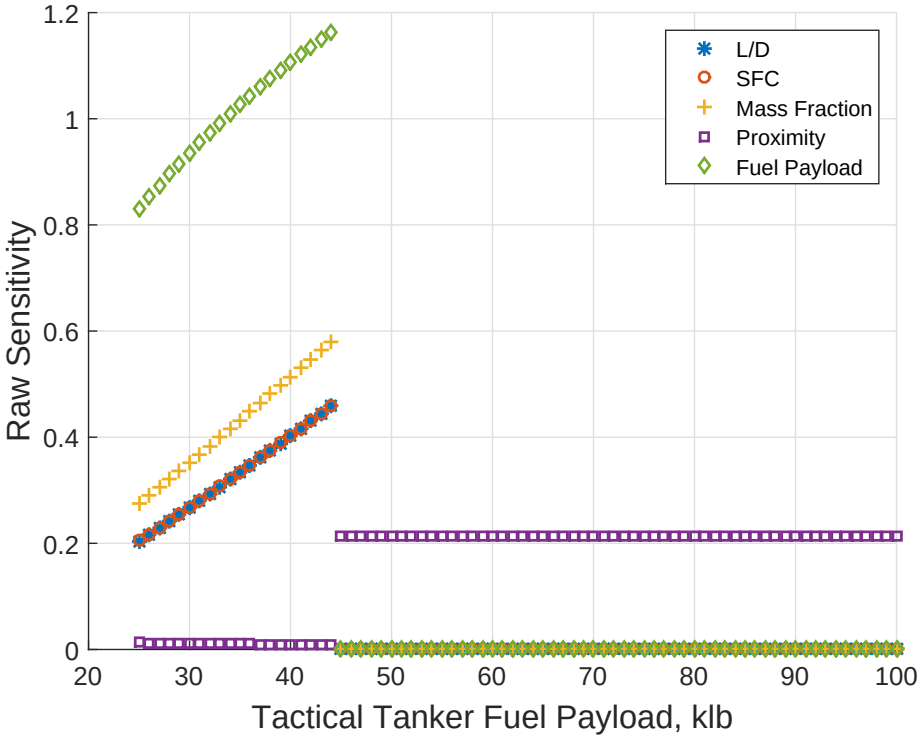

Figure 23. DCA Scenario 1: Sensitivity of CAP Loiter Effectiveness at varying tactical tanker fuel payloads.

Figure 23 shows the sensitivity of CAP Loiter Effectiveness to TPM changes. CAP Loiter Effectiveness is calculated by dividing the fighter's loiter time by the loiter time

achievable without the tactical tanker for each cycle, as shown in Equation 35.

$$DCACAPLoiterEffectiveness = \frac{DCAFtrLoiterTime}{DCAFtrLoiterTimeWOTT} \tag{35}$$

This MOE is sensitive to four of the TPMs beneath the critical 45000 lb fuel payload, because of the affect these TPMs have on the tanker's fuel burn rate. A decrease in fuel burn rate enables the fighters to receive more fuel than they otherwise would have received. Fuel payload has the highest sensitivity in this region because it impacts both fuel burn rate and the fuel quantity available to offload. Mass fraction, L/D, and SFC, on the other hand, only impact the fuel burn rate. The fighter has a full fuel tank above 45000 lb fuel payload, so a technological change in tactical tanker fuel burn rate or fuel payload does not have a corresponding performance impact. Only a change in the proximity of the tactical tanker to the contested airspace has an impact in this region, because a change in tactical tanker location will alter the distance the fighter must travel to refuel.

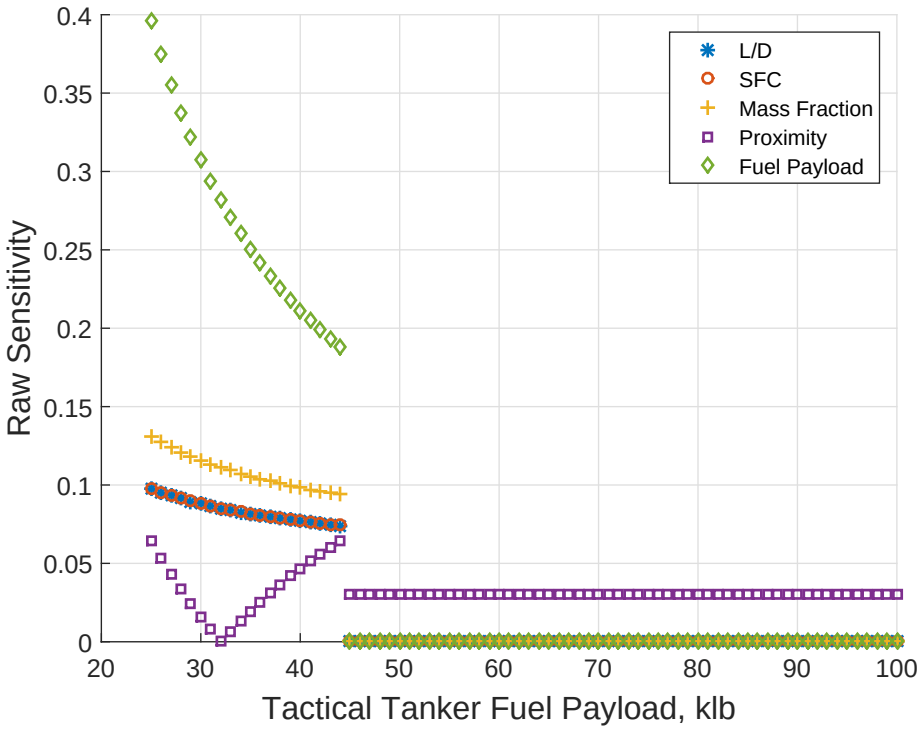

Figure 24. DCA Scenario 1: Sensitivity of CAP Loiter Percent Effectiveness at varying tactical tanker fuel payloads.

Figure 24 shows the sensitivity of CAP Loiter Percent Effectiveness to TPM changes. CAP Loiter Percent Effectiveness, shown in Equation 36 differs from CAP Loiter Effectiveness because it is calculated using percentages of achievable loiter time, not the actual loiter time value in minutes. CAP Loiter Percent Effectiveness describes the fighter's effectiveness over the entire mission duration, while CAP Loiter Effectiveness measures their effectiveness on each cycle. The denominator is constant for each scenario, meaning the sensitivity is driven by the percentage time the fighters spend loitering over their target.

$$DCACAPLoiterPercentEffectiveness = \frac{DCAFtrPctLoiterTime}{DCAFtrPctLoiterTimeWOTT} \quad (36)$$

The MOE is sensitive to all TPMs below the 45000 lb fuel cutoff, and thereafter

displays sensitivity only to proximity changes. On the left side of the discontinuity, the MOE's sensitivity to fuel payload decreases rapidly. This drop occurs because the tactical tanker provides the highest relative benefit at small fuel payloads when compared to a mission flown with only a traditional tanker. The sensitivity to changes in the proximity TPM decreases to nearly zero at 32000 lb fuel payload before increasing.

4.3.2 Offensive Counterair

When examining sensitivities to TPM changes for the OCA MOEs, recall that the baseline tactical tanker configuration could maximize fighter penetration range at fuel payloads of 37000 lb or higher.

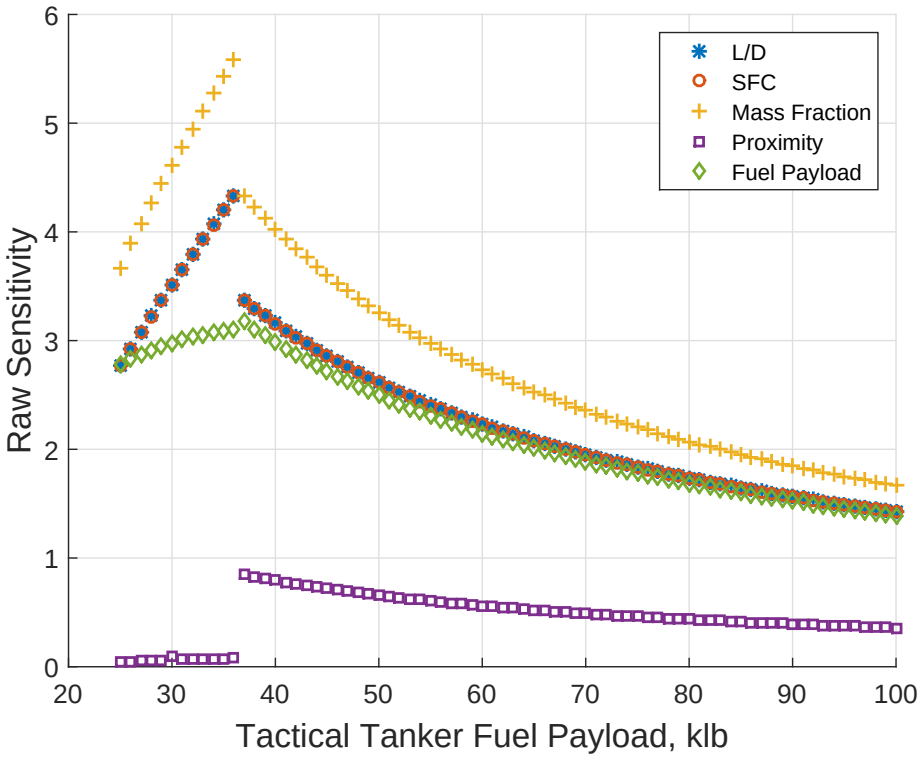

Figure 25. OCA Scenario 1: Sensitivity of Tactical Tanker Fuel Effectiveness at varying tactical tanker fuel payloads.

Figure 25 depicts the sensitivity of Tactical Tanker Fuel Effectiveness to TPM changes. This MOE is the ratio of fuel offloaded to fuel burned, multiplied by a

penetration radius correction factor, as shown in Equation 37.

$$OCATactTankerFuelEffectiveness = \frac{OCATactTankerFuelOffloaded}{OCATactTankerFuelBurned} * \frac{OCAFtrPenetrationRadius}{OCAFtrPenetrationRadius_{max}} \quad (37)$$

This MOE is sensitive to all TPMs at all fuel payloads, but displays a change in behavior near the 37000 lb critical fuel payload. Beneath 37000 lb, the tactical tanker cannot support the maximum penetration radius. At these small fuel payloads, the MOE is highly sensitive to changes in mass fraction, L/D, SFC, and fuel payload. Approaching 37000 lb, the penetration radius correction factor levels off at one, which explains the decreasing trend in fuel payload sensitivity. At higher fuel payloads, mass fraction, SFC, and L/D display roughly similar behavior because of their effect on tactical tanker fuel burn rate. The MOE is least sensitive to proximity changes at all fuel payloads, however the sensitivity is higher when the tactical tanker can fully fill the fighter's fuel tanks.

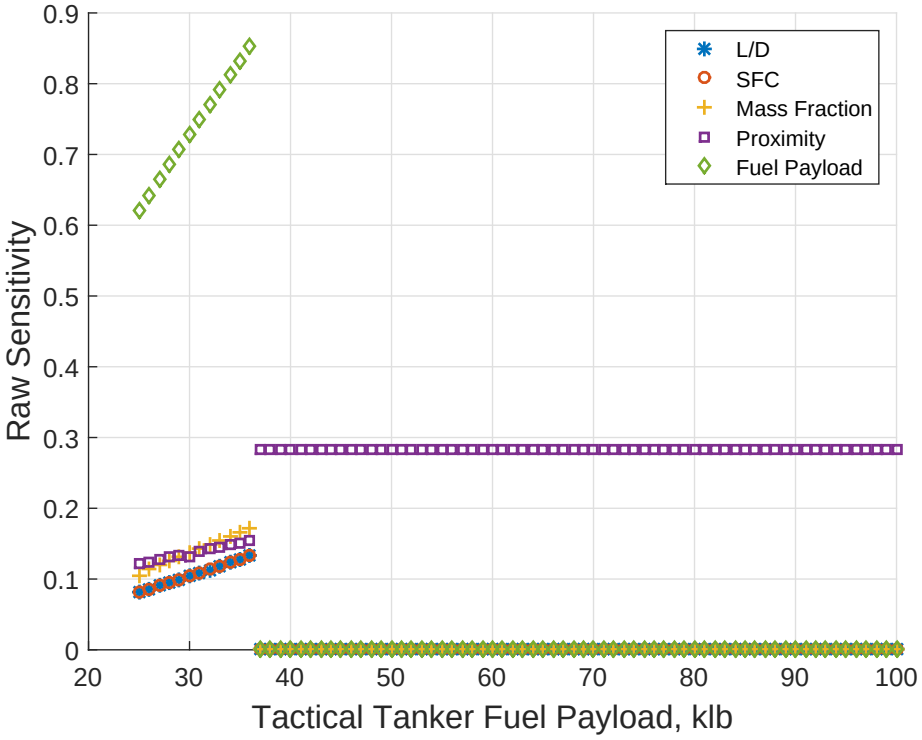

Figure 26. OCA Scenario 1: Sensitivity of CAP Effectiveness at varying tactical tanker fuel payloads.

Figures 26 and 27 show the sensitivity of the OCA CAP Effectiveness and OCA CAP Penetration Effectiveness MOEs. These two MOEs have similar equations, which causes their sensitivity behavior to show similar trends. OCA CAP Penetration Effectiveness is calculated by dividing the fighter's penetration radius by the achievable penetration radius in a scenario without the tactical tanker. OCA CAP Effectiveness finds the same ratio, but uses the fighter's total distance from the traditional tanker instead of solely the penetration radius. Equations for both MOEs are shown below in Equations 38 and 39. Distance from the traditional tanker is the sum of the distance between the traditional and tactical tankers, the distance from the tactical tanker to the ingress point, and the penetration radius.

$$OCACAPEffectiveness = \frac{OCAFtrDistancefromTradTanker}{OCAFtrDistancefromTradTankerWOTT} \quad (38)$$

$$OCACAPPenetrationEffectiveness = \frac{OCAFtrPenetrationRadius}{OCAFtrPenetrationRadiusWOTT} \quad (39)$$

These two figures display sensitivity to all five TPMs below 37000 lb fuel payload, become sensitive only to proximity changes. Fuel payload displays the highest sensitivity below 37000 lb because it has a large impact on the fuel available for offload to the fighter. The fighter's fuel tank is full above 37000 lb, so the only way to change penetration radius is to change the location where the fighters separate from the tactical tanker and begin flying towards the ingress point.

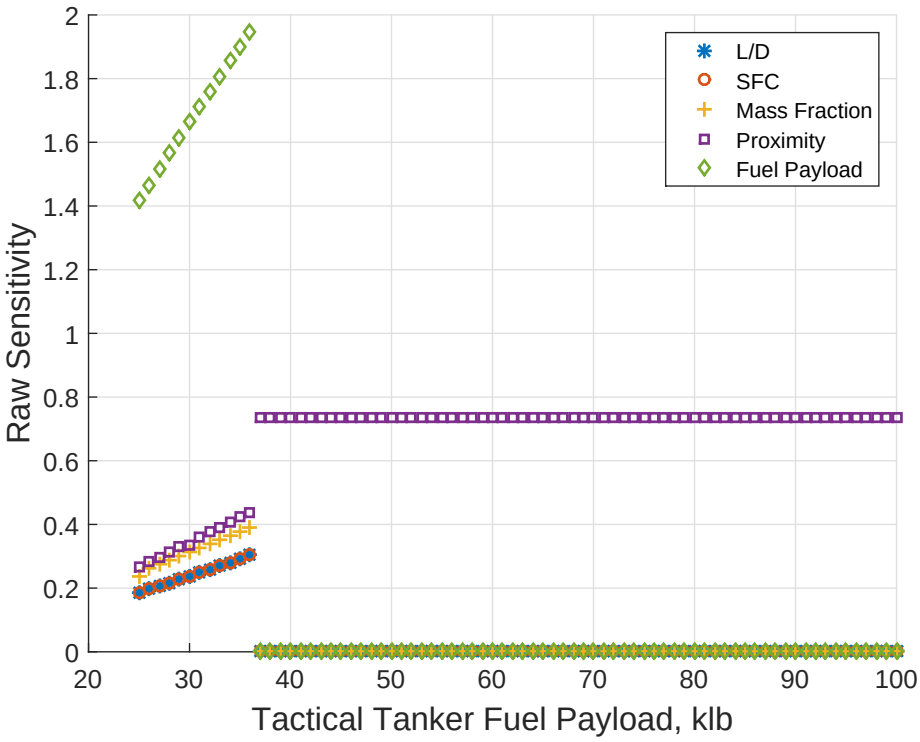

Figure 27. OCA Scenario 1: Sensitivity of CAP Penetration Effectiveness at varying tactical tanker fuel payloads.

4.4 Design of Experiments

A full factorial DOE trade space was conducted for a tactical tanker with a baseline fuel payload of 40000 lb conducting OCA and DCA missions using the distances from Scenario 1. In Scenario 1, the traditional tanker orbits 300 miles from the main operating base and 200 miles from contested airspace. The tactical tanker orbits at 100 miles from contested airspace, halfway between the traditional tanker and the ingress point. The red dot on each plot represents the baseline tactical tanker configuration, which has a 40000 lb fuel payload, 0.437 mass fraction, 100 NM proximity, and unadjusted L/D and SFC. The blue asterisks represent the remaining 3124 design vectors. Baseline and alternate TPM values are shown in Table 8. Full factorial trade spaces for Scenarios 2 and 3 are included in Appendix A.

Table 8. Range of possible TPM values.

Parameter	-20%	-10%	Baseline	+10%	+20%
SFC, 1/hr	0.458	0.515	0.572	0.629	0.686
L/D	12.8	14.4	16.0	17.6	19.2
Mass Fraction	0.365	0.411	0.456	0.502	0.548
Fuel Payload, lb	32000	36000	40000	44000	48000
Proximity, NM	80	90	100	110	120

4.4.1 Offensive Counterair

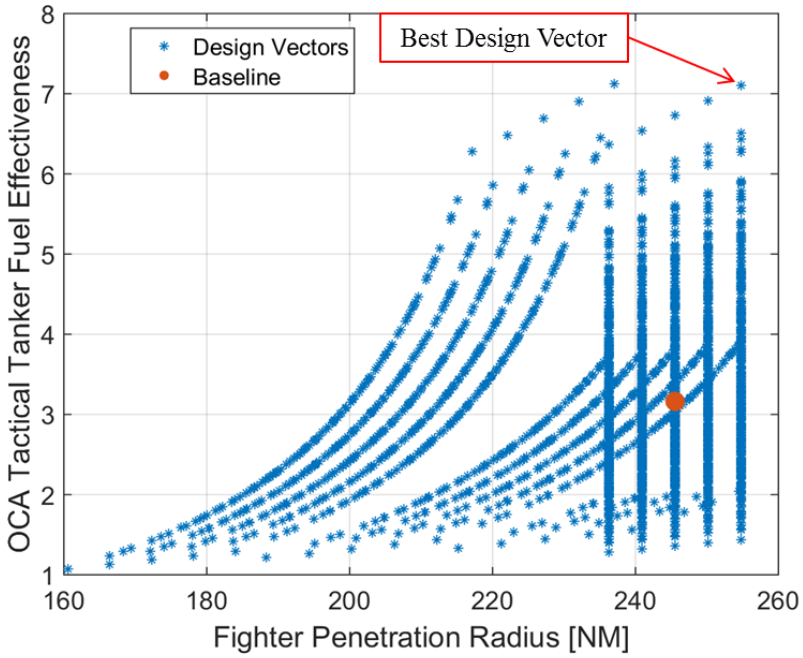

Figure 28. OCA Scenario 1: Full factorial trade space of OCA Tactical Tanker Fuel Effectiveness vs. Penetration Radius at baseline 40000 lb fuel payload.

Figure 28 depicts the full factorial DOE trade space for OCA Tactical Tanker Fuel Effectiveness versus Fighter Penetration Radius. The plot can be broken down into two distinct regions: curved lines and straight lines. The first region includes the curved lines on the plot's left side. Fighters flying with the tactical tanker design vectors in this region are unable to reach the maximum penetration range, which occurs when the fighter departs the tactical tanker with less than full fuel tanks.

These design vectors are unable to fully fuel the fighters because they have either decreased fuel payload or technology detriments which decrease the tactical tanker's fuel consumption or cruise efficiency. Each of the lines represents a different level of the proximity technology, beginning with technology detriments on the left and technology improvements towards the right. The second region includes the five vertical lines on the plot's right side. Like the first region, the five lines show the impact of the five proximity levels. On each of these five lines, the tactical tanker has enough fuel to fully fill the fighter's fuel tanks. Since the fighter's tanks are completely full, the only technology that impacts their penetration radius is the proximity factor. Penetration range increases as the tactical tanker gets closer to the contested airspace.

The best design vectors occur near the plot's top right corner, where both Tactical Tanker Effectiveness and Penetration Range are maximized. Utility is maximized when the tactical tanker is sized to fill the fighter's fuel tanks, with no excess fuel. Excess fuel payload increases the tactical tanker's weight and fuel burn rate, which decreases effectiveness. The best design vector is denoted by the red arrow. This design vector has the peak MOE value out of the design vectors which enable the fighters to maximize penetration range. This design vector has 20% improvements in SFC, L/D, mass fraction, and proximity, and a 10% fuel decrease. Consulting Figure 19, the maximum penetration radius was achieved for fuel payloads above 37000 lb in Scenario 1. A 10% fuel payload decrease, from 40000 lb to 36000 lb is below the 37000 lb cutoff. However, the technology improvements enable the tactical tanker to support the full penetration radius with as little as 35000 lb payload, a decrease of 12.5% from the 40000 lb baseline.

The design vectors shown in Figure 28 have significantly higher Tactical Tanker Fuel Effectiveness values than the baseline values shown in Figure 16. This MOE, calculated in Equation 85, is found by the ratio of fuel offloaded to fuel burned,

then multiplied by a penetration radius scaling factor. Once penetration radius is maximized, the amount of fuel offloaded is constant, therefore the MOE is driven by the amount of fuel burned. The technology improvements decrease the tactical tanker's fuel burn rate from 53 lb/min to 25 lb/min, which increases the MOE value. Fuel burn rate (see Equation 47) is a good indicator of how technology improvements interact to produce a better aircraft. Fuel burn rate was cut in half, even though none of the individual technology improvements was more than 20%.

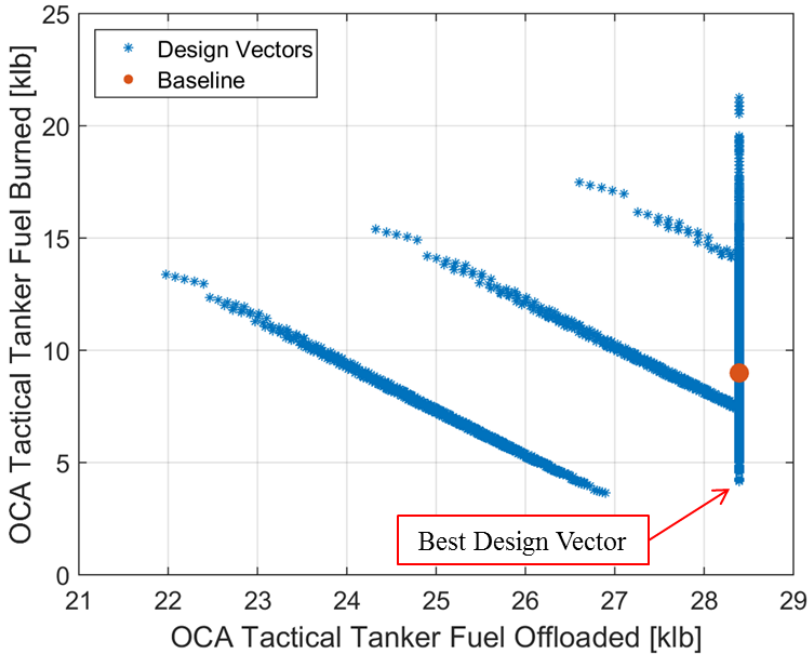

Figure 29. OCA Scenario 1: Full factorial trade space of Tactical Tanker Fuel Burned vs. Tactical Tanker Fuel Offloaded at baseline 40000 lb fuel payload.

Figure 29 shows the relationship between Tactical Tanker Fuel Burned and Tactical Tanker Fuel Offloaded. As previously discussed, the amount of offloaded fuel reaches a maximum when the fighter's tanks are full. Each fighter has a maximum fuel capacity of approximately 6000 lb. The amount of fuel burned is simply the fuel burn rate multiplied by mission duration. On this plot, the best design vector is located near the bottom right, and burns the least amount of fuel of all the design

vectors which completely fill the fighter's fuel tanks. The design vector is the same design vector that performed the best in Figure 28, and burns approximately 4150 lb of fuel during the 170 minute flight. The design vector at the top right of the plot also maximizes fighter penetration radius, but does so inefficiently. This design vector burns over 21000 lb of fuel, and has a lower L/D and higher SFC, mass fraction, and fuel payload. The tactical tanker design vector with the absolute minimum fuel burned has high efficiency due to low fuel burn rate, but does not have enough fuel to fully fill the fighter's tanks.

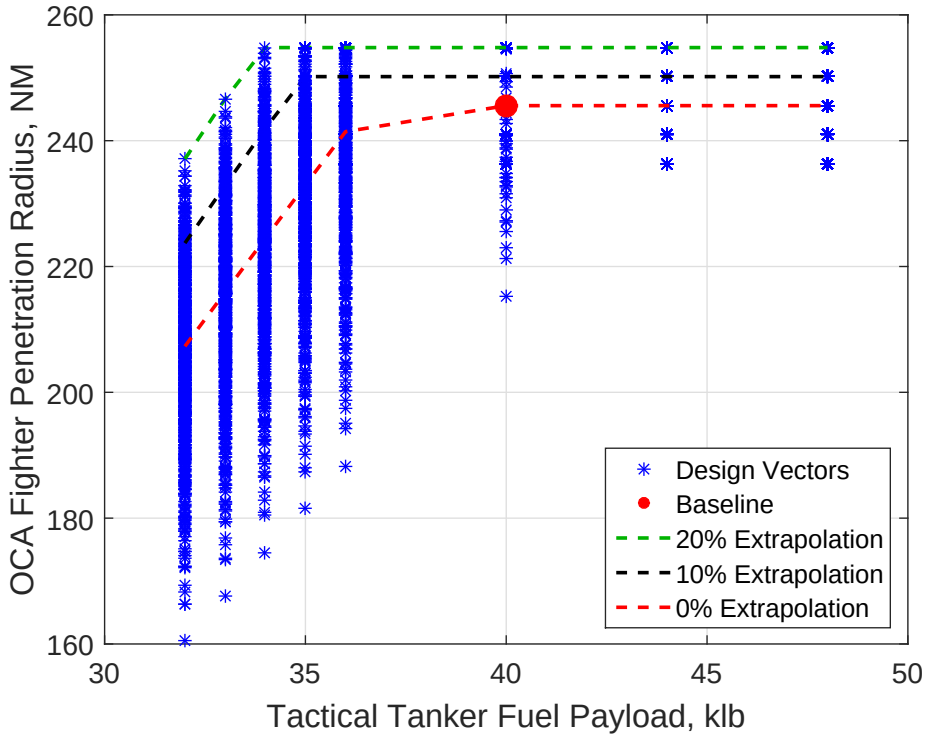

Figure 30. OCA Scenario 1: Full factorial trade space showing Fighter Penetration Radius vs. Tactical Tanker Fuel Payload at baseline 40000 lb fuel payload.

Figure 30 shows how TPM changes impact penetration radius. The five vertical lines show constant fuel payload, and the blue asterisks along each line are design vectors with ranges of TPM improvements or decrements for SFC, L/D, mass fraction, and proximity. The design vectors cluster into five groups at each fuel payload on the

right side of the plot because only the proximity TPM impacts penetration range. The green, black, and red extrapolation lines show 20%, 10%, and 0% TPM improvements at each fuel payload. 1875 additional trials were conducted to provide data at 33000 lb, 34000 lb, and 35000 lb. These data enable higher fidelity knowledge of performance in the extrapolation curve region. In general, TPM improvements are beneficial at low fuel payloads, but have no impact on penetration radius at higher fuel payloads.

4.4.2 Defensive Counterair

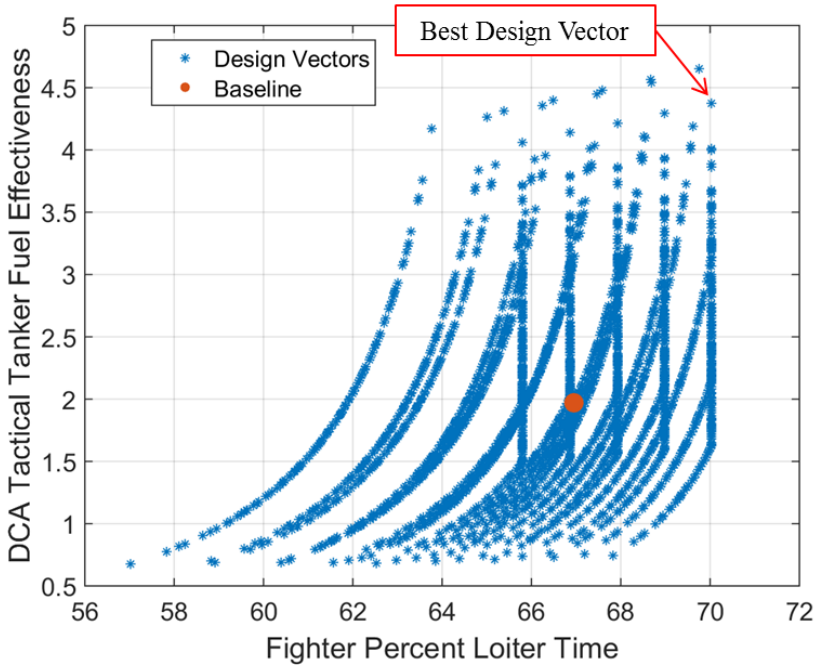

Figure 31. DCA Scenario 1: Full factorial trade space of Tactical Tanker Fuel Effectiveness vs. Fighter Percent Loiter Time at baseline 40000 lb fuel payload.

Figure 31 shows the DCA full factorial trade space of Tactical Tanker Fuel Effectiveness versus Fighter Percent Loiter Time. Like the OCA plots, this plot is divided into regions of curved lines and straight lines. The curved lines include design vectors where the tactical tanker was undersized, inefficient, located far away from the loiter point, or a combination of these factors. The vertical straight lines represent

design vectors which enable the fighter to reach the maximum possible loiter percentage. Fighters accompanying tactical tankers defined by the vertical lines have full fuel tanks when heading for the loiter point, so the only factor impacting their loiter percentage is the proximity TPM. The vertical lines on the left have worse proximity TPMs than the right, meaning the fighter has to transit a larger distance when flying to and from the loiter point.

The baseline design vector enables the fighters to spend about 67% of each cycle at the loiter point, which means approximately 33% is spent off station. The best design vector achieves 70% of cycle time on station, and also more than doubles the fuel effectiveness MOE from 2.0 to 4.4. This design vector has 20% improvements in SFC, L/D, mass fraction, and proximity, and no change in fuel payload. These TPM changes enable the tactical tanker to support a full fighter loiter cycle at 40000 lb fuel payload, opposed to the 45000 lb payload required in Figure 18. The design vector located immediately to the best design's top and left is also very good. This design is identical to the best design except that it has a -10% fuel payload TPM, resulting in 36000 lb fuel payload. This design vector has a slightly better fuel effectiveness MOE due to its smaller size, and therefore lower fuel burn rate, but lacks enough fuel to fill top off the fighter's fuel tanks.

Undersized or inefficient tactical tankers prevent fighters from realizing their maximum potential time at the loiter point. These fighters must return for refueling more frequently, which increases the number of cycles they make to and from the tactical tanker during their 8 hour sortie. The impact of these undersized or inefficient tactical tankers is depicted in Figure 32.

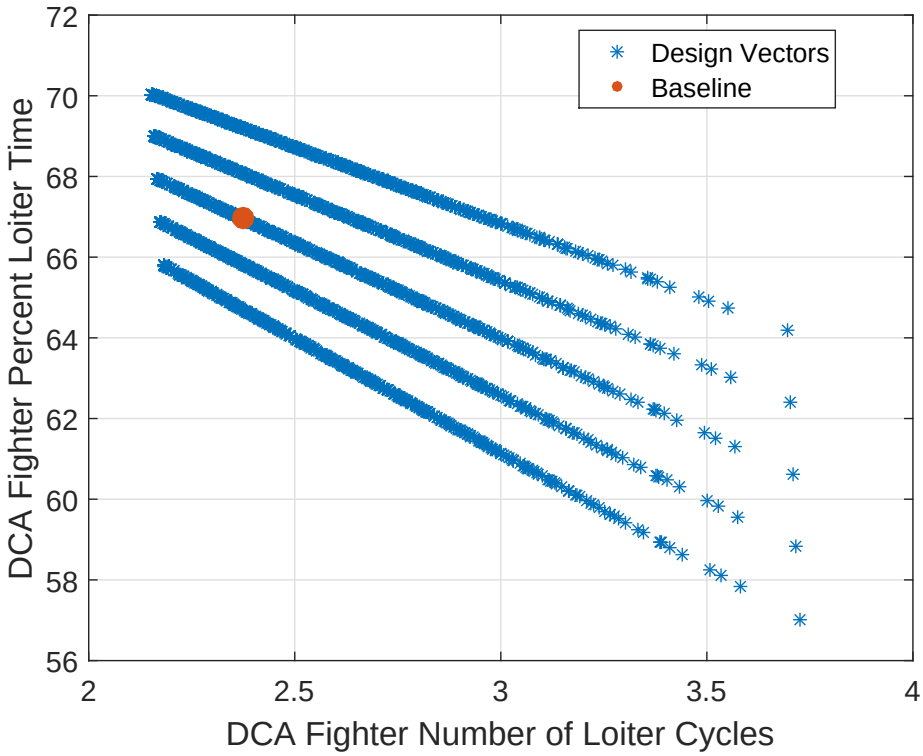

Figure 32. DCA Scenario 1: Full factorial trade space of Fighter Percent Loiter Time vs. Number of Loiter Cycles at baseline 40000 lb fuel payload.

Figure 33 shows the DCA full factorial trade space of Tactical Tanker Fuel Effectiveness versus Tactical Tanker Fuel Burned. The baseline design configuration with 40000 lb fuel payload has an effectiveness just below 2, can support 92% of a fighter loiter cycle (see Figure 18), and burns 25500 lb of fuel. Tactical tankers of a given size have the same fuel burn rate, but burn significantly more fuel on DCA missions than OCA missions because of the mission duration. OCA missions last about 3 hours because the fighter only penetrates the contested airspace one time. DCA missions last 8 hours, and consist of several loiter cycles. The user can change the maximum mission duration inside the quick look model based on the needed scenario.

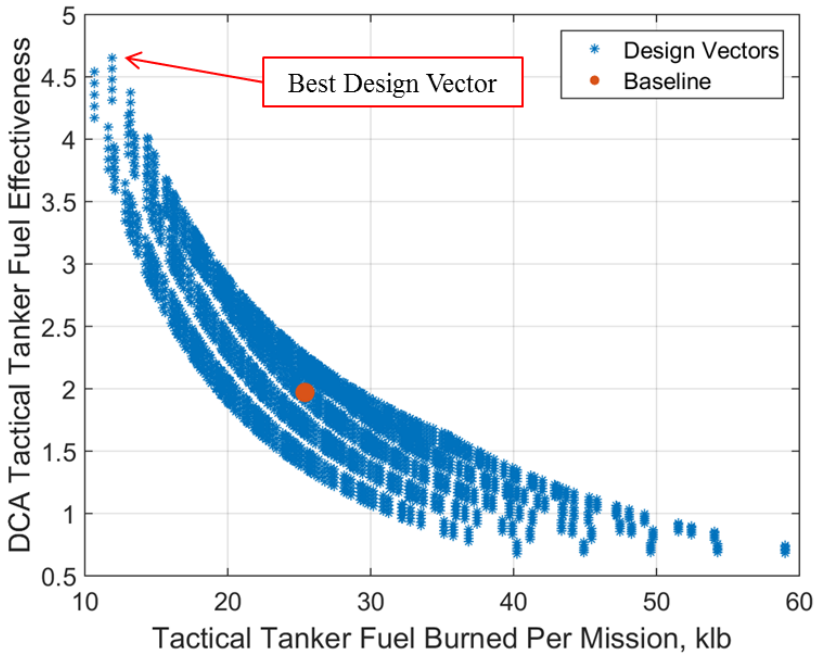

Figure 33. DCA Scenario 1: Full factorial trade space of Tactical Tanker Fuel Effectiveness vs. Fuel Burned at baseline 40000 lb fuel payload.

The best design vector in Figure 33 is located at the upper left, where the tactical tanker has the best effectiveness for least fuel burned. This design vector has the same TPM changes as the vector shown previously in Figure 31.

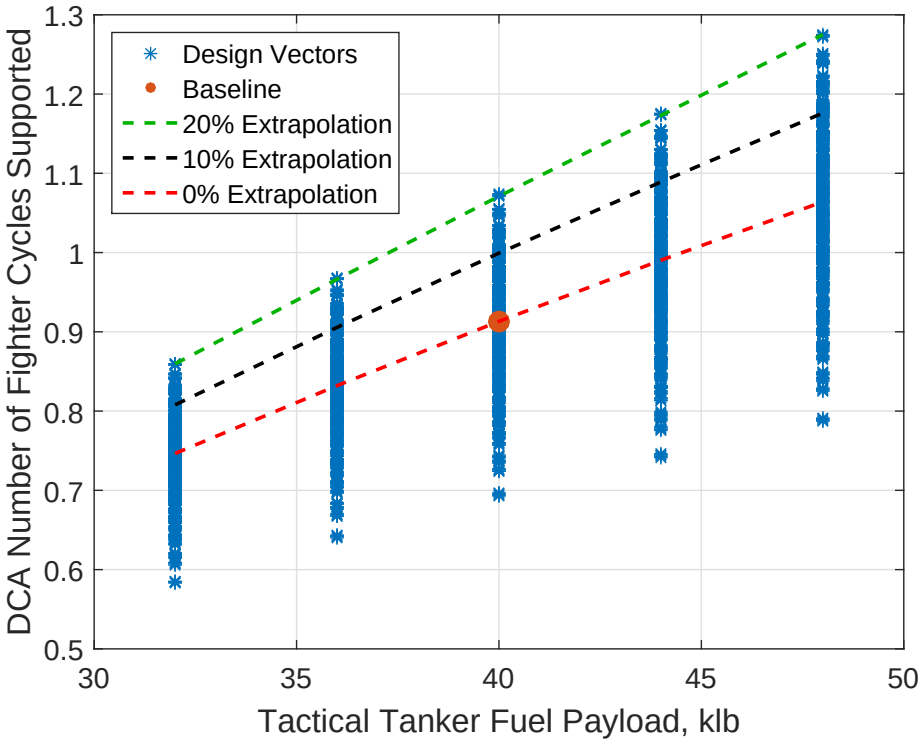

Figure 34. DCA Scenario 1: Full factorial trade space showing Number of Fighter Cycles Supported vs. Tactical Tanker Fuel Payload at baseline 40000 lb fuel payload.

When four of the TPMs are maximized, the tanker needs a 37500 lb fuel payload to support a loiter cycle, as shown in Figure 34 where the 20% improvement extrapolation crosses 1 on the y-axis. The black 10% extrapolation shows that 10% improvements in SFC, L/D, mass fraction, and proximity are enough to support a fighter cycle at the 40000 lb baseline fuel payload. The red 0% extrapolation line shows the number of fighter cycles supported if four TPMs are held constant and only the fuel payload changes. Further extrapolations can be made to estimate a design vector's performance with different TPM percentage changes.

V. Conclusions and Recommendations

5.1 Objective 1

The first objective of this research effort was to investigate the performance benefits of augmenting current capabilities with a tactical tanker air refueling aircraft. To this end, a baseline conceptual aircraft design was created and imported into a low-fidelity, quick look operational assessment model. The tactical tanker's performance was judged according to seven Measures of Effectiveness which investigated the tactical tanker's own performance as well as its impact on the performance of the fighters it was tasked to support in either offensive or defensive missions.

Outputs from the quick look model and MOE values showed the combination of a tactical tanker with a traditional tanker outperformed a traditional tanker alone. The presence of a tactical tanker in both OCA and DCA missions provided several benefits to traditional tankers and fighters. The tactical tanker enabled traditional tankers to safely remain in permissive airspace far from the contested area. The tactical tanker's ability to accompany the fighter gave the fighters increased fuel at their time of departure from the tactical tanker.

In the OCA case, the fighters used this extra fuel to penetrate farther into contested airspace. Extra penetration radius gives mission planners the ability to hold more targets at risk. Fighters performing DCA missions alongside a tactical tanker had greater flexibility than fighters supported only by a traditional tanker. The fighters spent a much greater percentage of their time actually defending friendly assets rather than transiting to and from a traditional tanker. In both OCA and DCA, the fighters became more effective because they are able to spend a greater proportion of mission time in contested airspace.

The Measures of Effectiveness evaluated in the quick look model showed that

tactical tankers with 45000 lb fuel payloads or higher were able to maximize fighter penetration radius and loiter time. However, this fuel payload is heavily influenced by gameboard distances, the ratio of fighters to tactical tankers, and the size of each fighter. A tactical tanker with a 45000 lb fuel payload has a total fuel capacity of about 78000 lb and weighs 138000 lb at takeoff. The tactical tanker is considerably smaller than the KC-135 traditional tanker, which carries a 200000 lb total fuel load and weighs 322500 lb at takeoff. The KC-46 and KC-10 are even larger.

5.2 Objective 2

The second objective was to investigate alternate tactical tanker designs by changing five technological parameters: lift to drag ratio, engine specific fuel consumption, mass fraction, fuel payload, and proximity. A sensitivity analysis was conducted using finite difference techniques to find which TPMs had the greatest impact on effectiveness. Proximity and mass fraction were typically the most sensitive technologies, with L/D and SFC next showing equal sensitivity and fuel payload slightly lower. These results suggest that investments in technologies to improve proximity and mass fraction parameters may provide the largest benefit to a tactical tanker.

A full factorial design of experiments trade space was set up in parallel with the sensitivity analysis. This trade space was created to see the results of TPM variations of up to 20%. The trade space included technology improvements as well as detriments to account for interactions between TPMs. 20% technology improvements may not be achievable in the short term, but they provide a glimpse of future performance increases for planning purposes.

5.3 Recommendations

1. Investigate similar scenarios using a mix of different fighter sizes and gameboard layouts.

2. Investigate potential integration issues of a flying boom type fuel system onto a small aircraft. This research was agnostic to the type of fuel delivery system (flying boom vs. probe and drogue) used by the tactical tanker. However, it was noted that Air Force tactical aircraft are incompatible with probe and drogue delivery systems.

3. Conduct a statistical analysis of the full factorial trade space to identify correlations between TPM predictors and MOE responses.

4. Search for links between investment costs and technology improvements. This research found that sensitivities to SFC and L/D were identical. If, for example, aerodynamic performance can be improved for less money than engine efficiency, then research to improve L/D may be more effective from a cost and payoff perspective.

VI. List of Acronyms

A2/AD Anti-access/Area Denial

AFRL Air Force Research Laboratory

AR Aspect Ratio

DCA Defensive Counterair

DOE Design of Experiments

GTOW Gross Takeoff Weight

HVAA High Value Airborne Asset

IADS Integrated Air Defense System

IP Ingress Point

L/D Lift-to-Drag Ratio

MATLAB Matrix Laboratory

MOE Measure of Effectiveness

NATO North Atlantic Treaty Organization

OA Operational Assessment

OCA Offensive Counterair

OEC Overall Evaluation Criteria

SAC Strategic Air Command

SFC Specific Fuel Consumption

TAC Tactical Air Command

TARP Tactical Aerial Refueling Platform

TOP Takeoff Parameter

TPM Technological Performance Measure

TRL Technology Readiness Level

TTT Tactical Tanker Trade Space

US United States

USAF United States Air Force

WOTT Without Tactical Tanker

Appendix A. Sensitivity Analysis and Factorial Studies for Scenarios 2 and 3

1.1 Sensitivity Analysis

Sensitivity plots for Scenarios 2 and 3 are shown below. Similar plots for Scenario 1 were covered in Chapter IV.

Apparent outliers in Figures 39, 42, and 44, occur due to the step size (+0.1%) used in the finite difference calculation. For example, at certain tactical tanker fuel payloads, a 0.1% increase in a TPM is enough to jump from supporting less than one fighter loiter cycle to supporting more than one cycle. Decreasing the finite difference step size below 0.1% would fix remove these anomalies, but may also increase rounding error.

1.1.1 Scenario 2

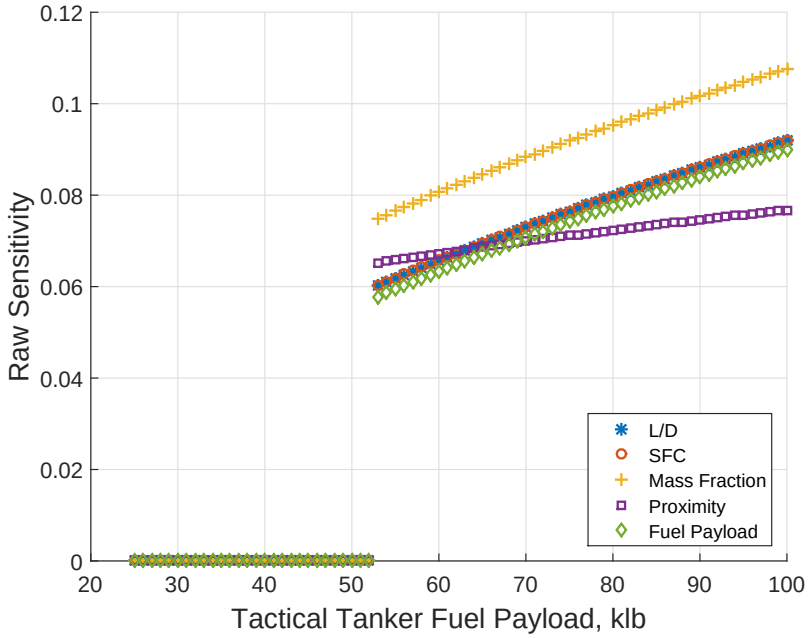

Figure 35. DCA Scenario 2: Sensitivity of Tactical Tanker Effectiveness at Varying Fuel Payloads.

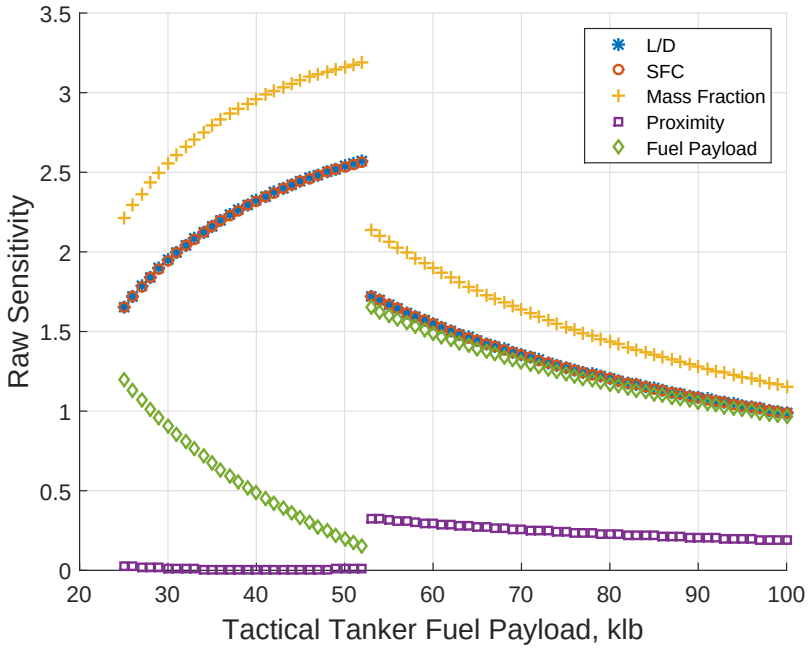

Figure 36. DCA Scenario 2: Sensitivity of Tactical Tanker Fuel Effectiveness at Varying Fuel Payloads.

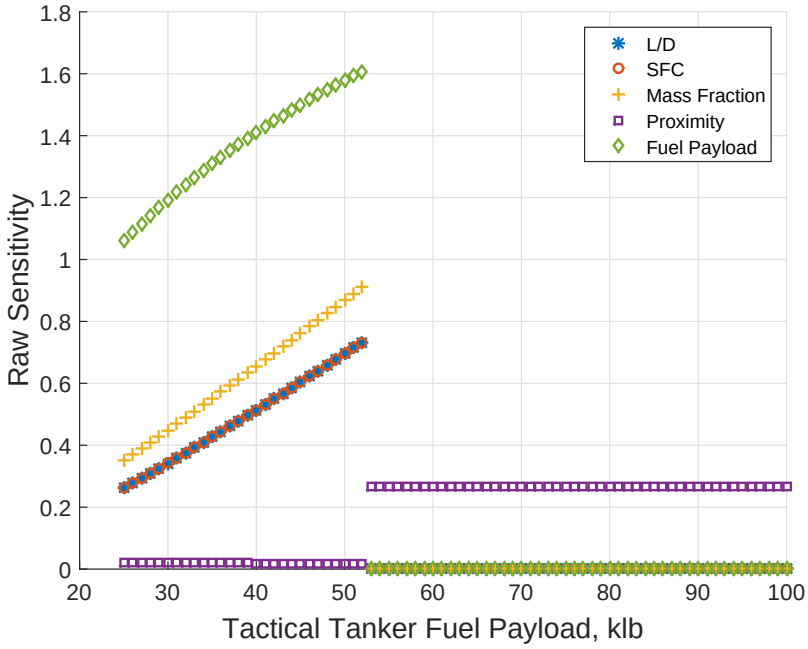

Figure 37. DCA Scenario 2: Sensitivity of CAP Loiter Effectiveness at Varying Fuel Payloads.

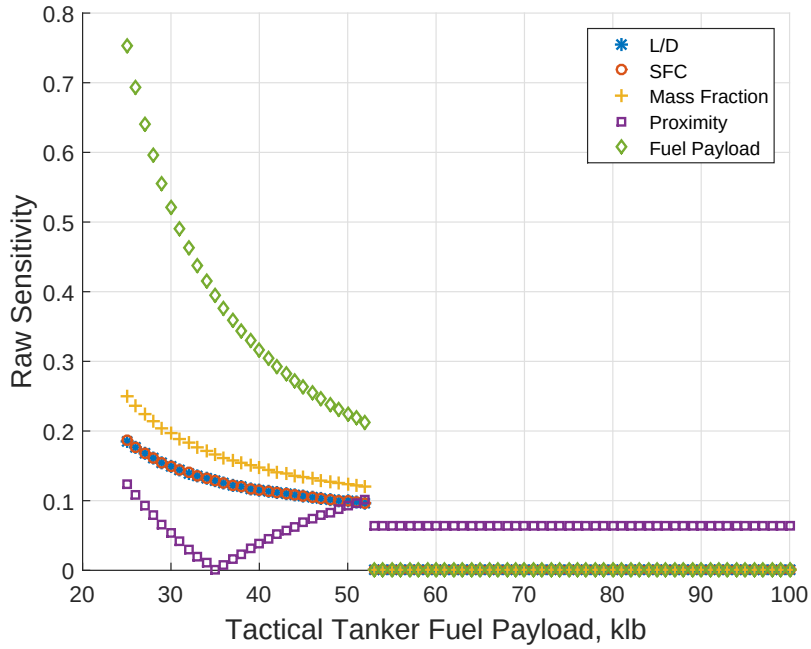

Figure 38. DCA Scenario 2: Sensitivity of CAP Loiter Percent Effectiveness at Varying Fuel Payloads.

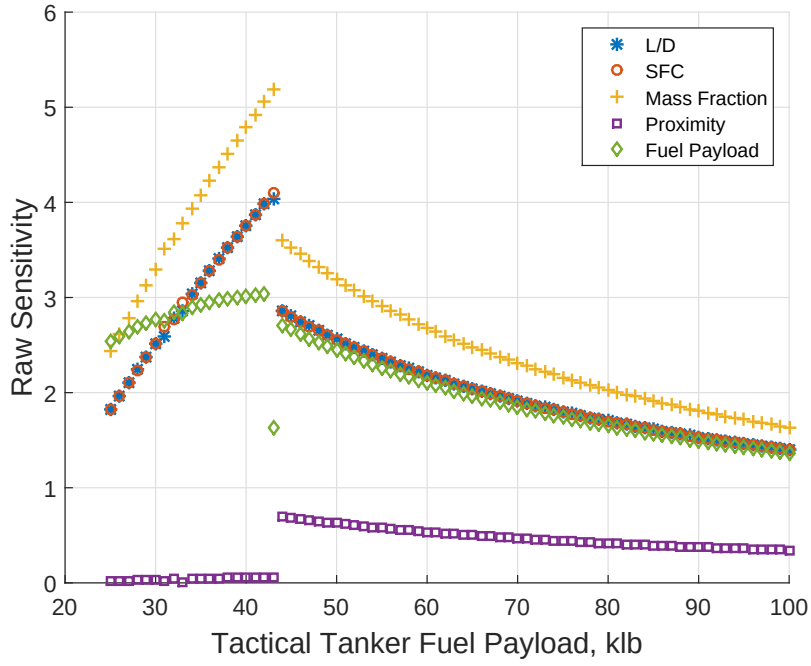

Figure 39. OCA Scenario 2: Sensitivity of Tactical Tanker Effectiveness at Varying Fuel Payloads.

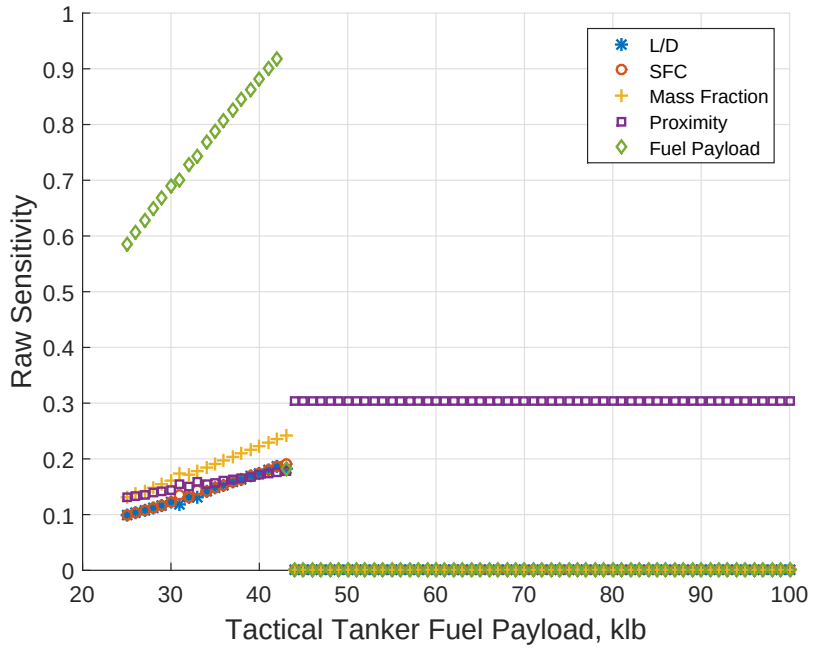

Figure 40. OCA Scenario 2: Sensitivity of CAP Effectiveness at Varying Fuel Payloads.

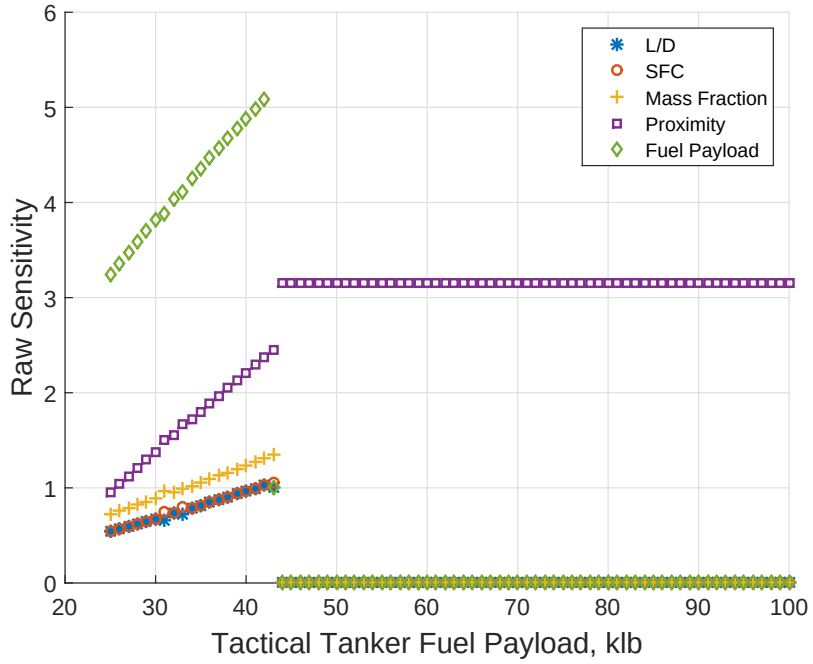

Figure 41. OCA Scenario 2: Sensitivity of CAP Penetration Effectiveness at Varying Fuel Payloads.

1.1.2 Scenario 3

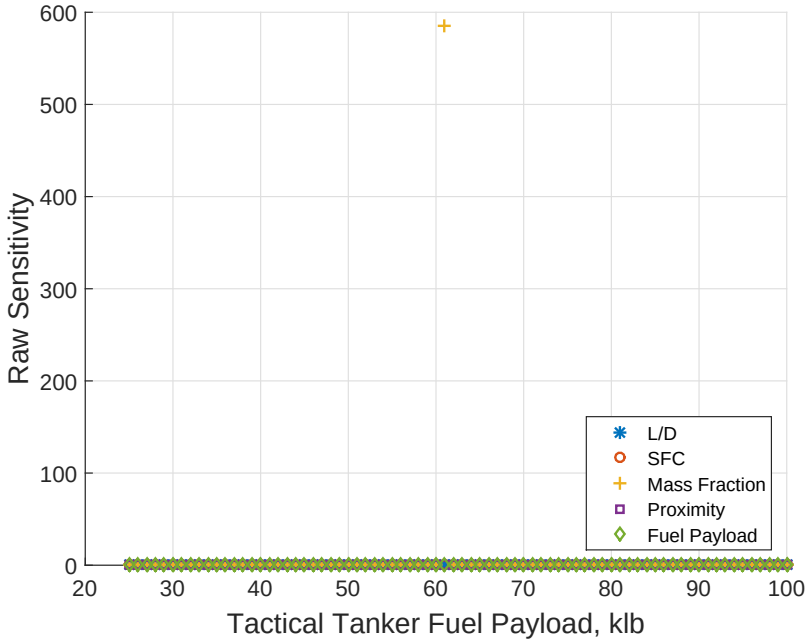

Figure 42. DCA Scenario 3: Sensitivity of Tactical Tanker Effectiveness at Varying Fuel Payloads.

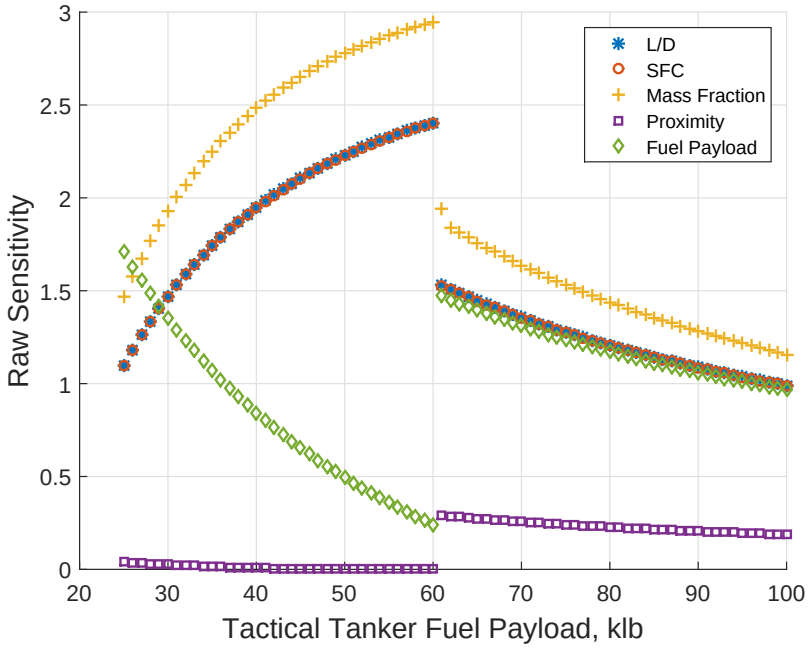

Figure 43. DCA Scenario 3: Sensitivity of Tactical Tanker Fuel Effectiveness at Varying Fuel Payloads.

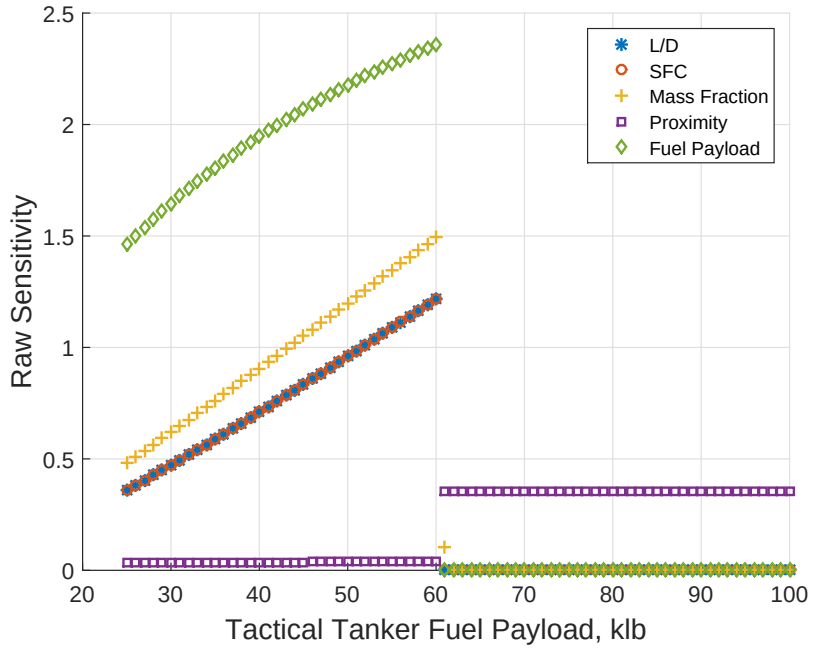

Figure 44. DCA Scenario 3: Sensitivity of CAP Loiter Effectiveness at Varying Fuel Payloads.

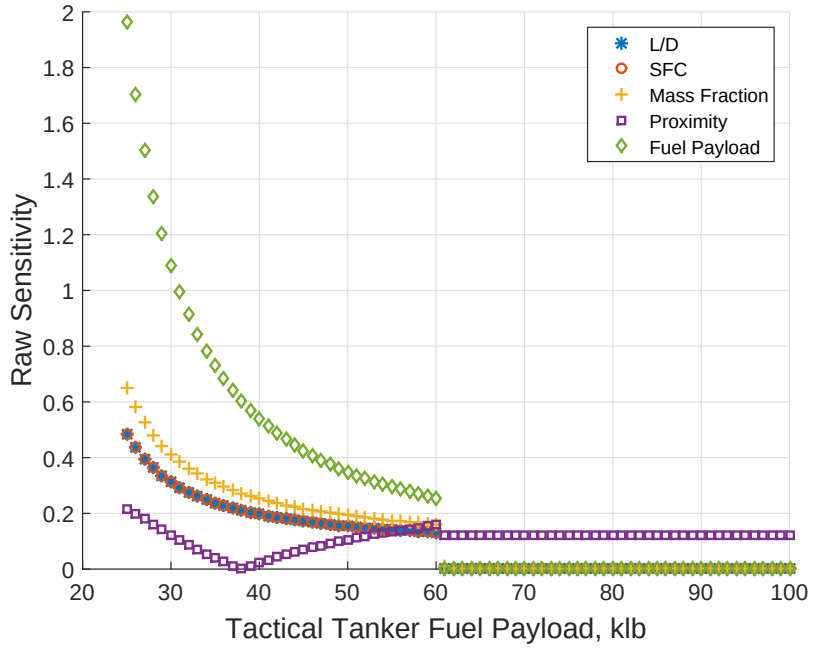

Figure 45. DCA Scenario 3: Sensitivity of CAP Loiter Percent Effectiveness at Varying Fuel Payloads.

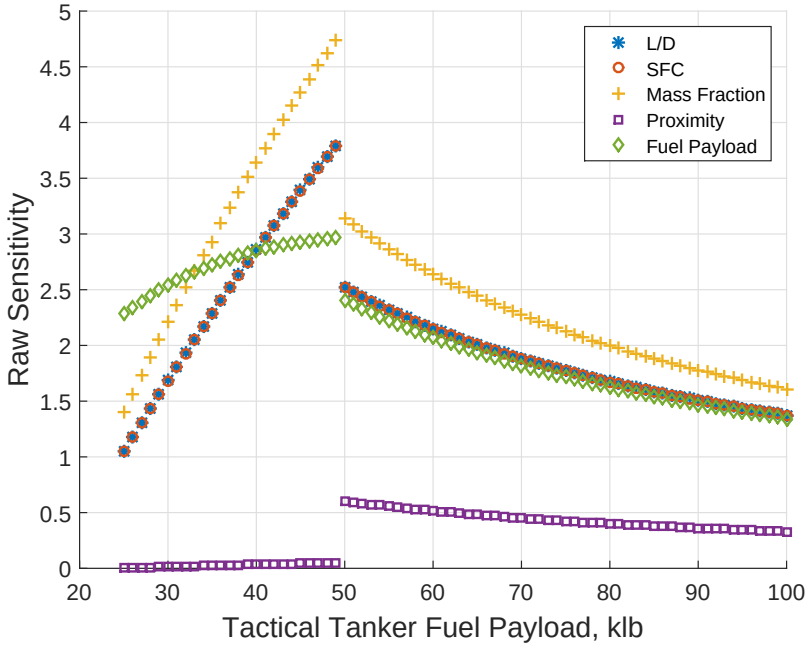

Figure 46. OCA Scenario 3: Sensitivity of Tactical Tanker Effectiveness at Varying Fuel Payloads.

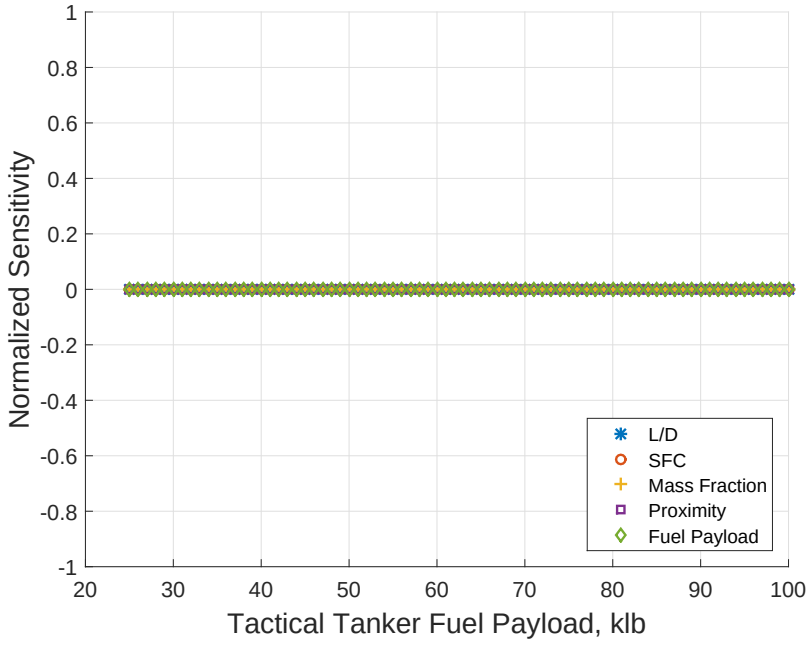

Figure 47. OCA Scenario 3: Sensitivity of CAP Effectiveness at Varying Fuel Payloads.

Figures 47 and 48 show the Fighter CAP Effectiveness MOE and Penetration MOE are insensitive to technology changes in the Tactical Tanker. These MOEs

show zero sensitivity because the MOEs are calculated by comparing the fighter's performance with and without the tactical tanker. In Scenario 3, the distance from the traditional tanker to the OCA ingress point is 400 miles. The fighter cannot cover this distance without help from the tactical tanker, so the penetration radius without the tactical tanker is zero nautical miles. These MOEs are insensitive because the calculation attempts to divide by zero.

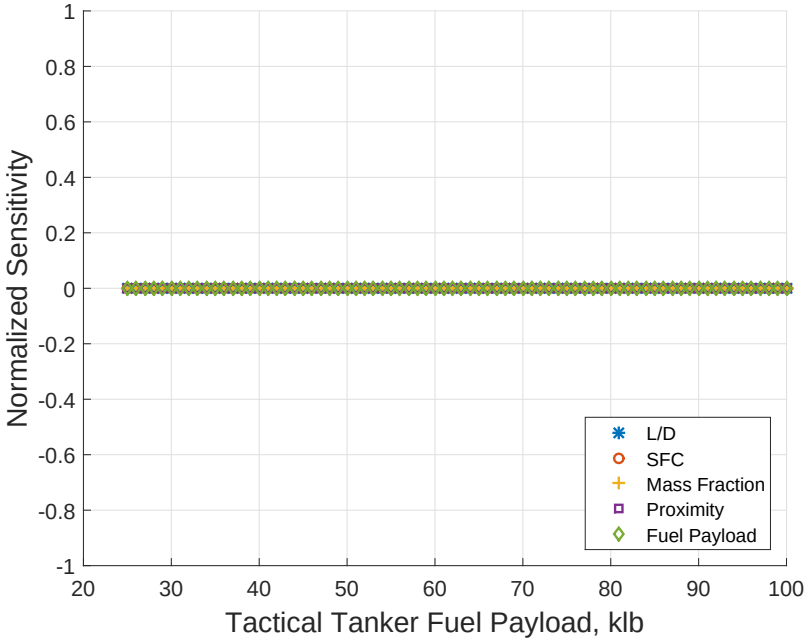

Figure 48. OCA Scenario 3: Sensitivity of CAP Penetration Effectiveness at Varying Fuel Payloads.

1.2 Design of Experiments

Full Factorial DOE trade spaces are shown below for Scenarios 2 and 3. Similar plots for Scenario 1 were shown and discussed in Chapter IV. Similar trends are present in these plots.

In the Scenario 1 plots shown previously, the baseline design vector had a 40000 lb fuel payload. 40000 lb was selected in order to show changes in behavior at up to 20% increases or decreases in fuel payload. Higher baseline fuel payloads were necessary

for Scenarios 2 and 3 in order to show these trends. For example, a 20% fuel payload increase (from a 40000 lb baseline) is 48000 lb. In Scenario 3, a 48000 lb tactical tanker cannot support maximum penetration radius or loiter time. Therefore,the baseline fuel payload is 50000 lb for Scenario 2, and 55000 lb for Scenario 3.

1.2.1 Scenario 2

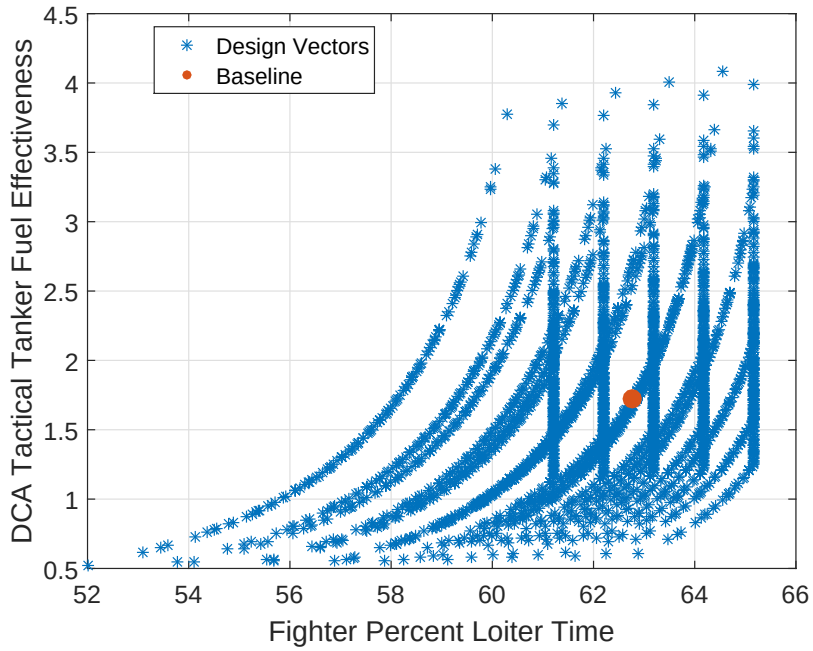

Figure 49. DCA Scenario 2: Full factorial trade space of Tactical Tanker Fuel Effectiveness vs. Fighter Percent Loiter Time at baseline 50000 lb fuel payload.

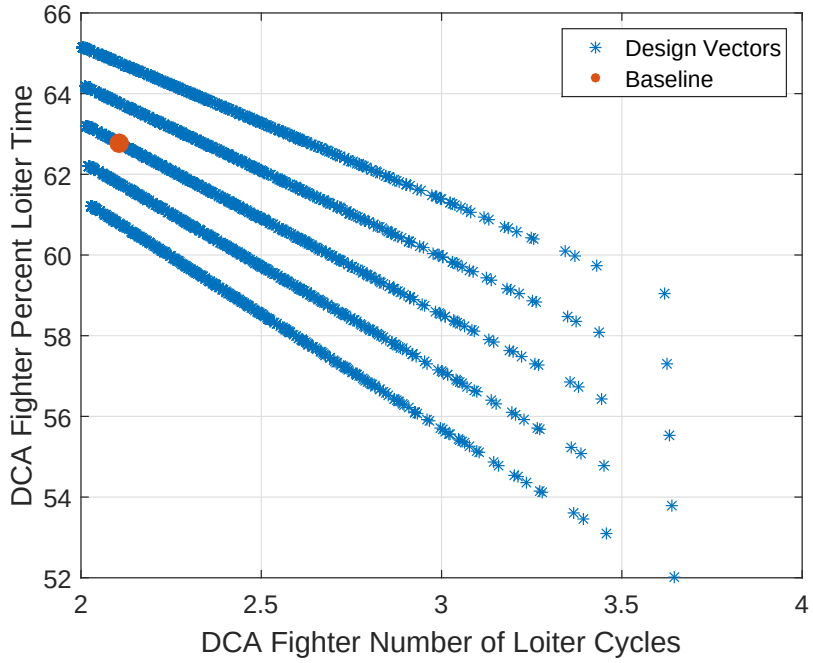

Figure 50. DCA Scenario 2: Full factorial trade space of Fighter Percent Loiter Time vs. Number of Loiter Cycles at baseline 50000 lb fuel payload.

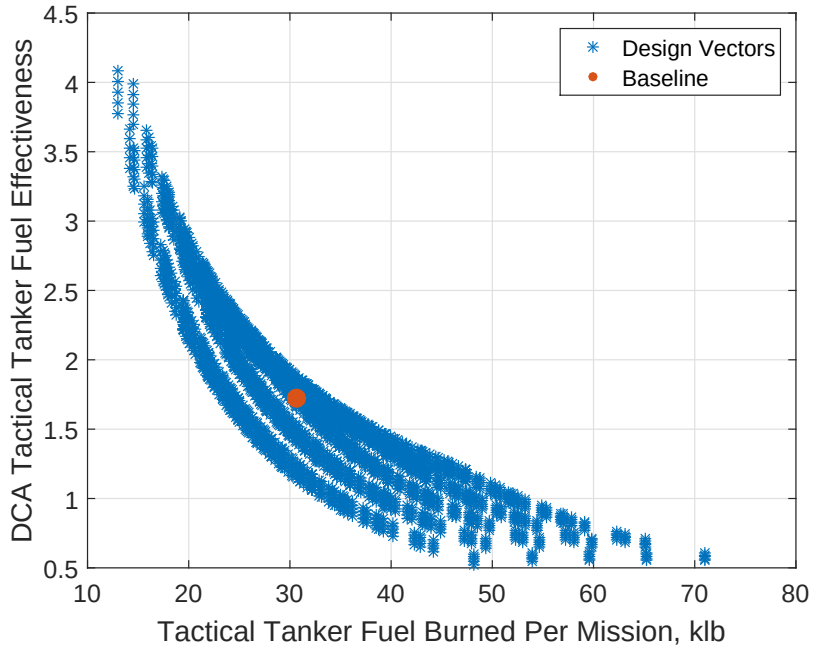

Figure 51. DCA Scenario 2: Full factorial trade space of Tactical Tanker Fuel Effectiveness vs. Fuel Burned at baseline 50000 lb fuel payload.

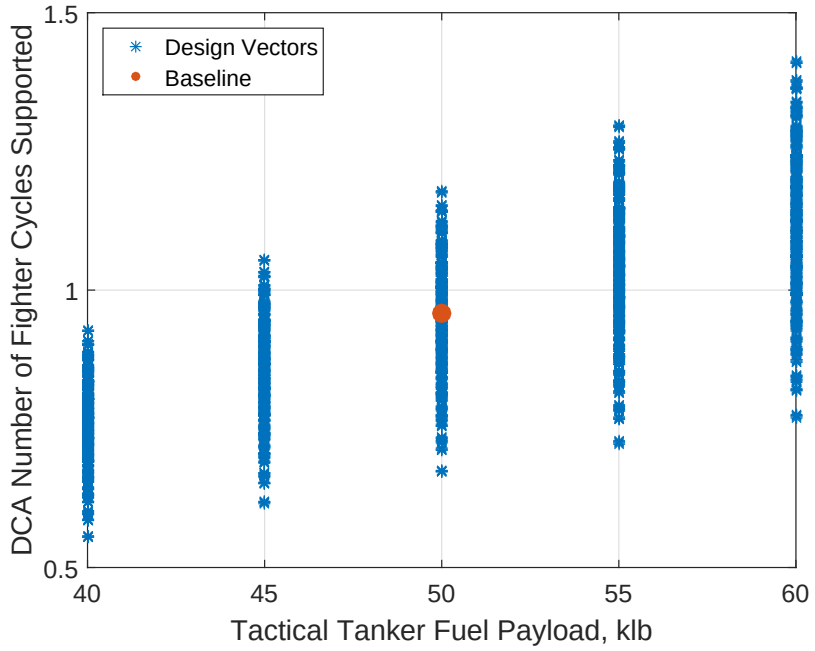

Figure 52. DCA Scenario 2: Full factorial trade space showing Number of Fighter Cycles Supported vs. Tactical Tanker Fuel Payload at baseline 50000 lb fuel payload.

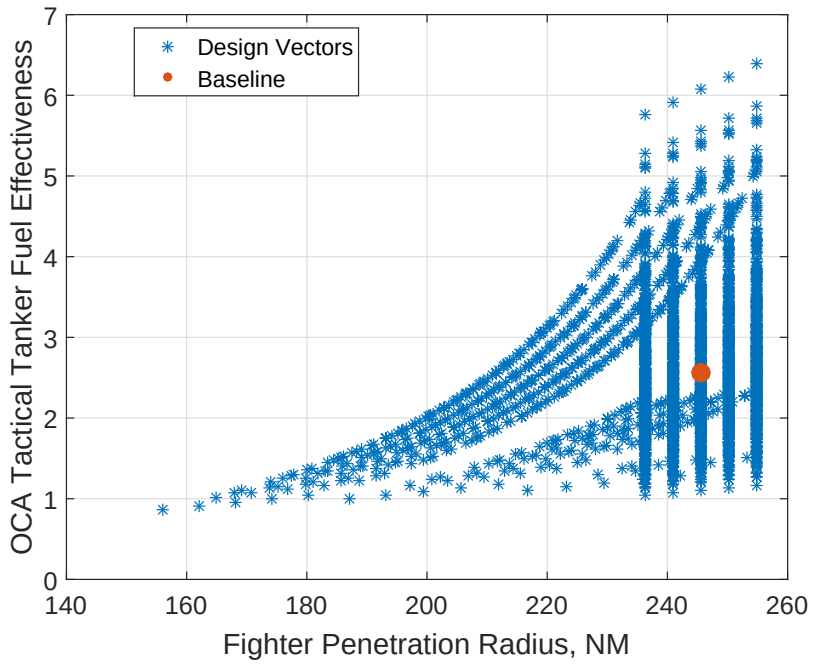

Figure 53. OCA Scenario 2: Full factorial trade space of OCA Tactical Tanker Fuel Effectiveness vs. Penetration Radius at baseline 50000 lb fuel payload.

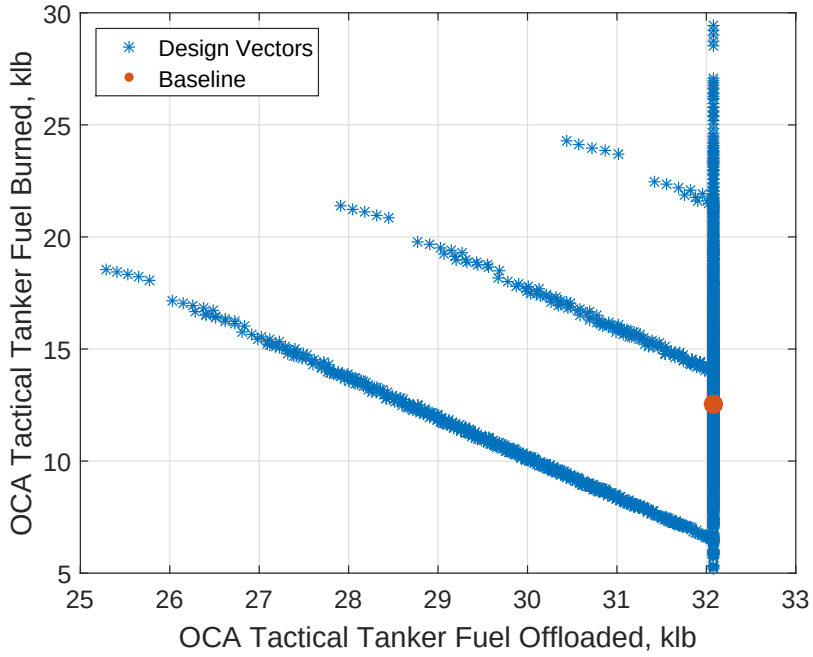

Figure 54. OCA Scenario 2: Full factorial trade space of Tactical Tanker Fuel Burned vs. Tactical Tanker Fuel Offloaded at baseline 50000 lb fuel payload.

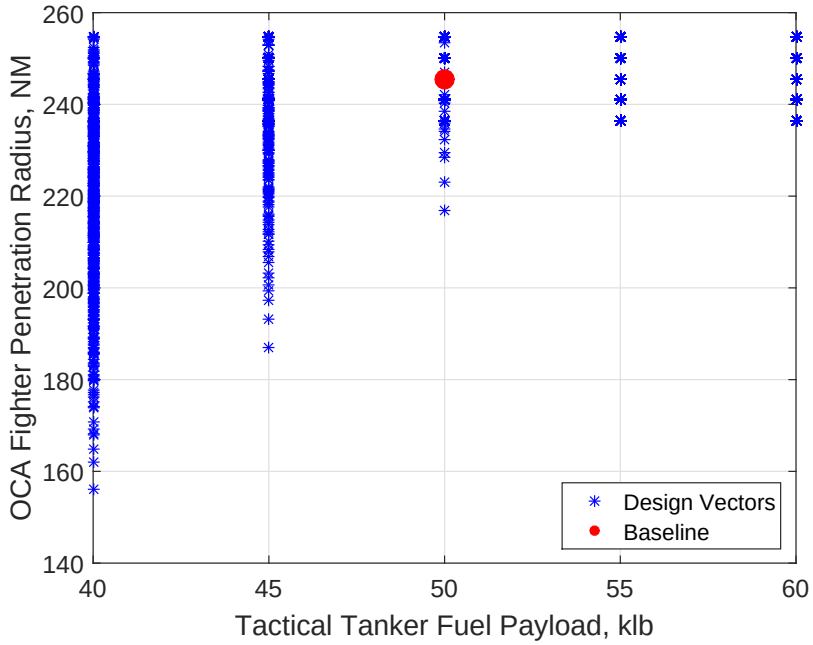

Figure 55. OCA Scenario 2: Full factorial trade space showing Fighter Penetration Radius vs. Tactical Tanker Fuel Payload at baseline 50000 lb fuel payload.

1.2.2 Scenario 3

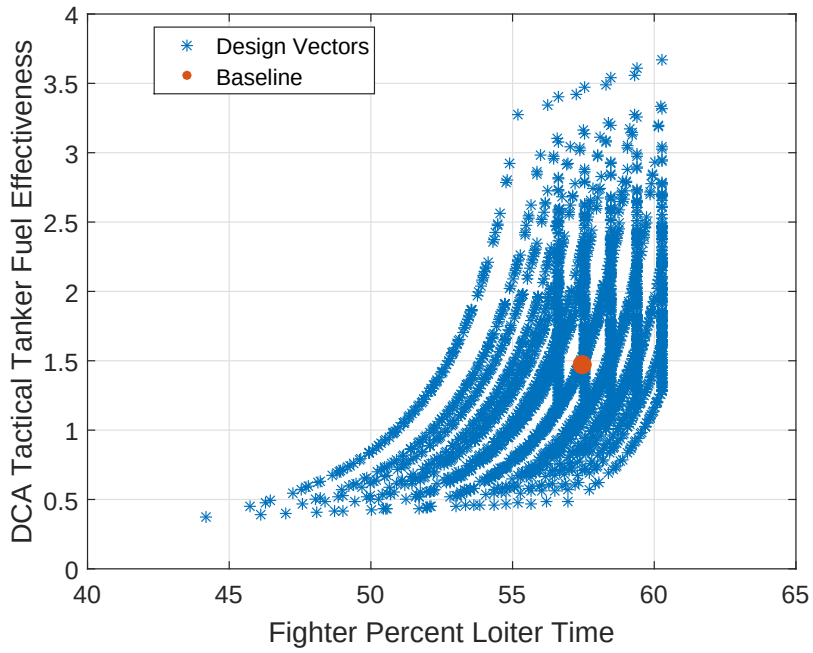

Figure 56. DCA Scenario 3: Full factorial trade space of Tactical Tanker Fuel Effectiveness vs. Fighter Percent Loiter Time at baseline 55000 lb fuel payload.

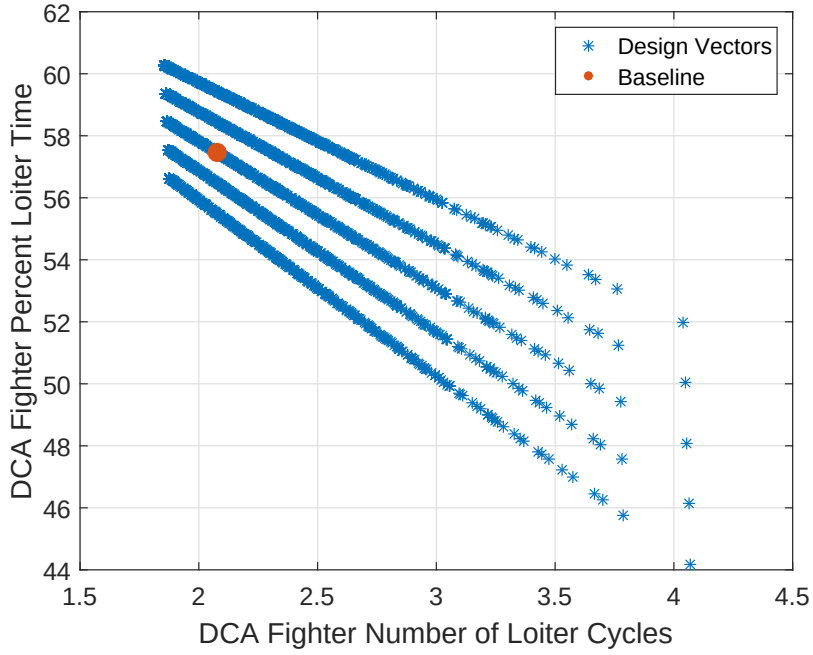

Figure 57. DCA Scenario 3: Full factorial trade space of Fighter Percent Loiter Time vs. Number of Loiter Cycles at baseline 55000 lb fuel payload.

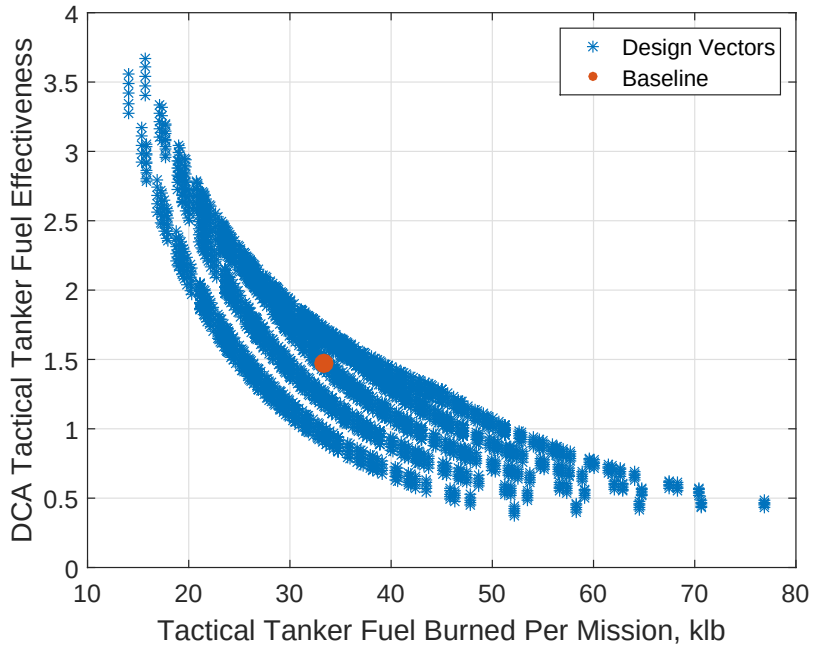

Figure 58. DCA Scenario 3: Full factorial trade space of Tactical Tanker Fuel Effectiveness vs. Fuel Burned at baseline 55000 lb fuel payload.

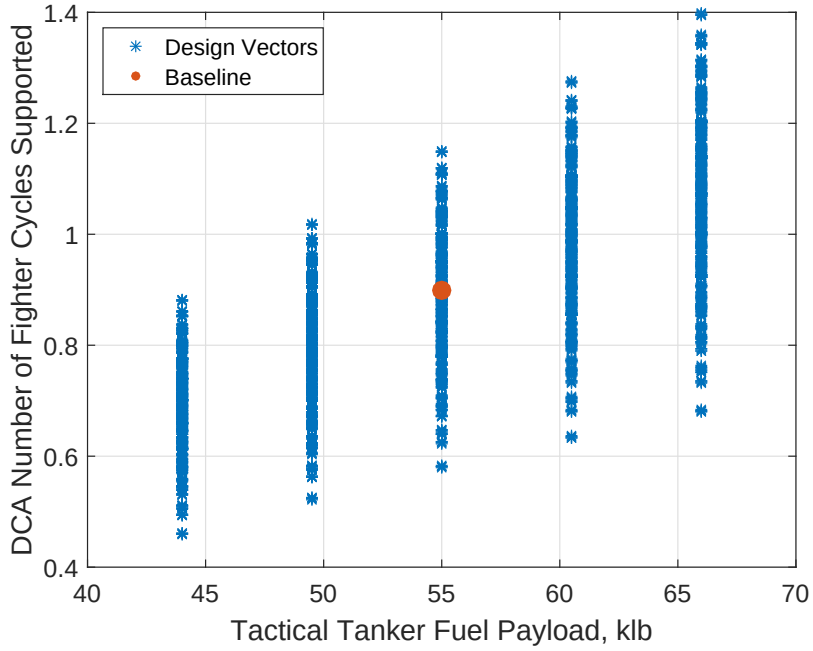

Figure 59. DCA Scenario 3: Full factorial trade space showing Number of Fighter Cycles Supported vs. Tactical Tanker Fuel Payload at baseline 55000 lb fuel payload.

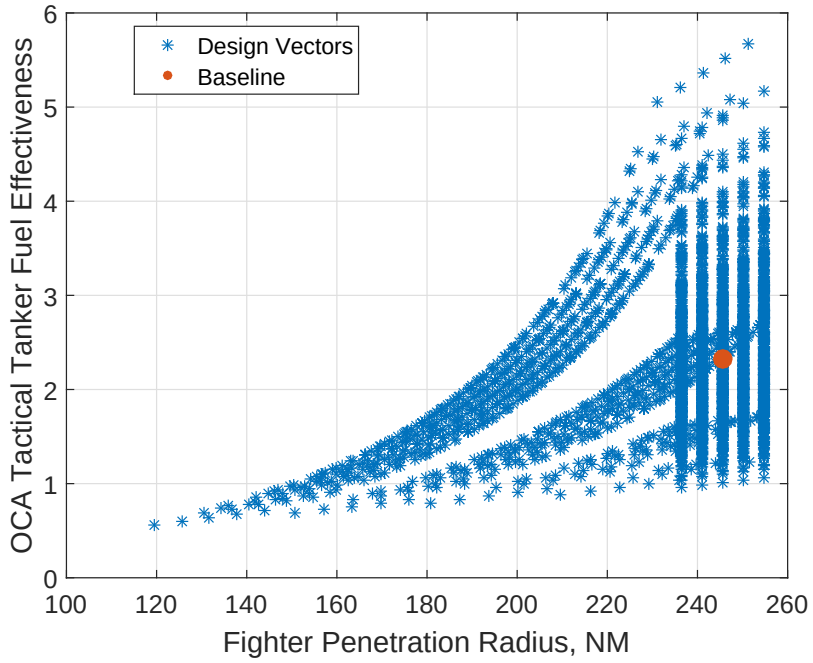

Figure 60. OCA Scenario 3: Full factorial trade space of OCA Tactical Tanker Fuel Effectiveness vs. Penetration Radius at baseline 55000 lb fuel payload.

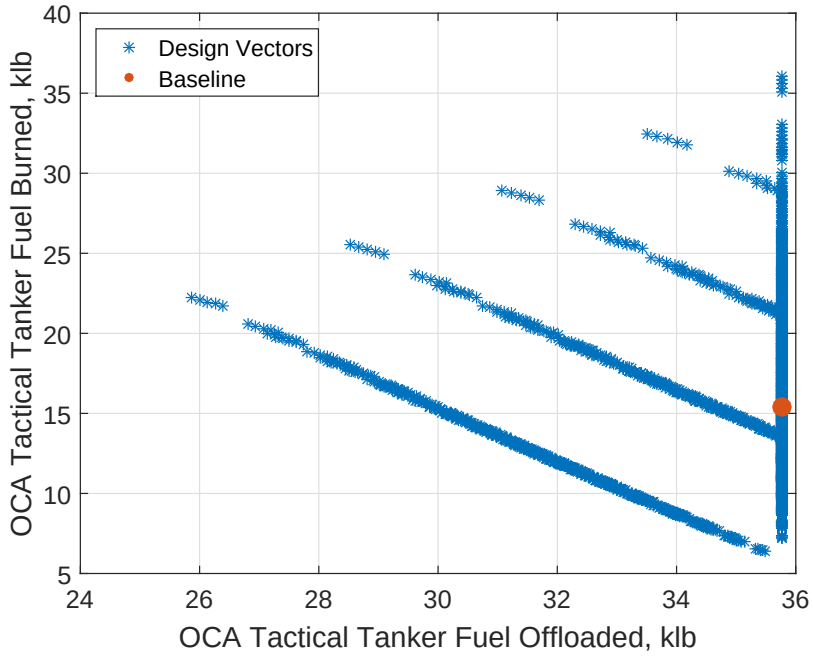

Figure 61. OCA Scenario 3: Full factorial trade space of Tactical Tanker Fuel Burned vs. Tactical Tanker Fuel Offloaded at baseline 55000 lb fuel payload.

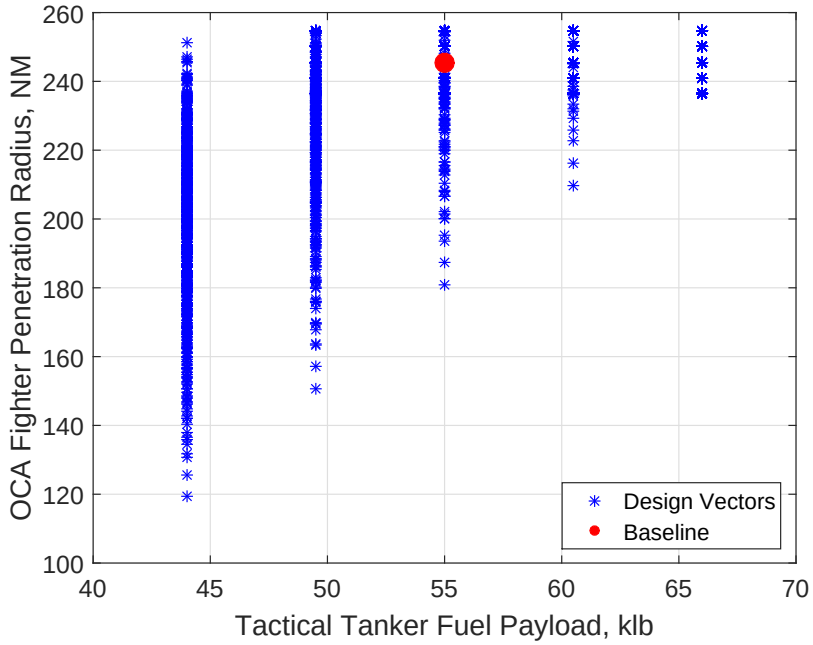

Figure 62. OCA Scenario 3: Full factorial trade space showing Fighter Penetration Radius vs. Tactical Tanker Fuel Payload at baseline 55000 lb fuel payload.

Appendix B. Selected Model Equations

Selected equations from the TTT quick look model are included below.

$$FtrFuelCapacity = GTOW - GTOW * massfraction \tag{40}$$

$$FighterFBR_i = \frac{FtrFuelCapacity * SFC_i}{60 * L/D_i * \ln(1/massfraction)} \tag{41}$$

$$FtrFuelReserves = FtrFuelCapacity * FtrPercentFuelReserves \tag{42}$$

$$FtrCruiseTimeFirstLeg = \frac{TradTankerOrbitDistanceFromBase}{FtrCruiseSpeed} * \frac{2}{60 min/hr} \tag{43}$$

$$FtrFuelConsumedinCruiseFirstLeg = FtrCruiseTimeFirstLeg * FtrCruiseFBR \tag{44}$$

$$FtrNumberTankingsDuringCruiseFirstLeg = \frac{FtrFuelConsumedinCruiseFirstLeg}{FtrFuelCapacity * FtrFuelReserves} \tag{45}$$

$$FtrCruiseRefuelTimeFirstLeg =$$

$$FtrNumberTankingsDuringCruiseFirstLeg* \left(2 + \frac{FtrFuelConsumedinCruiseFirstLeg}{5000lb/min}\right) \quad (46)$$

$$TactTankerFBR = \frac{FuelCapacity * SFC}{60 * L/D * \ln(1/massfraction)} \quad (47)$$

$$TactTankerFuelReserves =$$

$$TactTankerFuelCapacity * TactTankerPercentReserves \quad (48)$$

$$TactTankerCruiseTimeFirstLeg = \frac{TradTankerOrbitDistanceFromBase}{TactTankerBlockSpeed} * \frac{2}{60min/hr} \quad (49)$$

$$TactTankerFuelConsumedinCruiseFirstLeg =$$

$$TactTankerCruiseTimeFirstLeg * TactTankerFBR \quad (50)$$

$$TactTankerNumberTankingsDuringCruiseFirstLeg = \frac{TactTankerFuelConsumedinCruiseFirstLeg}{TactTankerFuelCapacity * TactTankerFuelReserves} \quad (51)$$

$$TactTankerCruiseRefuelTimeFirstLeg = TactTankerNumberTankingsDuringCruiseFirstLeg * (2 + \frac{TactTankerFuelConsumedinCruiseFirstLeg}{5000lb/min} \quad (52)$$

$$TradTankerFuelReserves = TradTankerFuelCapacity * TradTankerPercentReserves \quad (53)$$

$$TradTankerCruiseTimeFirstLeg = \frac{TradTankerOrbitDistanceFromBase}{TradTankerBlockSpeed} * \frac{2}{60min/hr} \quad (54)$$

$$TradTankerFuelConsumedinCruiseFirstLeg =$$

$$TradTankerCruiseTimeFirstLeg * TradTankerFBR$$

$$+ FtrFuelConsumedinCruiseFirstLeg * NumberFtrinFlight+$$

$$TactTankerFuelConsumedinCruiseFirstLeg \quad (55)$$

$$TradTankerFuelAvailablewhileonStation =$$

$$max(0, TradTankerFuelCapacity$$

$$- TradTankerFuelReserves - TradTankerFuelConsumedinCruiseFirstLeg)$$

$$(56)$$

$$FtrCruiseTimeSecondLeg =$$

$$\frac{TactTankerOrbitDistanceFromTradTanker}{FtrCruiseSpeed} * \frac{2}{60min/hr} \quad (57)$$

$$FtrFuelConsumedinCruiseSecondLeg =$$

$$FtrCruiseTimeSecondLeg * FtrCruiseFBR \quad (58)$$

$$FtrNumberTankingsDuringCruiseSecondLeg = \frac{FtrFuelConsumedinCruiseSecondLeg}{FtrFuelCapacity - FtrFuelReserves} \quad (59)$$

$$FtrCruiseRefuelTimeSecondLeg = FtrNumberTankingsDuringCruiseSecondLeg * \left(2 + \frac{FtrFuelConsumedinCruiseSecondLeg}{5000lb/min}\right) \quad (60)$$

$$TactTankerCruiseTimeSecondLeg = \frac{TactTankerOrbitDistanceFromTradTanker}{TactTankerBlockSpeed} * \frac{2}{60min/hr} \quad (61)$$

$$TactTankerFuelConsumedinCruiseSecondLeg = TactTankerCruiseTimeSecondLeg * TactTankerFBR + FtrFuelConsumedinCruiseSecondLeg * NumberFtrinFlight \quad (62)$$

$$OCATactTankerFuelAvailablewhileonStation =$$

$$max(0, TactTankerFuelCapacity - TactTankerFuelReserves$$

$$- TactTankerFuelConsumedinCruiseSecondLeg -$$

$$OCATactTankerLoiterFuelBurned_{guess}) \quad (63)$$

$$OCAFtrIngressEgressTime =$$

$$\frac{DistancefromTactTankertoLoiterorPenetration}{FtrIngressEgressSpeed} * \frac{2}{60min/hr} \quad (64)$$

$$OCAFtrFuelConsumedIngressEgress =$$

$$OCAFtrIngressEgressTime * FtrIngressEgressFBR \quad (65)$$

$$OCAFtrFuelforPenetration =$$

$$min(\frac{OCATactTankerFuelAvailablewhileonStation}{NumberFtrinFlight}$$

$$- OCAFtrFuelConsumedIngressEgress,$$

$$FtrFuelCapacity - FtrFuelReserves - OCAFtrFuelConsumedIngressEgress) \quad (66)$$

$$OCAFtrPenetrationDuration = \frac{OCAFtrFuelforPenetration}{FtrPenetrationFBR} \quad (67)$$

$$OCAFtrFuelConsumedPenetration =$$

$$OCAFtrPenetrationDuration * FtrPenetrationFBR \quad (68)$$

$$OCAFtrPenetrationRadius =$$

$$\frac{FtrPenetrationSpeed * OCAFtrPenetrationDuration}{2 * 60 min/hr} \quad (69)$$

$$OCATactTankerLoiterTime =$$

$$OCAFtrPenetrationDuration + OCAFtrIngressEgressTime \quad (70)$$

$$OCATactTankerLoiterFuelBurned =$$

$$TactTankerFBR * OCATactTankerLoiterTime \quad (71)$$

$$OCAFtrDistancefromTradTanker =$$

$$TactTankerOrbitDistanceFromTradTanker+$$

$$DistancefromTactTankertoLoiterorPenetration + OCAFtrPenetrationRadius \quad (72)$$

$$OCAFtrIngressDistanceWOTT =$$

$$TactTankerOrbitDistanceFromTradTanker+$$

$$DistancefromTactTankertoLoiterorPenetration \quad (73)$$

$$OCAFtrIngressEgressTimeWOTT =$$

$$\frac{OCAFtrIngressDistanceWOTT}{FtrIngressEgressSpeed} * 2 * 60min/hr \quad (74)$$

$$OCAFtrFuelConsumedIngressEgressWOTT =$$

$$OCAFtrIngressEgressTimeWOTT * FtrIngressEgressFBR \quad (75)$$

$$OCAFtrFuelatIPWOTT =$$

$$FtrFuelCapacity - FtrFuelReserves-$$

$$OCAFtrFuelConsumedIngressEgressWOTT-$$

$$FtrFuelConsumedinCruiseSecondLeg \quad (76)$$

$$OCAFtrPenetrationDurationWOTT = \frac{OCAFtrFuelatIPWOTT}{FtrPenetrationFBR} \quad (77)$$

$$OCAFtrPenetrationRadiusWOTT = \frac{OCAFtrPenetrationDurationWOTT * FtrPenetrationSpeed}{2 * 60 min/hr} \quad (78)$$

$$OCAFtrDistancefromTradTankerWOTT = OCAFtrIngressDistanceWOTT + OCAFtrPenetrationRadiusWOTT \quad (79)$$

$$OCAMissionDuration = TactTankerCruiseTimeFirstLeg + TactTankerCruiseTimeSecondLeg + OCAFtrIngressEgressTime + OCAFtrPenetrationDuration \quad (80)$$

$$OCATactTankerFuelOffloaded = NumberFtrinFlight * (FtrFuelConsumedinCruiseSecondLeg + OCAFtrFuelConsumedIngressEgress + OCAFtrFuelConsumedPenetration) \quad (81)$$

$$OCATactTankerFuelBurned = OCAMissionDuration * TactTankerFBR \quad (82)$$

$$OCACAPEffectiveness = \frac{OCAFtrDistancefromTradTanker}{OCAFtrDistancefromTradTankerWOTT} \quad (83)$$

$$OCACAPPenetrationEffectiveness = \frac{OCAFtrPenetrationRadius}{OCAFtrPenetrationRadiusWOTT} \quad (84)$$

$$OCATactTankerFuelEffectiveness = \frac{OCATactTankerFuelOffloaded}{OCATactTankerFuelBurned} * \frac{OCAFtrPenetrationRadius}{OCAFtrPenetrationRadius_{max}} \quad (85)$$

$$DCATactTankerFuelAvailablewhileonStation = max(0, TactTankerFuelCapacity - TactTankerFuelReserves - TactTankerFuelConsumedinCruiseSecondLeg) \quad (86)$$

$$DCAFtrTransitTime = \frac{DistancefromTactTankertoLoiterorPenetration}{FtrTransitSpeed} * 2 * 60min/hr \quad (87)$$

$$DCAFtrFuelConsumedinTransit = DCAFtrTransitTime * FtrTransitFBR \quad (88)$$

$$DCAFtrFuelforLoiter = FtrFuelCapacity - FtrFuelReserves - DCAFtrFuelConsumedinTransit \quad (89)$$

$$DCAFtrLoiterTime = min(\frac{DCAFtrFuelforLoiter}{FtrLoiterFBR}, MaxMissionDuration * 60min/hr - DCAFtrTransitTime - FtrCruiseTimeSecondLeg - FtrCruiseTimeFirstLeg) \quad (90)$$

$$DCAFtrAvailableCycleTime = MaxMissionDuration * 60min/hr - FtrCruiseTimeFirstLeg - FtrCruiseTimeSecondLeg \quad (91)$$

$$DCAFtrTimePerCycle = DCAFtrTransitTime + DCAFtrLoiterTime \quad (92)$$

$$DCAFtrNumberofCycles = \frac{DCAFtrAvailableCycleTime}{DCAFtrTimePerCycle} \quad (93)$$

$$DCAFtrPartialLoiterTime = PartialCycle$$
$$DCAFtrTimePerCycle - DCAFtrTransitTime \quad (94)$$

$$DCAFtrFuelforLoiterWOTT = FtrFuelCapacity-$$
$$FtrFuelReserves - DCAFtrFuelConsumedinTransit-$$
$$FtrFuelConsumedinCruiseSecondLeg \quad (95)$$

$$DCAFtrLoiterTimeWOTT = \frac{DCAFtrFuelforLoiterWOTT}{FtrLoiterFBR} \quad (96)$$

$$DCAFtrAvailableCycleTimeWOTT =$$
$$MaxMissionDuration * 60min/hr - FtrCruiseTimeFirstLeg \quad (97)$$

$$DCAFtrTimePerCycleWOTT = FtrCruiseTimeFirstLeg+$$
$$DCAFtrTransitTime + DCAFtrLoiterTimeWOTT \quad (98)$$

$$DCAFtrNumberofCyclesWOTT = \frac{DCAFtrAvailableCycleTimeWOTT}{DCAFtrTimePerCycleWOTT} \quad (99)$$

$$DCAFtrPctLoiterTimeWOTT = DCAFtrLoiterTimeWOTT* \frac{DCAFtrNumberofCyclesWOTT}{MaxMissionDuration * 60min/hr} \quad (100)$$

$$DCATactTankerFuelConsumedinCruiseSecondLeg = TactTankerCruiseTimeSecondLeg * TactTankerFBR \quad (101)$$

$$DCATactTankerMaxFuelAvailable = max(0, TactTankerFuelCapacity - TactTankerFuelReserves - DCATactTankerFuelConsumedinCruiseSecondLeg) \quad (102)$$

$$DCATactTankerOrbitMinFuelRequired = \frac{DCATactTankerFuelConsumedinCruiseSecondLeg}{2} + DCAFtrTimePerCycle * TactTankerFBR + NumberFtrinFlight * (FtrFuelCapacity - FtrFuelReserves) \quad (103)$$

$$DCATactTankerCycleTime = TactTankerCruiseTimeSecondLeg+ \left(\frac{DCATactTankerFuelLoadedfromTradTanker_{guess}}{5000lb/min} + 2min\right) \quad (104)$$

$$DCATactTankerMaxNumberFtrCyclesSupported = \frac{DCATactTankerMaxFuelAvailable}{TactTankerFBR * DCAFtrTimePerCycle + NumFtr * (FuelCap - FuelRes)} \quad (105)$$

$$DCAFtrTimePerCycleShortened = DCATactTankerMaxNumberFtrCyclesSupported * DCAFtrTimePerCycle \quad (106)$$

$$DCAFtrLoiterTime = DCAFtrTimePerCycleShortened - DCAFtrTransitTime \quad (107)$$

$$DCAFtrNumberofCycles = \frac{DCAFtrAvailableCycleTime}{DCAFtrTimePerCycleShortened} \quad (108)$$

$$DCAMissionDuration = TactTankerCruiseTimeFirstLeg+$$
$$TactTankerCruiseTimeSecondLeg+$$
$$DCAFtrTimePerCycleShortened * DCAFtrNumberofCycles \quad (109)$$

$$DCATactTankerActualNumberFtrCyclesSupported =$$
$$\frac{DCAMaxFuelAvailable - NumFtr * FtrFuelConsumedinCruiseSecondLeg}{TactTankerFBR * DCAFtrTimePerCycle + NumFtr * (FtrFuelCap - FtrFuelRes)} \quad (110)$$

$$DCATactTankerMaxIntegerNumberFtrCyclesSupported =$$
$$floor(DCATactTankerMaxIntegerNumberFtrCyclesSupported) \quad (111)$$

$$DCATactTankerFuelOffloadedPerTankerCycle =$$
$$DCATactTankerMaxIntegerNumberFtrCyclesSupported*$$
$$NumberFtrinFlight * (FtrFuelCapacity - FtrFuelReserves) \quad (112)$$

$$DCATactTankerFuelLoadedfromTradTanker =$$

$$DCATactTankerFuelConsumedinCruiseSecondLeg+$$

$$DCATactTankerMaxIntegerNumberFtrCyclesSupported*$$

$$\{FtrLoiterFBR * DCAFtrTimePerCycle + NumberFtrinFlight*$$

$$(FtrFuelCapacity - FtrFuelReserves)\} + \frac{NumFtr * FtrFuelConsCruiseSecondLeg}{2} \quad (113)$$

$$DCAFtrPctLoiterTime = DCAFtrLoiterTime*$$

$$\frac{DCAFtrNumberofCycles}{MaxMissionDuration * 60min/hr} \quad (114)$$

$$DCAMissionDuration = TactTankerCruiseTimeFirstLeg+$$

$$TactTankerCruiseTimeSecondLeg+$$

$$DCAFtrTimePerCycle * DCAFtrNumberofCycles \quad (115)$$

$$DCATactTankerFuelOffloaded = NumberFtrinFlight*$$

$$(FuelConsCruiseSecondLeg + FtrLoiterFBR * TimePerCycle * FtrNumCycles) \quad (116)$$

$$DCATactTankerFuelBurned = DCAMissionDuration * TactTankerFBR \quad (117)$$

$$DCACAPLoiterEffectiveness = \frac{DCAFtrLoiterTime}{DCAFtrLoiterTimeWOTT} \quad (118)$$

$$DCACAPLoiterPercentEffectiveness = \frac{DCAFtrPctLoiterTime}{DCAFtrPctLoiterTimeWOTT} \quad (119)$$

$$DCATactTankerEffectiveness = \frac{DCATactTankerFuelOffloadedPerTankerCycle}{DCATactTankerFuelLoadedfromTradTanker} \quad (120)$$

$$DCATactTankerFuelEffectiveness = \frac{DCATactTankerFuelOffloadedPerMission}{DCATactTankerFuelBurnedPerMission} * \frac{DCAFtrLoiterTime}{DCAFtrLoiterTime_{max}} \quad (121)$$

Bibliography

1. *Counterair Operations*. Technical report, LeMay Center for Doctrine, Maxwell AFB, AL, Aug 2014. URL `https://doctrine.af.mil/download.jsp?filename=3-01-ANNEX-COUNTERAIR.pdf`.

2. Aerospace Vehicles Division, Air Force Research Laboratory. *Aerospace Vehicle Concept Technology Validation*, 2015.

3. Air Force Research Laboratory. *Technology Milestones*, Jan 2006.

4. Allen, J. *Advertisement and Specification for a Heavier Than-Air Flying Machine*. Technical report, Signal Corps Specification, No. 486, Washington D.C., Jan 1908.

5. Arena, M., O. Younossi, K. Brancato, I. Blickstein, and C. I. Grammich. "Why Has the Cost of Fixed-Wing Aircraft Risen? A Macroscopic Examination of the Trends in U.S. Military Aircraft Costs over the Past Several Decades". *RAND Corporation*, 1–4, 2008.

6. Box, G. E. P., J. S. Hunter, and W. G. Hunter. *Statistics for Experimenters: Design, Discovery, and Innovation*. Wiley Interscience, Hoboken, NJ, 2nd edition, 2005.

7. Cobb, M. R. *Aerial Refueling: The Need for a Multipoint, Dual-System Capability*. Technical report, Airpower Research Institute, Maxwell AFB, AL, July 1987.

8. Cole, A. D. *The Need for a Tactical Aerial Refueling Platform*. Ph.D. thesis, Air War College, Maxwell Air Force Base, AL, March 1989.

9. Dacus, C. and S. Hagel. "A Conceptual Framework for Defense Acquisition Decision Makers: Giving the Schedule Its Due". *Defense Acquisition Research Journal*, 21(1):486–504, 2014.

10. DePauw, D. J. W. and P. A. Vanrolleghem. "Avoiding the Finite Difference Sensitivity Analysis Deathtrap by Using the Complex-Step Derivative Approximation Technique". *Proceedings of the 3rd Biennial Meeting of the International Environmental Modeling and Software Society*. Burlington, July 2006.

11. Diedrich, A. J. *The Multidisciplinary Design and Optimization of an Unconventional, Extremely Quiet Transport Aircraft*. Ph.D. thesis, Massachusetts Institute of Technology, Cambridge, MA, 2005.

12. Economon, T. D., S. R. Copeland, J. J. Alonso, M. Zeinali, and D. Rutherford. "Design and Optimization of Future Aircraft for Assessing the Fuel Burn Trends of Commercial Aviation". *49th AIAA Aerospace Sciences Meeting including the New Horizons Forum and Aerospace Exposition*. Orlando, FL, Jan 2011.

13. Fisher, R. A. *The Design of Experiments*. Hafner Press, New York, 8th edition, 1974.

14. Fulghum, D. A., R. Wall, and A. Nativi. "Combat in Libya Takes Place". *Aviation Week and Space Technology*, 25, Apr 2011.

15. Green, J. M. "Establishing System Measures of Effectiveness". *AIAA 2nd Biennial National Forum on Weapon System Effectiveness*, 2001.

16. Iannuzzi, P. A. *Proposal for United States Air Force Air Refueling Operations Doctrine*. Graduate research paper, Air Force Institute of Technology, Wright-Patterson AFB, OH, Nov 1996.

17. Kirby, M. R. *A Methodology for Technology Identification, Evaluation, and Selection in Conceptual and Preliminary Aircraft Design.* Thesis, Georgia Institute of Technology, Atlanta, GA, Mar 2001.

18. Mavris, D. N. and D. DeLaurentis. "An Integrated Approach to Military Aircraft Selection and Concept Evaluation". *1st Annual AIAA Aircraft Engineering, Technology, and Operations Congress*, 1995.

19. McManus, H. L., M. G. Richards, A. M. Ross, and D. E. Hastings. "A Framework for Incorporating ilities in Tradespace Studies". *AIAA SPACE Conference and Exposition*, 2007.

20. Oates, G. C. *Aircraft Propulsion Systems Technology and Design.* American Institute of Aeronautics and Astronautics, Reston, VA, 1989.

21. Osborne, A. "BAE Proposes Tactical Tanker Based on BAe 146". *Aerospace Daily and Defense Report*, 3, Sep 2013.

22. Owen, R. C. *Basing Strategies for Air Refueling Forces in Antiaccess/Area-Denial Environments.* Air University Press, Maxwell AFB, AL, 2015.

23. Panson, D. M., E. J. Alyanak, J. A. Dubois, and T. Van Woerkam. "Exploring the Next Generation Air Dominance Trade Space", 2015. Unpublished paper.

24. Raymer, D. *Enhancing Aircraft Conceptual Design Using Multidisciplinary Optimization.* Dissertation, Royal Institute of Technology, Stockholm, Sweden, 2002.

25. Raymer, D. P. *Aircraft Design: A Conceptual Approach, 4th Edition.* AIAA Education Series, Reston, VA, 2006.

26. Sadin, S. R., F. P. Povinelli, and R. Rosen. "The NASA Technology Push Towards Future Space Mission Systems". *Proceedings of the 39th Annual Interna-*

tional Astronautical Congress. National Aeronautics and Space Administration, Association for Computing Machinery, Bangalore, India, Oct 1988.

27. Spencer, B. W. *The Precious Sortie: The United States Air Force at the Intersection of Rising energy Prices, an Aging Fleet, a Struggling Recapitalization Effort, and Stressed Defense Budgets*. Thesis, United States Marine Corps Command and Staff College, Quantico, VA, 2009.

28. of Staff, U.S. Joint Chiefs. *Air Mobility Operations Joint Publication 3-17*. Technical report, U.S. Joint Chiefs of Staff, Washington, D.C., Sep 2013.

29. Tortorelli, D. A. and P. Michaleris. "Design Sensitivity Analysis: Overview and Review". *Inverse Problems in Engineering*, 1(1):71–105, Oct 1994.

REPORT DOCUMENTATION PAGE

Form Approved
OMB No. 0704–0188

1. REPORT DATE *(DD–MM–YYYY)*	2. REPORT TYPE	3. DATES COVERED *(From — To)*
24–03–2016	Master's Thesis	Sept 2014 — Mar 2016

4. TITLE AND SUBTITLE

Effectiveness Based Design of a Tactical Tanker Aircraft

5a. CONTRACT NUMBER

5b. GRANT NUMBER

5c. PROGRAM ELEMENT NUMBER

6. AUTHOR(S)

Petry, Andrew K., 1Lt, USAF

5d. PROJECT NUMBER

5e. TASK NUMBER

5f. WORK UNIT NUMBER

7. PERFORMING ORGANIZATION NAME(S) AND ADDRESS(ES)

Air Force Institute of Technology
Graduate School of Engineering and Management (AFIT/EN)
2950 Hobson Way
WPAFB OH 45433-7765

8. PERFORMING ORGANIZATION REPORT NUMBER

AFIT/GAE/ENY/16-M-233

9. SPONSORING / MONITORING AGENCY NAME(S) AND ADDRESS(ES)

Design and Analysis Branch, AFRL/RQVC
2210 8th Street
WPAFB OH 45433
DSN 713-7144, COMM 937-713-7144, edward.alyanak.1@us.af.mil

10. SPONSOR/MONITOR'S ACRONYM(S)

AFRL/RQVC

11. SPONSOR/MONITOR'S REPORT NUMBER(S)

12. DISTRIBUTION / AVAILABILITY STATEMENT

DISTRIBUTION STATEMENT A:
APPROVED FOR PUBLIC RELEASE; DISTRIBUTION UNLIMITED.

13. SUPPLEMENTARY NOTES

14. ABSTRACT

An approach to drive conceptual aircraft design using mission effectiveness parameters is described and applied to an operational scenario. The scenario includes traditional aircraft refueling tankers and a proposed tactical tanker concept supporting fighter aircraft conducting offensive (OCA) and defensive (DCA) counter air patrols. Traditional conceptual design methodologies were used to generate a baseline design for a tactical tanker aircraft, which was evaluated using a MATLAB-based model to investigate Measures of Effectiveness (MOE). The model holds the traditional tanker and fighter capabilities constant, while varying the tactical tanker's specific fuel consumption, lift-to-drag ratio, fuel payload, mass fraction, and proximity to contested airspace. A sensitivity analysis was conducted to show the effect of technology variations on MOEs. Results show with a minimum of 45000 lb fuel payload, the tactical tanker can increase the fighter OCA penetration radius by 57%, and the DCA loiter time by 48%. However; optimal size is heavily dependent on gameboard layout, fighter size, and number of aircraft tasked to the tanker. Sensitivity analysis and full factorial trade space exploration show the MOEs are most sensitive to changes in proximity and mass fraction. These results provide recommendations for the prioritization of research efforts if the US Air Force decides to develop a tactical tanker aircraft in the future.

15. SUBJECT TERMS

Tactical Tanker, Air Refueling, Aircraft Design, Measures of Effectiveness, Sensitivity Analysis, Full Factorial Tradespace

16. SECURITY CLASSIFICATION OF:			17. LIMITATION OF ABSTRACT	18. NUMBER OF PAGES	19a. NAME OF RESPONSIBLE PERSON
a. REPORT	b. ABSTRACT	c. THIS PAGE			Lt Col Anthony M. DeLuca, AFIT/ENY
U	U	U	UU	130	19b. TELEPHONE NUMBER *(include area code)* (937) 255-3636 x4537, anthony.deluca@afit.edu